การตรวจสอบการเปลี่ยนแปลงอัตราการไหวสะเทือนและขั้นตอนวิธี บริเวณ-เวลา-ความยาวรอยเลื่อน ตามแนวมุดตัวของแผ่นเปลือกโลกสุมาตรา-อันดามัน

นายสัณฑวัฒน์ สุขรังษี

จุฬาลงกรณ์มหาวิทยาลัย
Chulalongkorn University

บทคัดย่อและแฟ้มข้อมูลฉบับเต็มของวิทยานิพนธ์ตั้งแต่ปีการศึกษา 2554 ที่ให้บริการในคลังปัญญาจุฬาฯ (CUIR)
เป็นแฟ้มข้อมูลของนิสิตเจ้าของวิทยานิพนธ์ ที่ส่งผ่านทางบัณฑิตวิทยาลัย
The abstract and full text of theses from the academic year 2011 in Chulalongkorn University Intellectual Repository (CUIR)
are the thesis authors' files submitted through the University Graduate School.

วิทยานิพนธ์นี้เป็นส่วนหนึ่งของการศึกษาตามหลักสูตรปริญญาวิทยาศาสตรมหาบัณฑิต
สาขาวิชาโลกศาสตร์ ภาควิชาธรณีวิทยา
คณะวิทยาศาสตร์ จุฬาลงกรณ์มหาวิทยาลัย
ปีการศึกษา 2557
ลิขสิทธิ์ของจุฬาลงกรณ์มหาวิทยาลัย

SEISMICITY RATE CHANGE AND REGION-TIME-LENGTH ALGORITHM INVESTIGATIONS ALONG SUMATRA-ANDAMAN SUBDUCTION ZONE

Mr. Santawat Sukrungsri

A Thesis Submitted in Partial Fulfillment of the Requirements

for the Degree of Master of Science Program in Earth Sciences

Department of Geology

Faculty of Science

Chulalongkorn University

Academic Year 2014

Copyright of Chulalongkorn University

Thesis Title	SEISMICITY RATE CHANGE AND REGION-TIME-LENGTH ALGORITHM INVESTIGATIONS ALONG SUMATRA-ANDAMAN SUBDUCTION ZONE
By	Mr. Santawat Sukrungsri
Field of Study	Earth Sciences
Thesis Advisor	Assistant Professor Santi Pailoplee, Ph.D.

Accepted by the Faculty of Science, Chulalongkorn University in Partial Fulfillment of the Requirements for the Master's Degree

.....Dean of the Faculty of Science

(Professor Supot Hannongbua, Dr.rer.nat.)

THESIS COMMITTEE

.....Chairman

(Assistant Professor Sombat Yumuang, Ph.D.)

.....Thesis Advisor

(Assistant Professor Santi Pailoplee, Ph.D.)

.....Examiner

(Kruawun Jankaew, Ph.D.)

.....External Examiner

(Paiboon Nuannin, Ph.D.)

จุฬาลงกรณ์มหาวิทยาลัย
CHULALONGKORN UNIVERSITY

สัณฑวัฒน์ สุขรังษี : การตรวจสอบการเปลี่ยนแปลงอัตราการไหวสะเทือนและขั้นตอนวิธี บริเวณ-เวลา-ความยาวรอยเลื่อน ตามแนวมุดตัวของแผ่นเปลือกโลกสุมาตรา-อันดามัน (SEISMICITY RATE CHANGE AND REGION-TIME-LENGTH ALGORITHM INVESTIGATIONS ALONG SUMATRA-ANDAMAN SUBDUCTION ZONE) อ.ที่ปรึกษาวิทยานิพนธ์หลัก: สันติ ภัยหลบลี้, 108 หน้า.

การศึกษานี้ มีวัตถุประสงค์หลักในการตรวจสอบพื้นที่เสี่ยงที่มีโอกาสเกิดแผ่นดินไหวขนาดใหญ่ ตามแนวมุดตัวของแผ่นเปลือกโลกสุมาตรา-อันดามัน ด้วยวิธีการทางแผ่นดินไหววิทยาเชิงสถิติ (statistical seismology) 2 วิธีคือ 1) การเปลี่ยนแปลงอัตราการไหวสะเทือน (seismicity rate change หรือ Z value) และ 2) ขั้นตอนวิธี บริเวณ-เวลา-ความยาวรอยเลื่อน (RTL) ซึ่งหลังจากตรวจสอบปรับปรุงข้อมูลทางสถิติ ข้อมูลเหตุการณ์แผ่นดินไหวที่มีขนาด 4.4 ตามมาตราโมเมนต์ ที่บันทึกไว้ในช่วงปี ค.ศ. 1980-2014 ถูกประเมินว่าเป็นฐานข้อมูลที่บันทึกไว้อย่างครบถ้วนสมบูรณ์ และแสดงถึงพฤติกรรมการเกิดแผ่นดินไหวตามแนวมุดตัวของแผ่นเปลือกโลกสุมาตรา-อันดามันอย่างแท้จริง ค่าลักษณะเฉพาะ (characteristic parameters) ที่เหมาะสมถูกนำมาใช้ในการวิเคราะห์พื้นที่เสี่ยงต่อการเกิดแผ่นดินไหวด้วยวิธี Z value และ RTL ที่มีการแปรผันในเชิงเวลา และสามารถแสดงถึงภาวะเงียบสงบของกิจกรรมแผ่นดินไหวที่ค่า Z 6.7 และ RTL-0.3 ก่อนเกิดแผ่นดินไหวขนาดใหญ่ประมาณ 1-7 ปี นอกจากนี้การตรวจสอบในเชิงพื้นที่ยังพบว่าภาวะเงียบสงบของกิจกรรมแผ่นดินไหวเกิดขึ้นในบริเวณจุดศูนย์กลางแผ่นดินไหวขนาดใหญ่ตามแนวมุดตัวของแผ่นเปลือกโลกสุมาตรา-อันดามัน สืบเนื่องจากในการศึกษานี้ไม่พบการไหวสะเทือนที่เกิดจากมนุษย์ ดังนั้นค่าผิดปกติของ Z value และ RTL ที่ตรวจพบทั้งในเชิงพื้นที่และเวลาจึงแสดงถึงสัญญาณเตือนก่อนเกิดแผ่นดินไหว จากลักษณะเฉพาะที่เหมาะสมข้างต้นเมื่อนำมาวิเคราะห์แผนที่ Z และ RTL โดยใช้ข้อมูลแผ่นดินไหวล่าสุดในปัจจุบัน ผลการศึกษาตรวจพบค่าผิดปกติของ Z value และ RTL หนึ่งบริเวณ แต่ยังไม่เกิดแผ่นดินไหวขนาดใหญ่ คือ บริเวณหมู่เกาะนิโคบาร์ ดังนั้นการวางแผนอย่างมีประสิทธิภาพเพื่อลดผลกระทบควรดำเนินการอย่างเร่งด่วน

ภาควิชา ธรณีวิทยา ลายมือชื่อนิสิต .....

สาขาวิชา โลกศาสตร์ ลายมือชื่อ อ.ที่ปรึกษาหลัก .....

ปีการศึกษา 2557

5572235923 : MAJOR EARTH SCIENCES

KEYWORDS: SEISMICITY / RTL ALGORITHM / Z VALUE / QUIESCENCE

SANTAWAT SUKRUNGSRI: SEISMICITY RATE CHANGE AND REGION-TIME-LENGTH ALGORITHM INVESTIGATIONS ALONG SUMATRA-ANDAMAN SUBDUCTION ZONE. ADVISOR: ASST. PROF. SANTI PAILOPLEE, Ph.D., 108 pp.

In this study, prospective areas of the forthcoming major earthquakes were investigated along the Sumatra-Andaman Subduction Zone (SASZ) using simultaneously 2 seismological techniques called 1) seismicity rate change (Z value) and 2) region-time-length (RTL). After statistical investigation, the earthquake dataset with Mw 4.4 recorded during 1980-2014 were defined as the completeness data representing directly the seismotectonic activities along the SASZ. Using suitable characteristic parameters, both Z value and RTL reveal temporally the anomalous seismic quiescence, i.e., Z 6.7 and RTL -0.3, within 1-7 year before the major earthquakes. In addition, regarding spatial investigation, the quiescence illustrates in the vicinity of the epicenters of major earthquakes generated previously along the SASZ. Due to there is no evidence of man-made seismicity, both temporal and spatial Z-value and RTL anomalies obtained in this study, therefore, imply empirically the precursor of the earthquake. Base on the suitable conditions of both Z and RTL, the present-day Z and RTL maps were also contributed. The results reveal that there is only one location of Z and RTL anomalies which still quiescence from the major earthquakes, i.e., the segment in the vicinity of the Nicobar Islands. Therefore, the effective mitigation plan should be contributed urgently.

Department:	Geology	Student's Signature.....
Field of Study:	Earth Sciences	Advisor's Signature.....
Academic Year:	2014	

ACKNOWLEDGEMENTS

I sincerely thank my Advisor, Assistant Professor Dr. Santi Pailoplee, Department of Geology, Faculty of Science, Chulalongkorn University for his supports, encouragements, critically advises and reviews of thesis.

I would like to thank Miss Boossarasiri Thana, Department of Geology, Faculty of Sciences, Chulalongkorn University for her valuable suggestion.

I thank to Mr. Prayot Puangjuntha, Mr. Karun Taraka, and all of my friends for their kindly help throughout my study at the university.

I am grateful to Thai Meteorological Department who gave me opportunity to this study.

Finally, I express my deep respectfulness and gratitude to my family for their inspiration on scientific thinking is greatly appreciated.

จุฬาลงกรณ์มหาวิทยาลัย
Chulalongkorn University

CONTENTS

Page

จุฬาลงกรณ์มหาวิทยาลัย
Chulalongkorn University

Page

จุฬาลงกรณ์มหาวิทยาลัย
Chulalongkorn University

Page

จุฬาลงกรณ์มหาวิทยาลัย
Chulalongkorn University

LIST OF TABLES

Page

LIST OF FIGURES

Page

Page

จุฬาลงกรณ์มหาวิทยาลัย
Chulalongkorn University

Page

Page

จุฬาลงกรณ์มหาวิทยาลัย
Chulalongkorn University

Page

Chulalongkorn University

Page

จุฬาลงกรณ์มหาวิทยาลัย
CHULALONGKORN UNIVERSITY

Page

Page

จุฬาลงกรณ์มหาวิทยาลัย
CHULALONGKORN UNIVERSITY

CHAPTER I
INTRODUCTION

1.1 Background

Among the tectonic plate boundaries, the Sumatra–Andaman subduction zone (SASZ) is defined as one of the most seismically active (Pailoplee and Choowong, 2014). Tectonically, the SASZ formed according to the Indo-Australian and Eurasian plate collision and subduction with the rate of plate movement around 46 mm/year (Oishi and Sato, 2007). The average dip angle of subduction estimated from the cross section earthquakes distribution is ~20°, and the earthquakes were observed down to the depths of 700 km.

Based on literature review, the seismic history of the SASZ from the late 1600s through the early instrumental period (starting about 1900) were reported in the large number of previous works e.g., Banghar (1987); Dasgupta and Mukhopadhyay (1993); Dasgupta et al. (2003); Eguchi et al. (1979); Kumar Ravi et al. (1996); Sun and Pan (1995). The significant earthquakes were assigned very approximate magnitudes of 8.9 (in 1833) and 8.5 (in 1861). In addition, the evidences for moderate sized (M_w<8.0) subduction earthquakes in 1847, 1881, and 1941 was presented by Bilham et al. (2005). The 1881 event produced a tsunami that was recorded in the Bay of Bengal (Ortiz and Bilham, 2003).

Moreover based on around 50-year time span of the instrumental earthquake records, the SASZ still posed continuously a number of hazardous earthquakes (Figure 1.1). Among these, the Mw-9.0 earthquake generated on December 26th, 2004 was defined as the third largest earthquake in the world since 1900 (Park et al., 2005). This Mw-9.0 earthquake caused ground shaking in the countries surrounding its source including Thailand (Figure1.2); (Martin, 2005). In addition according to this giant earthquake, the tsunami devastated severely the number of coastal communities located along the Indian Ocean killing over 230,000 people in fourteen countries (Figure 1.3). Based on Paris et al. (2007), it was one of the deadliest natural disasters in

recorded history. In addition, not only was the last tsunami originated by a Mw-9.0 earthquake on December 26th, 2004, but also paleotsunami evidence supports that the SASZ is a significant tsunamogenic source (Jankaew et al., 2008; Monecke et al., 2008).

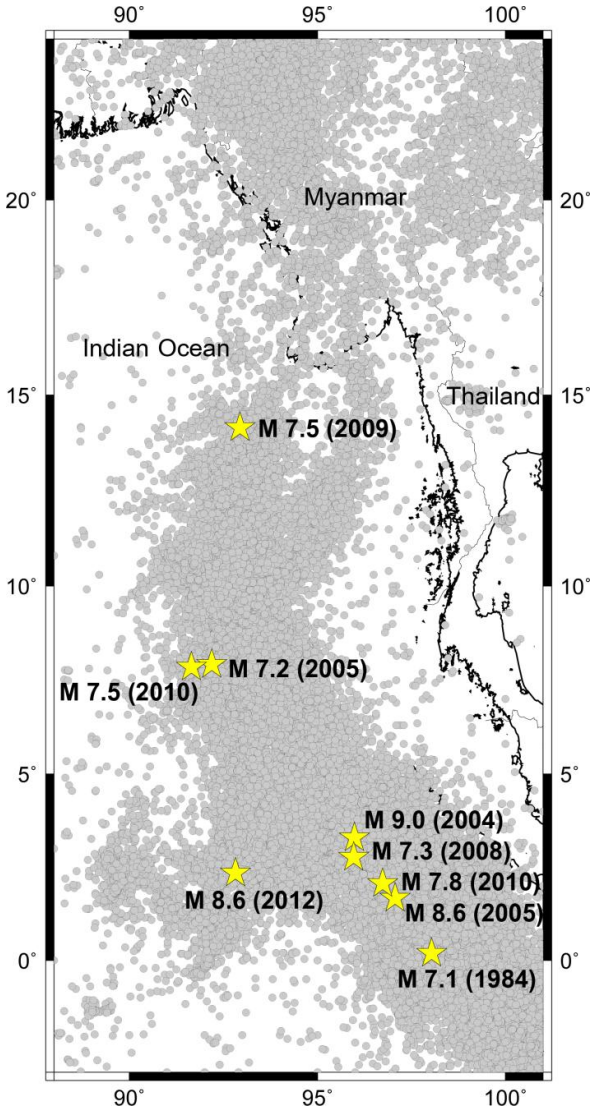

Figure 1.1. Map of the SASZ showing the boundary of study area. Grey circles is the epicentral distribution of the earthquake recorded instrumentally along the SASZ. The yellow stars denote some significant hazardous earthquake.

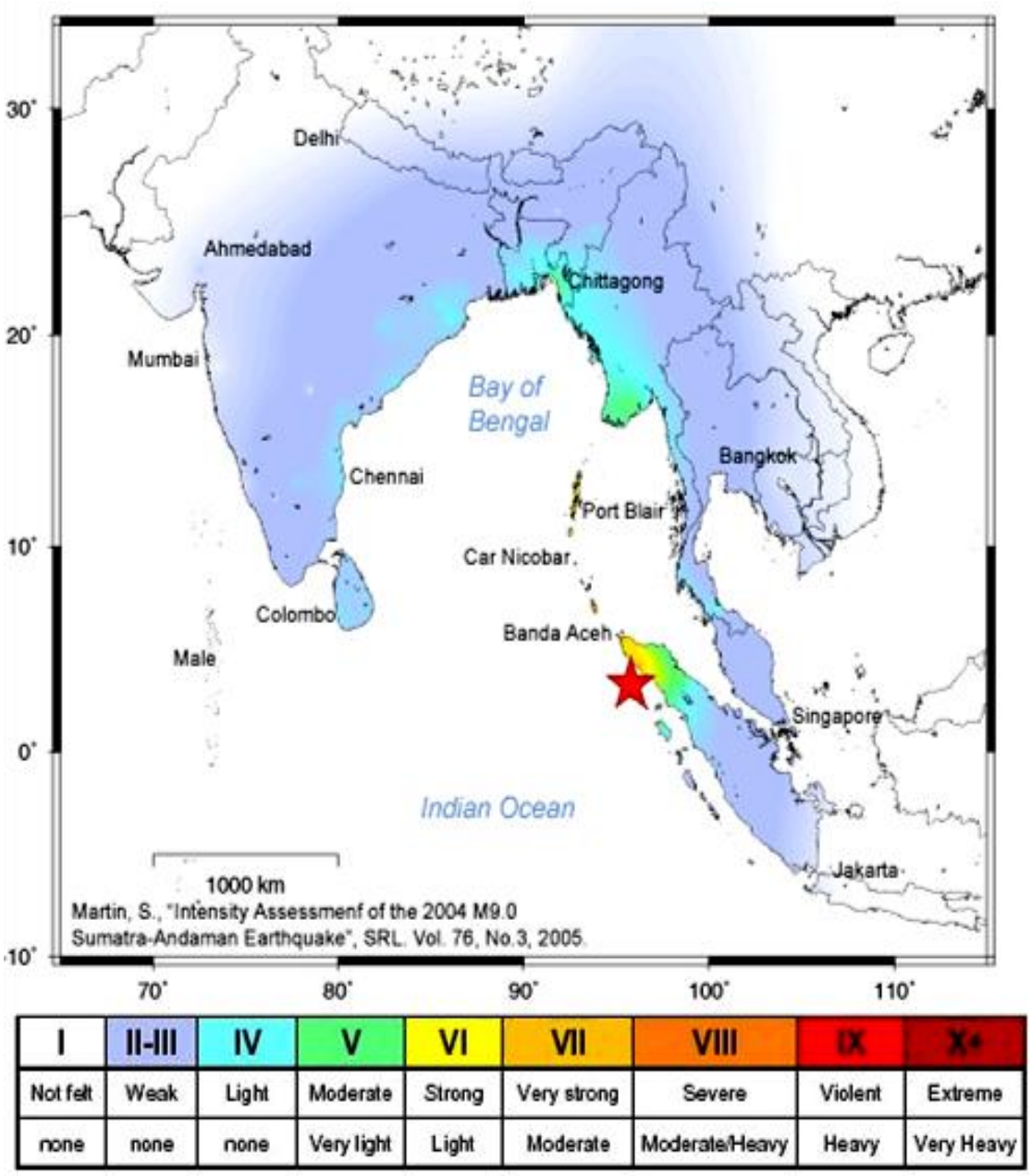

Figure 1.2. Map of the Mainland Southeast Asia showing location of the Mw-9.0 Sumatra-Andaman earthquakes (red star) and the area over which it was felt by the earthquake ground shaking. Colored shades depict the maximum observed European Macro-seismic Scale intensity (Martin, 2005).

Geographically, the tsunami hazard created here impacts upon a number of countries surrounding the Indian Ocean. And also such far-field SASZ earthquakes

normally generate long-period ground motions that directly affect tall buildings, and in particular in Bangkok, the capital city of Thailand. Hence, some researchers have attempted to clarify both the seismogenic and tsunamogenic situation along the SASZ (Gahalaut et al., 2006; Jankaew et al., 2008)

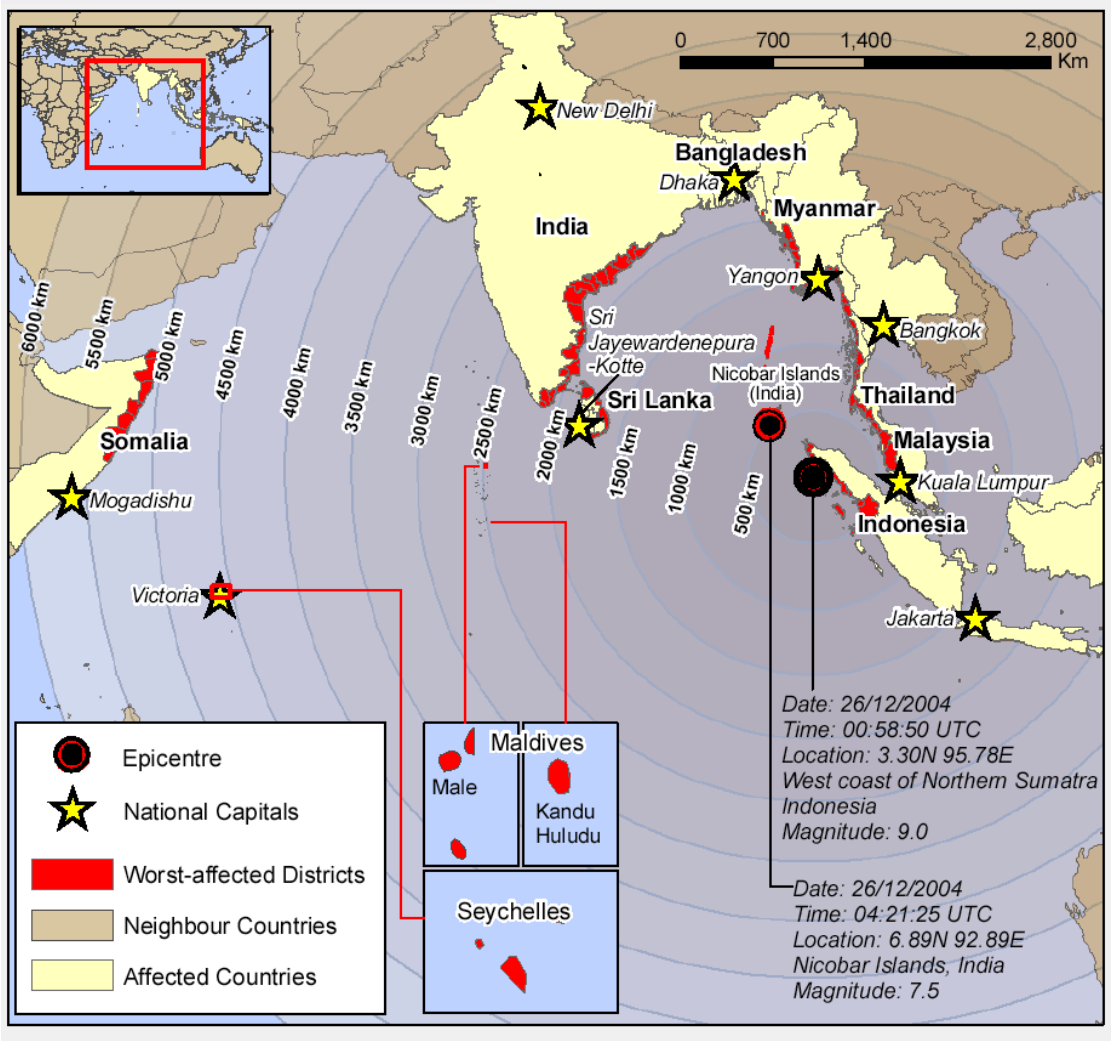

Figure 1.3. Map of the countries located along the Indian Ocean showing the worst-affected districts (red area) and tsunami affected countries (yellow area) according to the tsunami posed in December 26th, 2004 (Jaffe et al., 2006).

In addition, according to statistical seismology, the prospective areas of the upcoming earthquakes were also clarified along the SASZ. After the M_w-9.0 earthquake, Nuannin et al. (2005) estimated b values from the frequency-magnitude distribution

model (FMD); (Gutenberg and Richter, 1944) in the southern segment of the SASZ. They concluded that using 50 closest earthquake events of each site of interest, the comparatively low of b values are strongly related to the seismotectonic stress accumulated and the following major earthquakes. Thereafter, based mainly on the Nuannin et al. (2005)'s assumption, Pailoplee et al. (2013) investigated further to the northern segment of the SASZ. They proposed 3 prospect areas that might generate the hazardous earthquakes in the future (Figure 1.4), i.e., southern and northern offshore of Nicobar Islands including the inland Sittwe city, western Myanmar. However up to the present of 2015, no earthquake has been posed hazardously in the vicinity of those mentioned prospective areas so as to need monitoring carefully.

Since the last 2 decades, Sobolev (1995) proposed the existing of seismicity rate change, i.e., quiescence and or activation stages, preceding the strong-to-major earthquake. A number of research works, investigating such changes, have done successfully based mainly on 3 statistical approaches, i.e., β-value (Matthews and Reasenberg, 1988), Z value (Wiemer and Wyss, 1994), and region-time-length (RTL) algorithm (Huang et al., 2001). Among these approaches, Z value is one of the alternative technique that detecting effectively the precursory seismic quiescence of the strong-to-major earthquakes as mentioned by Chouliaras and Stavrakakis (2001), Rudolf-Navarro et al. (2010), Katsumata (2011a), and Kawamura et al. (2014).

In addition as a result of extended practice, a number of RTL investigations have revealed the successful correlation between the quiescent and/or activation stages and the subsequent moderate-to-major earthquakes in various seismogenic settings, such as the M_w-7.2 Kobe earthquake, Japan (Huang et al., 2001), M_w-6.8 Nemuro earthquake, Japan (Huang and Sobolev, 2002), M_w-7.3 Izmit earthquake, Turkey (Huang et al., 2002), M_S-7.3 Tottori earthquake, Japan (Huang and Nagao, 2002), earthquakes with $M_w \geq$ 5.0 in northern China (Jiang et al., 2004), earthquakes with $M_S \geq$ 6.0 in the Yunnan area (Liu and Su, 2006), M_w-7.3 Chi-Chi earthquake, Taiwan (Chen and Wu, 2006), M_w-8.0 Wenchuan earthquake, China (Huang, 2008) and the latest hazardous event of the M_w-9.0 Tohoku earthquake, Japan (Huang and Ding, 2012).

Therefore in order to investigate and constrain further the prospective areas of the forthcoming earthquakes proposed previously along the SASZ (Pailoplee et al., 2013), both approach of Z value and RTL algorithm, implying precursory seismic quiescence, were applied in this study to the most up-to-date seismicity data recorded along the SASZ.

1.2 Study Area and Scope of Study

In this study covering the SASZ is located between latitudes 2°S-24°N and longitudes 88°E-100°E. Geographically, if the segment ruptures of SASZ, in particular for vertical movement, the earthquake will generate the potential hazards of both ground shaking and local tsunami for Myanmar and India, including Thailand. This study, therefore, attempted to clarify the hazardous situation of the SASZ by investigating the anomalies in the Z value and RTL algorithm. The obtained results should be useful for preparing long-term mitigation plans for both seismic and tsunami hazards.

1.3 Objectives

The purposes of this study are,

- To evaluate the potential areas prior to large earthquakes along the SASZ according to the Z value.
- To evaluate the potential areas prior to large earthquakes along the SASZ according to the RTL algorithm.
- According to both Z value and RTL algorithm obtained above the prospective area prior to the large earthquake are interpreted along SASZ and proposed in this study.

จุฬาลงกรณ์มหาวิทยาลัย
Chulalongkorn University

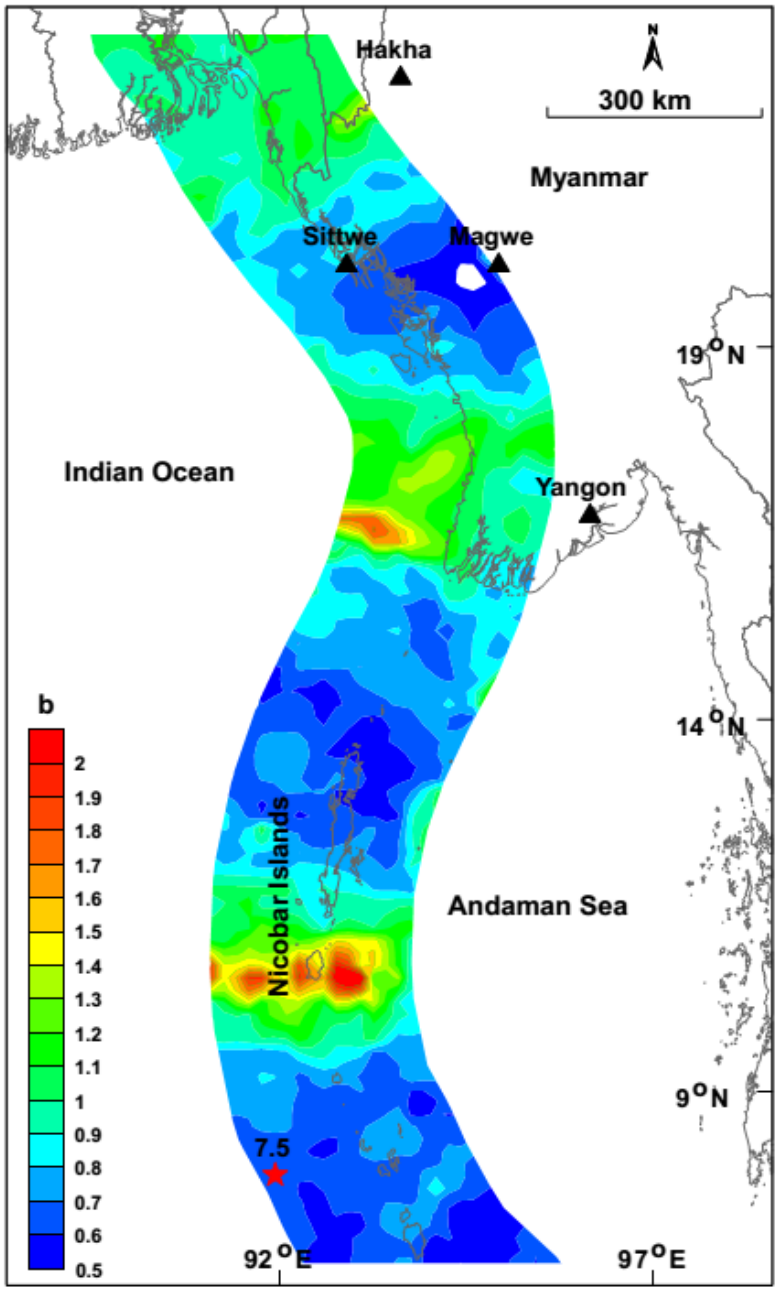

Figure 1.4. Distribution of b-values along the Northern segment of the SASZ, as derived using the seismicity data recorded during 1980–2010. Red star indicate earthquakes with $m_b \geq 7.0$ that was generated after the utilized seismicity data set (Pailoplee et al., 2013).

CHAPTER II
THEORY AND METHODOLOGY

2.1 Theory

2.1.1 Z-value

In order to find out the precursory seismic quiescence which is a significant decrease of the mean seismicity rate as compared to the background rate in the same crustal volume (Figure 2.1), the statistic method called Z value was applied in this study using the Long Term Average or LTA (t) function as expressed in Equation (2.1) (Wiemer and Wyss, 1994).

$$Z = \frac{R_{bg} - R_w}{\sqrt{\frac{S_{bg}}{N_{bg}} + \frac{S_w}{N_w}}} \tag{2.1}$$

where Z detects the seismic quiescence in terms of the difference between the average seismicity rate within considered time window (R_w) and the background rate outside the window recognized (R_{bg}). S_w and S_{bg} are the standard deviation whereas N_w and N_{bg} denote the corresponding number of earthquake data considered the seismicity rate, respectively (see also Figure 2.1b). Seismically, positive and negative values of Z imply that the seismicity rate is lower, and higher, than the background rate, respectively.

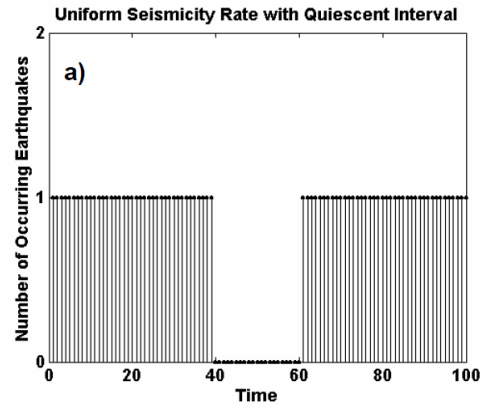

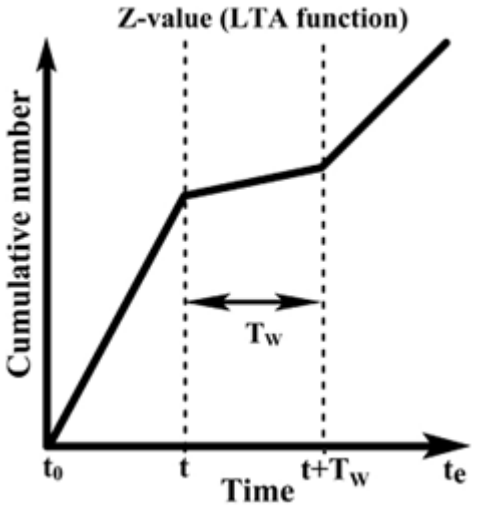

(b)

Figure 2.1. Simplified model of quiescent interval. (a) the number of earthquakes against time. (b) cumulative number as a function of time.

2.1.2 RTL algorithm

As mentioned previously, i.e., Sobolev (1995), laboratory rock experiments indicates the acoustic emissions may accelerate as load increases. However, the number of relatively weak signals tends to decrease after loading reaches a maximum, because small cracks are no longer generated due to a partial reduction in stress. During the final stage before the main rupture, acoustic activity increases again. In other words, acoustic emission passes through stages of quiescence and activation prior to the main rupture Sobolev (1995).

Theoretically, the RTL algorithm (Huang et al., 2001; Sobolev and Tyupkin, 1997) takes into account the influence weight of each prior event in the main event under investigation depends on all three parameters (time, place and magnitude) of earthquakes. The weight becomes larger when the prior earthquake is larger in magnitude or is closer to the investigated place or time. Mathematically, the RTL parameter is defined as the product of the following three functions after normalized by their standard deviations: epicentral distance, R(x, y, z, t); time, T (x, y, z, t); and rupture length, L(x, y, z, t) (equations (2.2-2.4)),

$$R(x,y,z,t) = \left[\sum_{i=1}^{n}\exp(-\frac{r_i}{r_0})\right] - R_{bk}(x,y,z,t), \quad (2.2)$$

$$T(x,y,z,t) = \left[\sum_{i=1}^{n}\exp(-\frac{t-t_i}{t_0})\right] - T_{bk}(x,y,z,t), \quad (2.3)$$

$$L(x,y,z,t) = \left[\sum_{i=1}^{n}(\frac{l_i}{r_i})\right] - L_{bk}(x,y,z,t), \quad (2.4)$$

where R, T, L are functions of space (x, y, z) and time (t), l_i , t_i, and r_i are the rupture dimension (a function of magnitude M_i), the occurrence time, and the distance from the position (x, y, z) to the epicenter of the i^{th} event, respectively; $R_{bk}(x, y, z, t)$, $T_{bk}(x, y, z, t)$ and $L_{bk}(x, y, z, t)$ are the trends (background values) of R(x, y, z, t), T (x, y, z, t) and L(x, y, z, t); r_0 and t_0 are a characteristic distance and time-span, respectively; n is the number of events satisfying some criteria, e.g., $M_i \geq M_{min}$ (M_i is the magnitude of the i^{th} earthquake and M_{min} is the cut-off magnitude ensuring the completeness of the earthquake catalogue), $r_i \leq R_{max} = 2r_0$ and $(t - t_i) \leq T_{max} = 2t_0$. Thus, the RTL parameter describes the deviation from the background level of seismicity and is in units of the standard deviation and normalized (Equation 2.5)

$$RTL(x,y,z,t) = \frac{R(x,y,z,t)}{R(x,y,z,t)_{\max}} \cdot \frac{T(x,y,z,t)}{T(x,y,z,t)_{\max}} \cdot \frac{L(x,y,z,t)}{L(x,y,z,t)_{\max}}, \quad (2.5)$$

According to the Equation (2.5), it makes the RTL function changing within [-1, 1] and the expectation value is zero. RTL>0 or RTL<0 imply respectively seismic activation or quiescence upon background values.

In addition according to (Huang et al., 2002), the parameter Q(x, y, z, t1, t2), representing as an average of the RTL values over some time window [t1, t2], was adopted newly to quantify the seismic quiescence at position (x, y, z) during [t1, t2]. The parameter Q(x, y, z, t1, t2) is defined as Equation 2.6.

$$Q(x,y,z,t1,t2) = \frac{1}{m}\sum_{i=1}^{m} RTL(x, y, z, t_i), \quad (2.6)$$

where m is the number of data points of RTL in the window [t1, t2] (RTL parameter is calculated by Equation (2.4)) available in [t1, t2]. Thus, one can obtain the spatial distribution of seismic quiescence as a function of position.

2.2 Literature Review

2.2.1 Z-value

Ozturk and Bayrak (2009) identified the starting time and duration of precursory quiescence prior to the Bingol earthquake, Turkey with the magnitude 6.4 Mw. Based on the iterative test of Z-value investigation, a decrease of the seismicity rate was found with the Zmax = 2.5 level on the date 1997.6. After that around 5.73 years, the Bingol earthquake posed on May 1st, 2003 followed an outstanding seismic quiescence. (Figure 2.2).

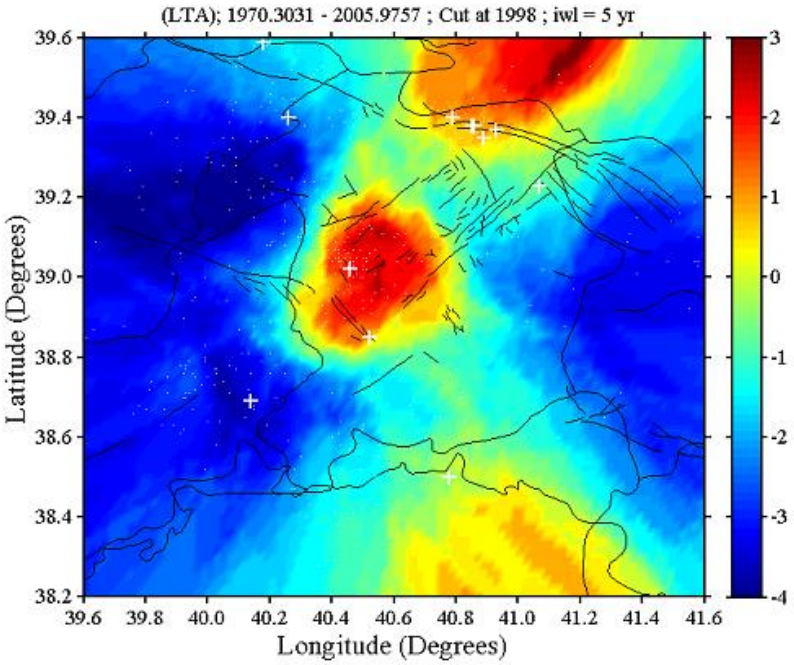

Figure 2.2. Map of eastern Turkey showing the distribution of Z values evaluated at the time slice 1997.6. The epicenter of main shocks with MD≥5.0 is indicated

by “+” symbol. Red color represents a decrease in the seismicity rate (Ozturk and Bayrak, 2009).

Katsumata (2011a) investigated the variations in seismicity pattern in the Japan region before the Mw-8.3 Tokachi-Oki, Japan, earthquake by calculating the standard normal deviate of the Z value. Based on careful investigation, Katsumata (2011a) found that the 2003 Tokachi-oki earthquake is preceded by two neighboring seismic quiescence anomalies (Figure 2.3a). As shown in Figures 2.3b and c., the maximum value of Z are +3.9 and +4.0 that started around the beginning of 1999, 5 years prior to the main shock occurred (Figure 2.3).

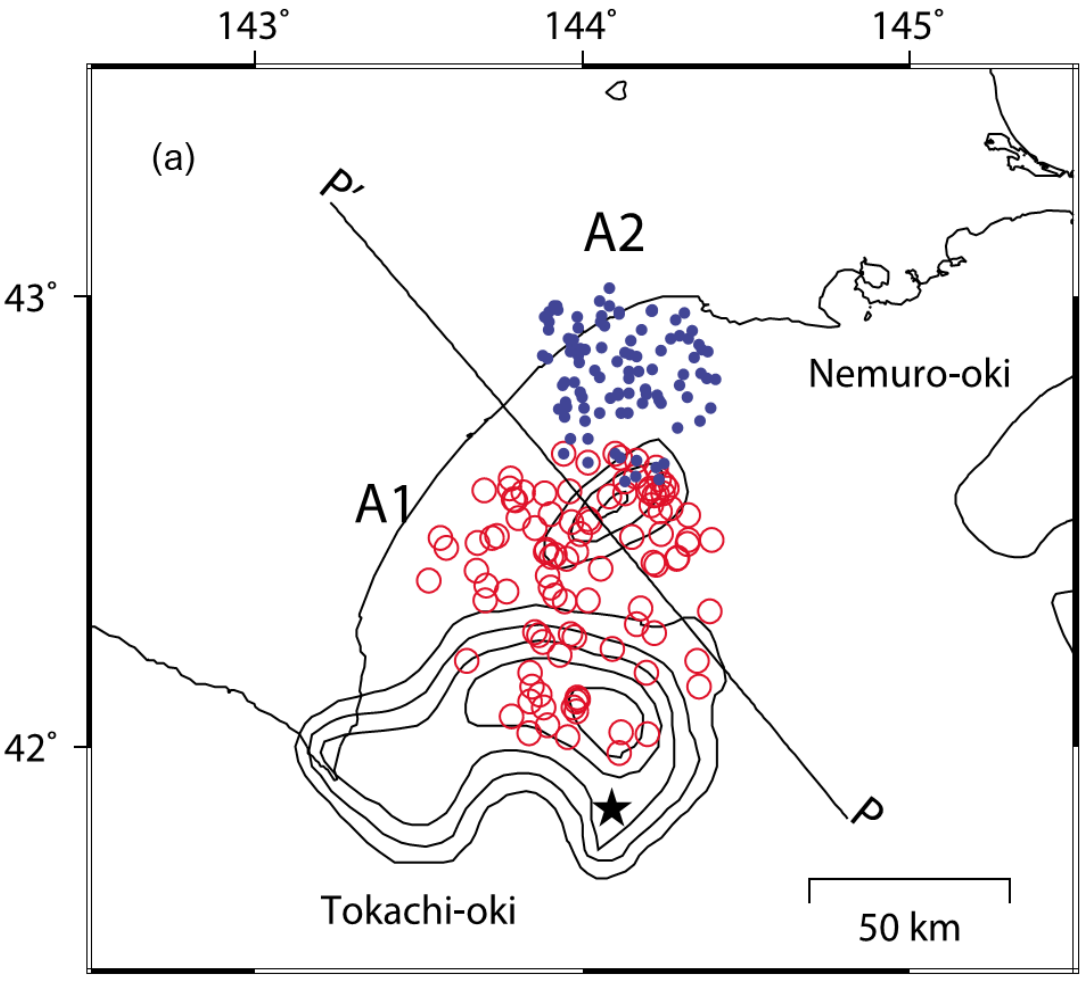

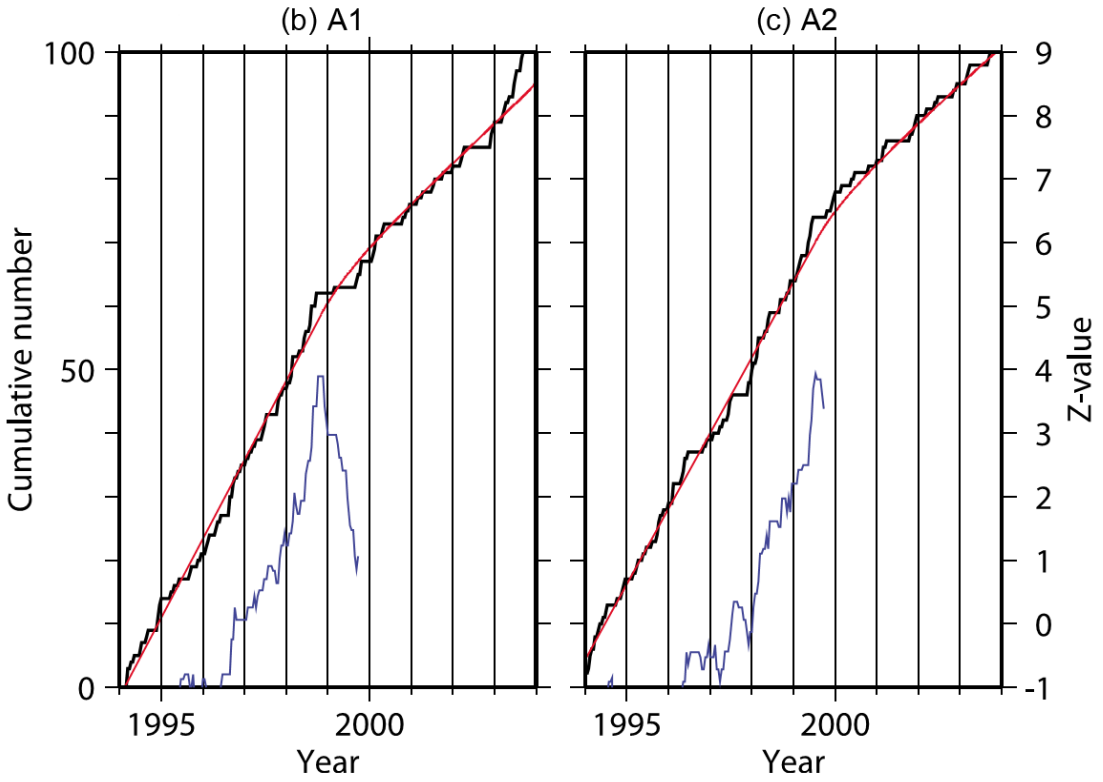

Figure 2.3. (a) Distribution of epicenters in the areas of Anomaly 1 (A1, red open circles) and Anomaly 2 (A2, closed blue circles). (b and c) show the cumulative number (black line), the Z value (blue line), and a theoretical curve for the cumulative number, assuming that the stressing rate ratio is 0.5 (red line) (Katsumata, 2011a).

จุฬาลงกรณ์มหาวิทยาลัย
Chulalongkorn University

Katsumata (2011b) found that a long-term seismic quiescence started 23.4 years before the 2011 off the Pacific coast of Tohoku Earthquake, Japan (Mw = 9.0). The quiescence-anomaly area is located around the deeper edge of the asperity ruptured by the main shock, and the maximum Z value was estimated around +4.9 (Figure 2.4).

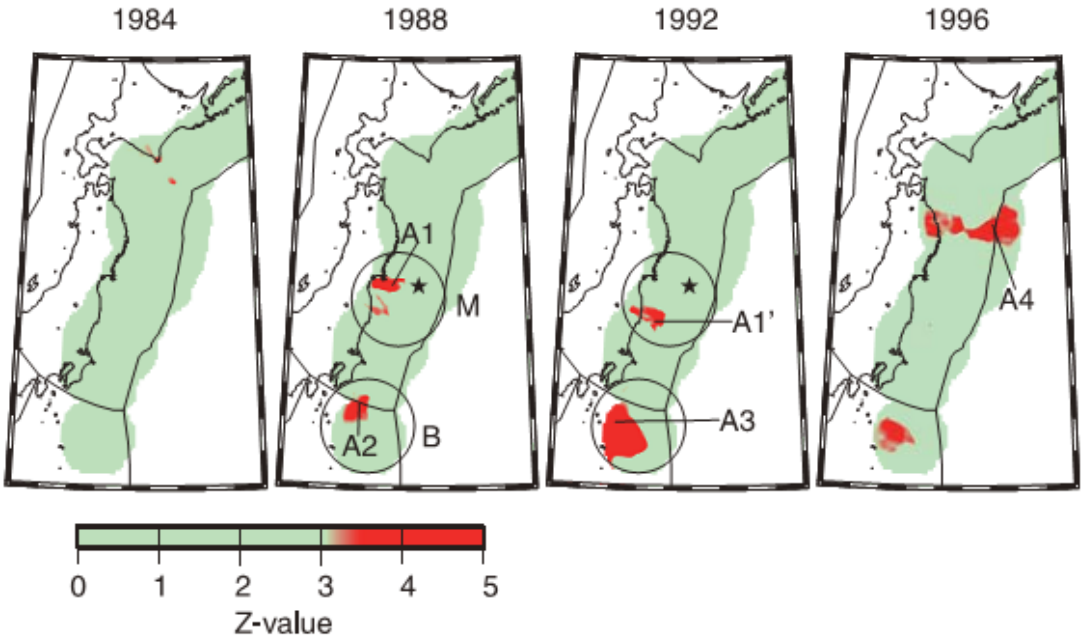

Figure 2.4. Maps of Japan showing Z value distribution at different time slide of interest, i.e., 1984-1996. The Z obtained here were estimated using the Japan Meteorological Agency (JMA) earthquake catalogue. A red color area (positive Z value) represents a decrease in the seismicity rate (Katsumata, 2011b). Black stars denote the epicenter of the Mw-9.0 Tohoku earthquake.

Sorbi et al. (2012) investigated the variations of seismicity rate changes prior to the September 10th, 2008 (Mw = 6.1) Qeshm earthquake, Southern Iran. Both temporal and spatial of Z values was investigated. Regarding to temporal investigation, the cumulative number and the Z value as a function of time illustrates a precursory seismic quiescence, i.e., Zmax = 3.0, preceding the 2008 Qeshm earthquake. The spatial distribution map of the standard deviation, Z, also exhibits an obvious precursory seismic quiescence region located in the vicinity of the epicenter of the Qeshm earthquake (Figure 2.5). Interestingly, the precursory seismic anomaly region is approximately consistent with the comparatively low b value anomaly region, implying the comparatively high of the seismotectonic stress accumulated in the region.

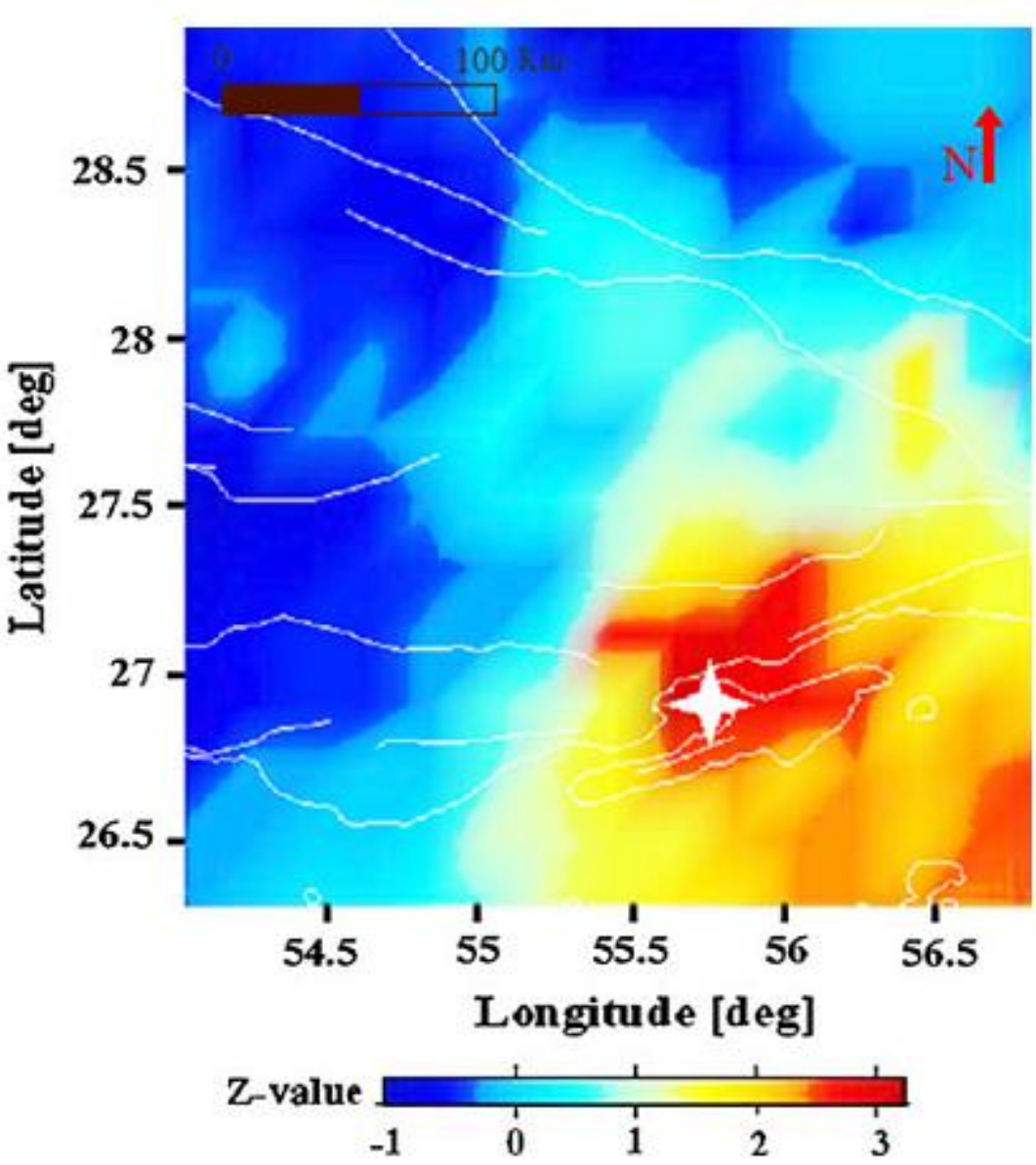

Figure 2.5. Map of Southern Iran showing the distribution of Z values. The white star marks the epicenter of the 2008 Qeshm main shock. Red color means positive Z value, that is, decrease in seismicity rate and blue color refer to increase at the seismicity rate (Sorbi et al., 2012).

2.2.2 RTL algorithm

Huang and Sobolev (2002) investigated the characteristics of the precursory seismicity change associated with the Mw = 6.8 Nemuro Peninsula earthquake posed on January 28th, 2000. The RTL parameters at the earthquake epicenter (Figure 2.6) indicated that a seismic quiescence started in 1995 and reached its minimum during October 1996. An activation stage with a duration of about eight months, followed (Figure 2.7).

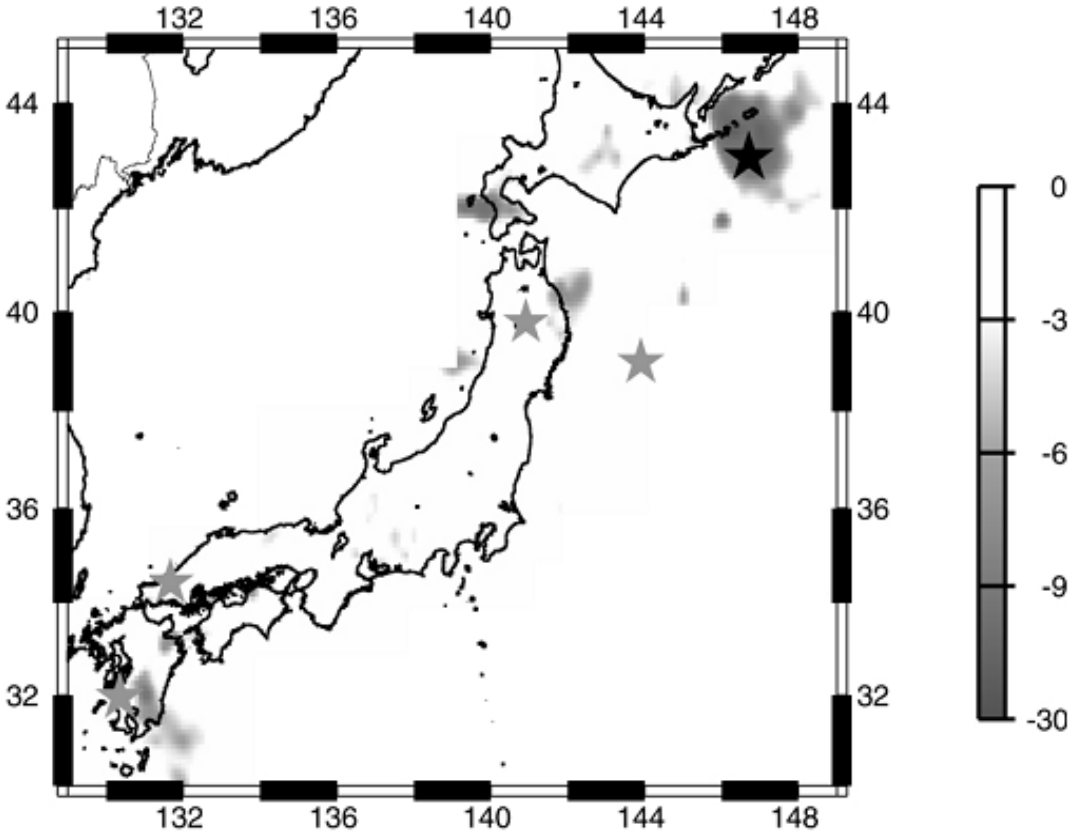

Figure 2.6. The spatial distribution of seismic quiescence in 1996. A significant seismic quiescence appeared three years before the Nemuro Peninsula earthquake. The scale on the right corresponds to the RTL value in units of standard deviation. The black star represents the epicenter of the Nemuro Peninsula earthquake (146.71E, 42.98N) (Huang and Sobolev, 2002).

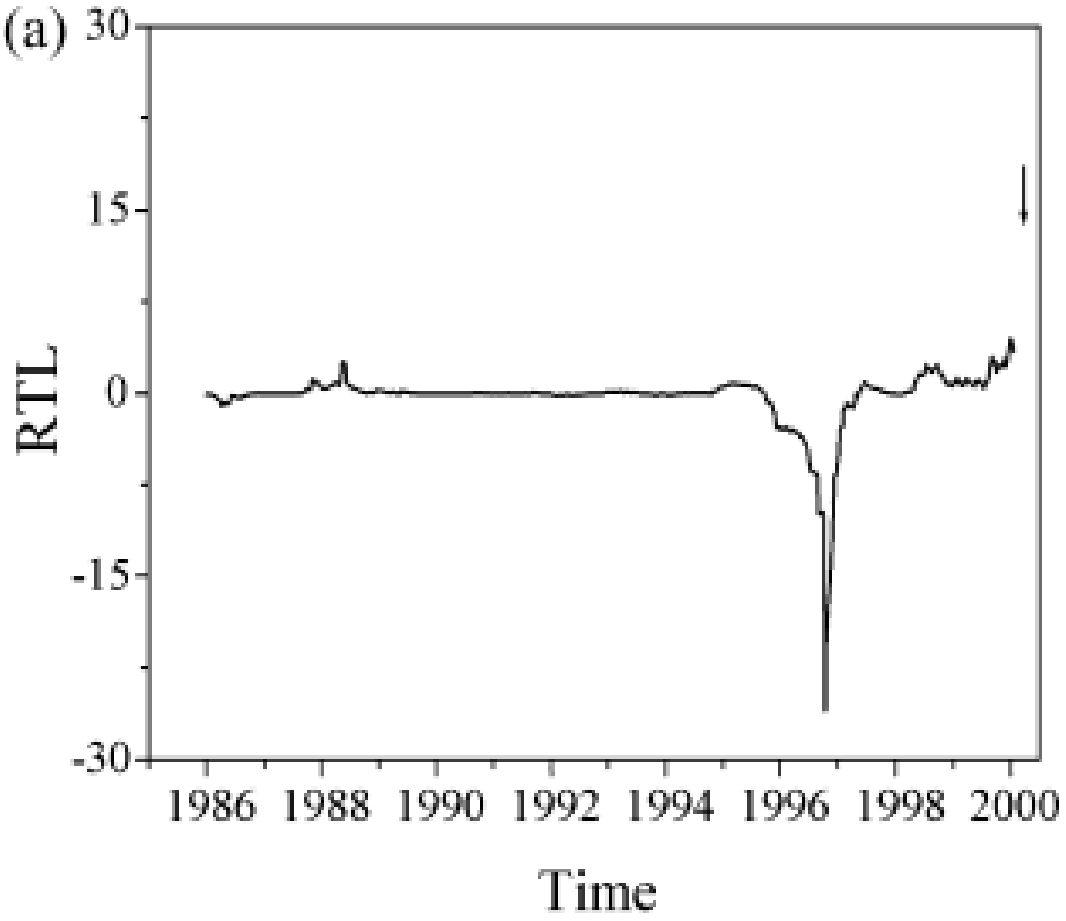

Figure 2.7. The temporal distribution of RTL score varies with time evaluated at the epicenter of the 2000 Nemuro Peninsula earthquake. A significant quiescence appeared in 1996, followed by an activation pattern. The arrow indicates the occurrence time of the main shock.

Jiang et al. (2004) applied retrospective examinations of RTL algorithm in North China and found that the anomalies obtained by the RTL algorithm show the short or intermediate-short term precursory features in most cases of some hazardous earthquake recognized (Figure 2.8).

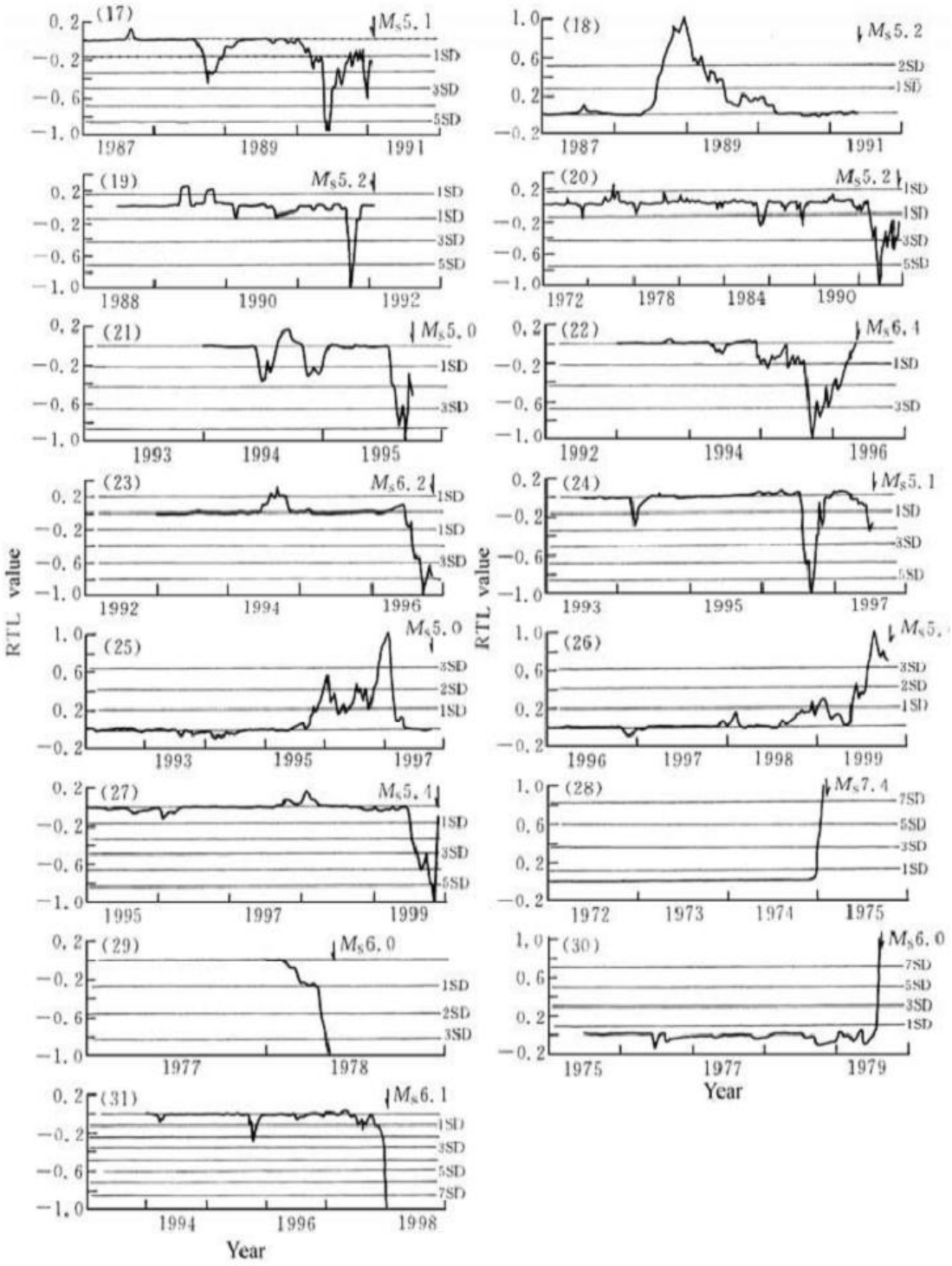

Figure 2.8. Temporal variation of VRTL curves before 15 events of the moderate or strong earthquakes in North China (Jiang et al., 2004).

Chen and Wu (2006) examined the precursory seismic activities occurred prior to the 1999, Mw = 7.6, Chi-Chi earthquake around its epicenter. Based on the calculation of the RTL values, the epicentral area has been found to strongly exhibit the signs of anomalous activity, associated with the seismic quiescence and activation, before the main shock (Figure 2.9).

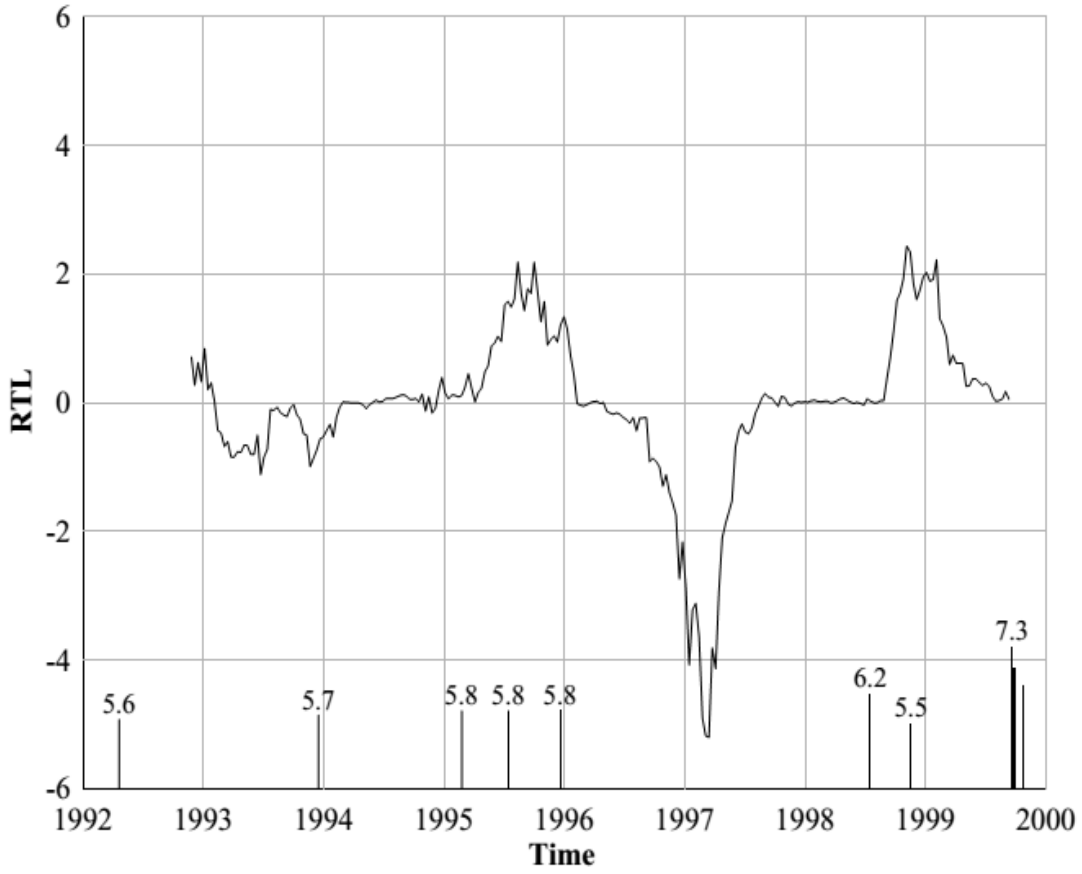

Figure 2.9. Temporal variation in the RTL function at the epicenter of the 1999 Chi-Chi earthquake. Seismic activation appeared around 1999 and seismic quiescence can be found around 1997 (Chen and Wu, 2006).

Shashidhar et al. (2010) investigated the seismicity patterns associated with the M~5 earthquakes in the artificial water reservoir triggered zone of the Koyna region situated near the west coast of India by means of the RTL algorithm. After careful

investigation, They found that epicentral area showed both of anomalous seismic activation and quiescence before the main earthquake posed (Figure 2.10).

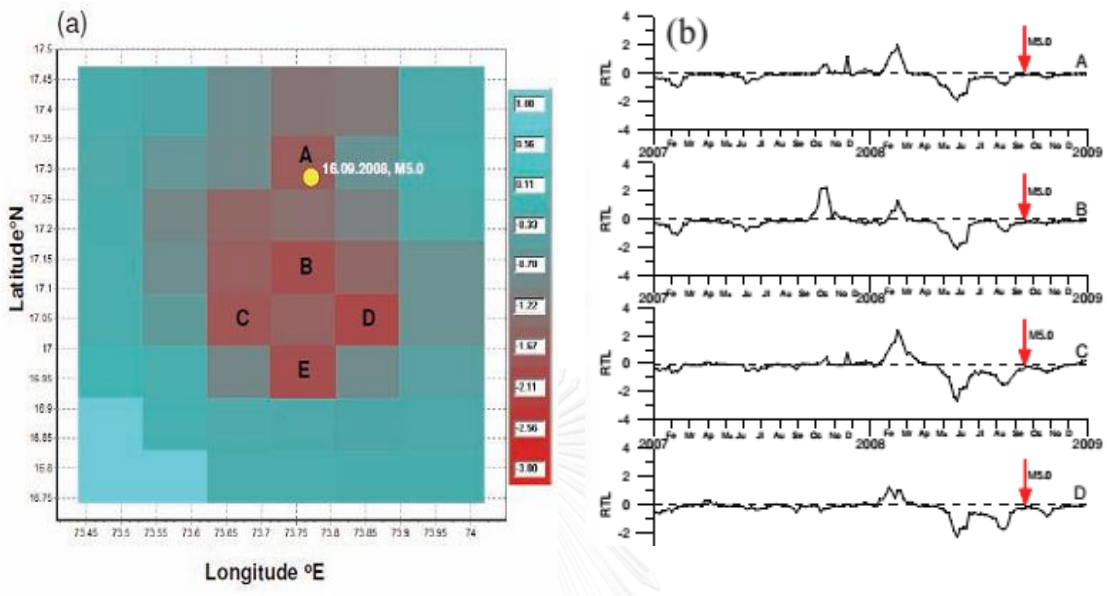

Figure 2.10. (a) Spatial variation of RTL score in the Koyna-Warna region during the observation period from 2007 to 2008. The scale on the right corresponds to the RTL value in the units of the standard deviation. (b) Temporal variation of RTL of the cells A, B, C, D shown in Figure.2.10a. The arrow indicates the occurrence time of the M 5.0 earthquake on 16 September 2008 (Shashidhar et al., 2010).

.

2.3 Methodology

In this study, the methodology for investigating both Z value and RTL algorithm are described consecutively as shown below (see also Figure 2.11).

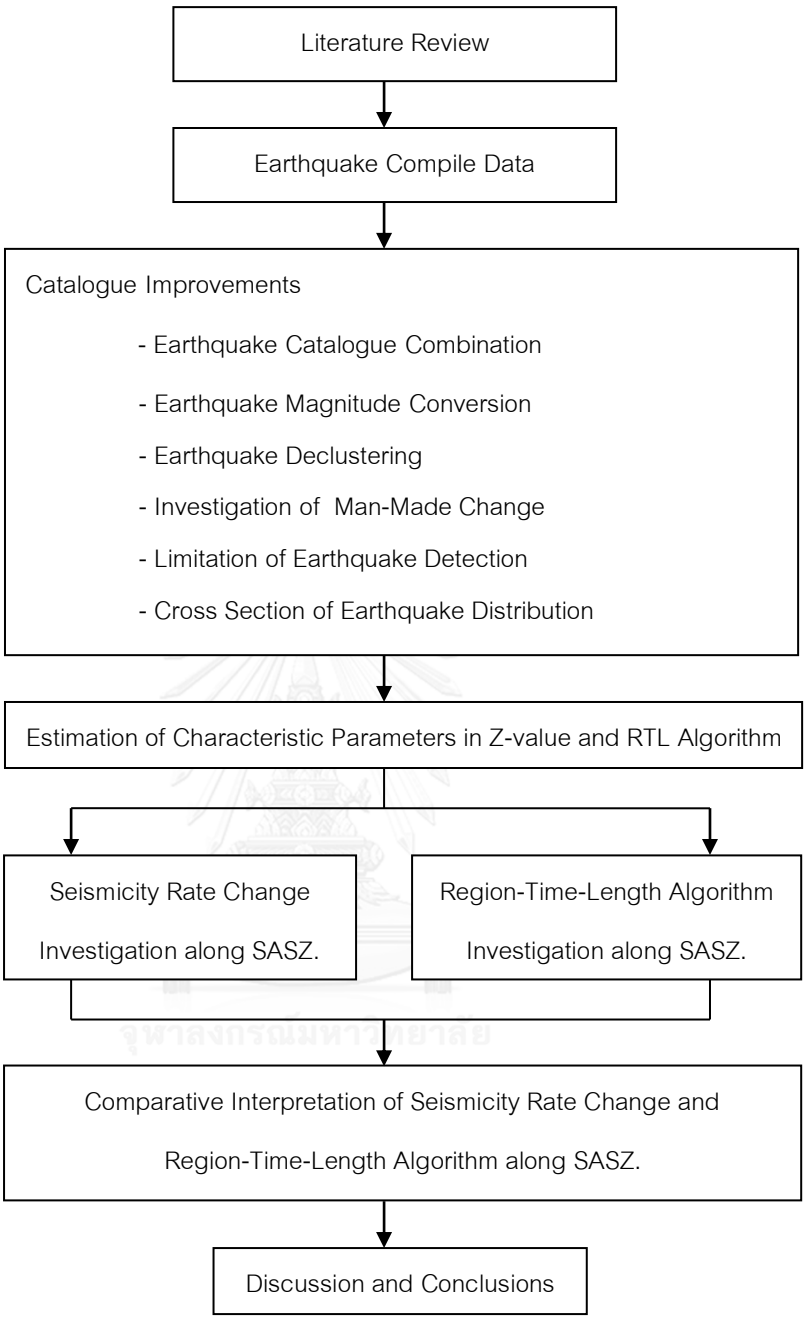

Figure 2.11. Simplified flow chart showing the methodology applied in this study.

2.3.1 Literature Review

Regarding to the section of literature review, the previous works, in particular for the theory aspect, were viewed. The main aim of this procedure is to summarize the methodology, including complying the variables, i.e., the number of earthquakes and the time window for Z investigation, and radius and time window for RTL investigation, used in various areas. The outcome obtained in this section is the guideline of using the variable useful for finding out the most suitable variable for the study area, i.e., SASZ.

2.3.2 Catalogue Improvement

In the past, the obtained original earthquake catalogues have been recorded non-systematically in practice, those data are, therefore, un-reliable and not available for evaluation of the seismic activities. As a result, before any evaluation of statistical seismology, the obtained earthquake catalogue must be improved. In this study, the improved methodology following Caceres and Kulhanek (2000) is applied as shown in Figure 2.11, and described in more detail in Chapter III.

2.3.3 Estimation of Characteristic Parameters in Z-value and RTL Algorithm

As mentioned above, both Z and RTL investigations need some variable suitable for any area of interest. Based on literature review, no guideline of previous work has been done successfully for the SASZ. Therefore, the variable of characteristic parameters should be analyzed which is the main aim of this study.

2.3.4 Seismicity Rate Change Investigation

According to the suitable characteristic parameters obtained from the previous section, the seismicity rate change, i.e., Z value, is analyzed using the most up-to-date data. The outcome obtained here is the maps showing Z anomalies implying the prospective areas of the upcoming earthquakes.

2.3.5 Region-Time-Length Algorithm Investigation

As similar as the section of seismicity rate change investigation, the RTL algorithm is also investigated simultaneously. According to the different assumption

between Z and RTL investigation, the result obtained in this section constrains the precision and accuracy of the prospective areas of the upcoming earthquakes

2.3.6 Comparative Interpretation of Rate Change and Region-Time-Length Algorithm

According to both Z and RTL investigations, the prospective area is interpreted and finally proposed in term of map showing distribution of the seismic anomalies implying the prospective areas might be posed by the forthcoming earthquake.

จุฬาลงกรณ์มหาวิทยาลัย
Chulalongkorn University

CHAPTER III
SEISMICITY DATA AND COMPLETENESS

Up to the present, it is worldwidely accepted that although the instrumental earthquake records cover a much shorter time period than paleo-seismological data, the instrumental earthquake records, i.e., earthquake catalogue, are a valuable result of fundamental seismological practice and they form the basis for seismicity, seismotectonic, seismic risk and hazard investigations. However, in practice, the existing earthquake catalogue is normally incomplete in terms of representing the seismotectonic activities of any time span and site specific of interest. This is because earthquake catalogs are produced by the recording of seismic waves in seismological networks that change in time and space with varying operational practices and procedures.

Therefore, in order to obtain reliable results from a statistical analysis, the critical issue to be addressed is to assess the quantity, quality, and consistency of those earthquake data. Consequently, the unified earthquake catalogue is needed. In this chapter, the seismicity data, i.e., earthquake catalogue, within the study area are clarified in order to improve the completeness of data meaningful for both Z and RTL investigation in the next chapter. The methodology for analyzing seismicity data is according to Caceres and Kulhanek (2000) as follows (see also Chapter 2 in Figure 2.11).

3.1 Earthquake Catalogue Combination

From earthquake catalogue investigation, some networks of instrumental earthquake recording stations, which recorded the present-day earthquakes covered the study area, have been developed. These include three global networks operated by the International Seismological Center (ISC), the National Earthquake Information Center (NEIC), and the Global Centroid Moment Tensor (GCMT) (Figure 3.1). The recorded earthquakes include location (longitude, latitude and depth), time (year, month, day,

hour, minute) and various kinds of magnitude are reported in these catalogues including the body wave magnitude (m_b), the surface wave magnitude (M_S), the moment magnitude (M_w) and some local magnitudes (M_L) (Table 3.1).

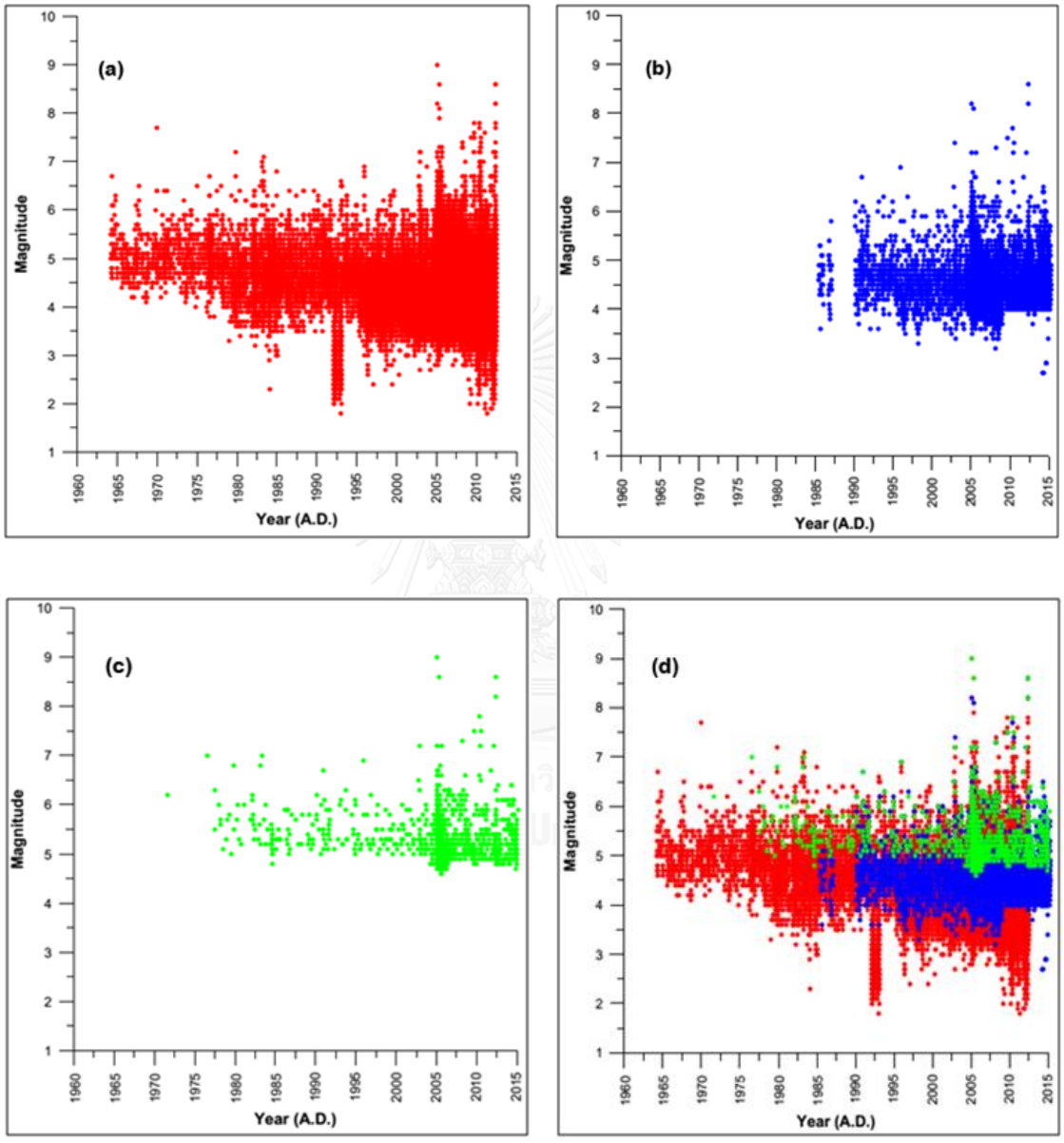

Figure 3.1. Relationships between the magnitude and date of earthquakes recorded in individual earthquake catalogues, (a) ISC (b) NEIC (c) GCMT, and (d) Composite.

Empirically, any earthquake catalogue is the result of seismological signals recorded on complex, spatially and temporally heterogeneous networks of seismometers, and processed using a variety of software, assumptions and also the judgments (Habermann, 1987; Habermann, 1991; Habermann and Creamer, 1994; Zuniga and Wiemer, 1999).

Table 3.1. Examples of earthquake catalogue.

Long	Lat	Year	Month	Day	Depth	Hour	Min	Sec	M_w	m_b	M_S	M_L
95.060	15.970	2010	5	22	0	23	7	22	-	3.6	-	3.8
95.140	5.520	2010	5	24	61	19	11	41	-	4.2	-	4.1
92.015	11.185	2010	5	25	0	0	51	55	-	4.3	3.7	3.9
94.250	11.850	2010	5	25	10	0	52	33	-	4.2	-	4.2
92.694	6.885	2010	5	25	0	9	4	32	-	3.4	-	-
92.847	13.684	2010	5	26	0	6	53	3	-	3.6	-	4.3
93.120	13.847	2010	5	26	0	19	39	41	-	3.4	-	3.2
93.534	11.529	2010	5	28	35	19	21	51	-	3.8	-	-
93.505	12.587	2010	5	28	101.7	19	22	3	-	3.3	-	4.0
92.645	11.681	2010	5	30	26	15	21	11	-	3.6	-	-
93.700	11.060	2010	5	31	122	19	51	48	6.4	6.2	-	6.7
92.994	15.958	2010	6	4	0	12	43	4	-	3.2	3.0	3.6
93.022	13.994	2010	6	4	41	16	24	5	-	3.5	-	-

จุฬาลงกรณ์มหาวิทยาลัย
Chulalongkorn University

The earthquake catalogues contributed by these different networks, therefore, have both advantages and disadvantages themselves in terms of the continuity, recording time span, and limit of the recordable magnitude range including the type of proposed magnitude scales of their records. The far-field global networks (i.e., ISC, NEIC, and GCMT) are recordable continuously with the large to medium size earthquakes over a long time span (see also Figure 3.1). In addition, in the magnitude scales, the GCMT catalogue records simultaneously the moment magnitude (M_w), surface wave magnitude (M_s), and body wave magnitude (m_b) for individual earthquake events whereas the rest catalogues record the earthquakes non-systematically in

different scales. The ISC and NEIC catalogues record variably the earthquake size in M_s, m_b, M_L, and M_w in the order of amount.

Statistically, the longer of earthquake recording time span, the wider detectable of the magnitude range including reliable recording magnitude scale cause the more accurate in the statistical analysis of seismic activity.

To improve the quantity and quality of earthquake data, combination a new earthquake catalogue is prepared. The earthquake catalogs are different in reported magnitude scales, period of availability and the number of the listed events (Table 3.2). All existing earthquake catalogues (i.e. ISC, NEIC, and GCMT) are merged in this study (See also Figure 3.1d).

Table 3.2. Parameters of catalogs used

Catalog	No. of events	Time period
ISC	59,815	1965-2012
NEIC	12,438	1985-2014
GCMT	1,330	1976-2014

As a result, the composite earthquake catalogue contains totally 73,583 number of data, ranging in M_w from 2.4 to 9.0 during the 50 year period from 1965–2014 in the study area (Figure 3.1d).

3.2 Earthquake Magnitude Conversion

After combining all earthquake data in the previous section, the new merged earthquake catalogue composed of the heterogeneous magnitude scales (including M_w, M_s, m_b, and M_L). In practically, it is noted that each scale is derived from a specific assumption and analytical method which have a valid but different value and unique meaning. The m_b analyzed is obtained from the first arrival P-wave from a seismogram and the M_s and M_L are from the surface wave and S-wave, respectively.

Based on Hanks and Kanamori (1979), M_w directly represents the physical properties of an earthquake source while the other scales may be affected by the "saturation phenomenon" particularly for large seismic moments (Figure 3.2) (Campbell, 1985). Therefore, in this study the different scales (i.e., $m_{b,}$ M_s, and M_L) were converted systematically to M_w in order to investigate the other qualities of the composite earthquake catalogue.

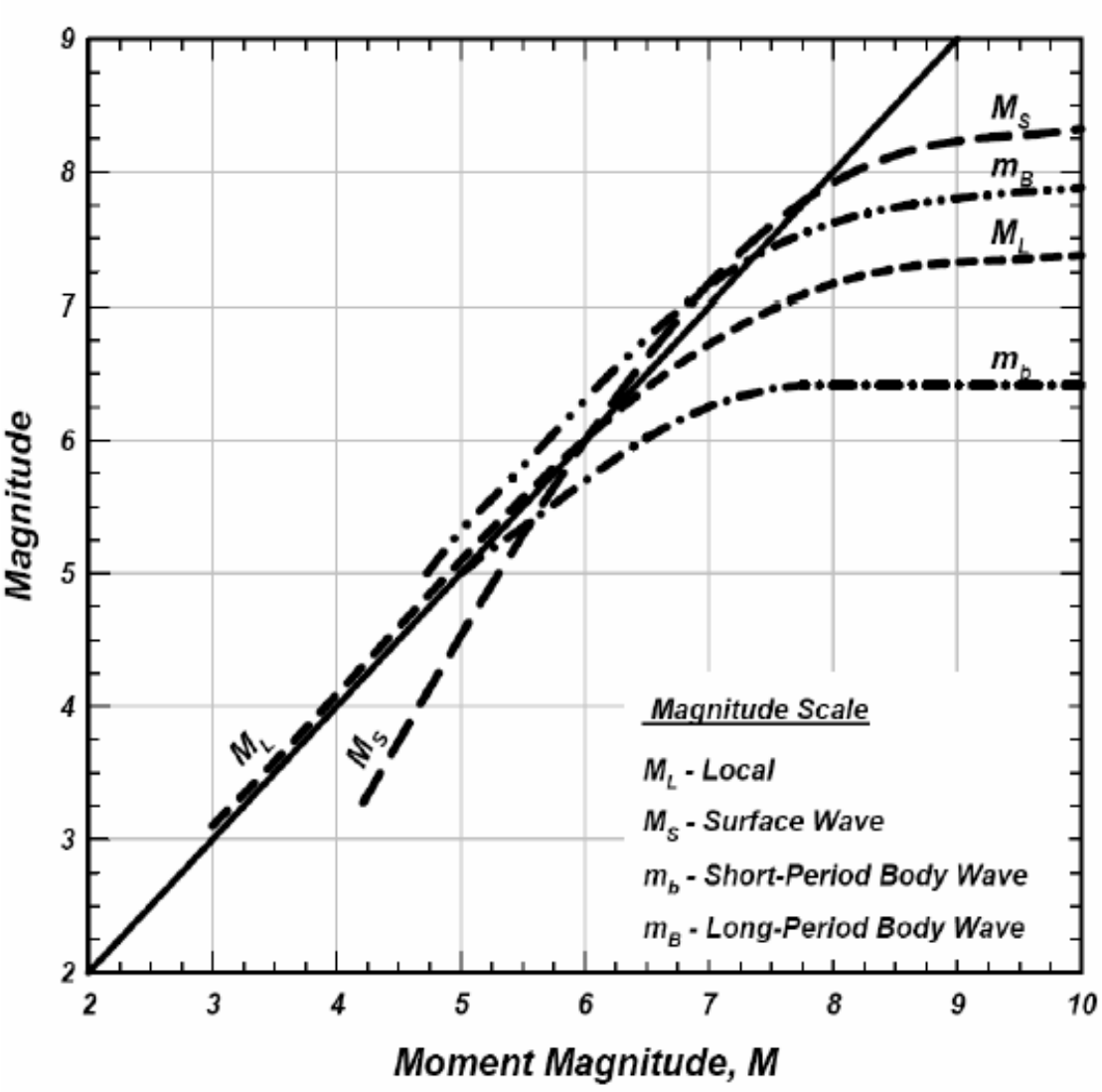

Figure 3.2. The graph shows the saturation of the various magnitude scales (Campbell, 1985).

At first, the earthquake data recorded in the study area are used to develop relationships between the different magnitude scales and thus converted the remains m_b, M_s, and M_L to the standard M_w. Based on those records that have reported simultaneously the different magnitude scales in the composite earthquake catalogue. These data are carefully used to calibrate the empirical relationships between these different scales are shown in Figure 3.3, along with the regression derived equation between each pair of different scales.

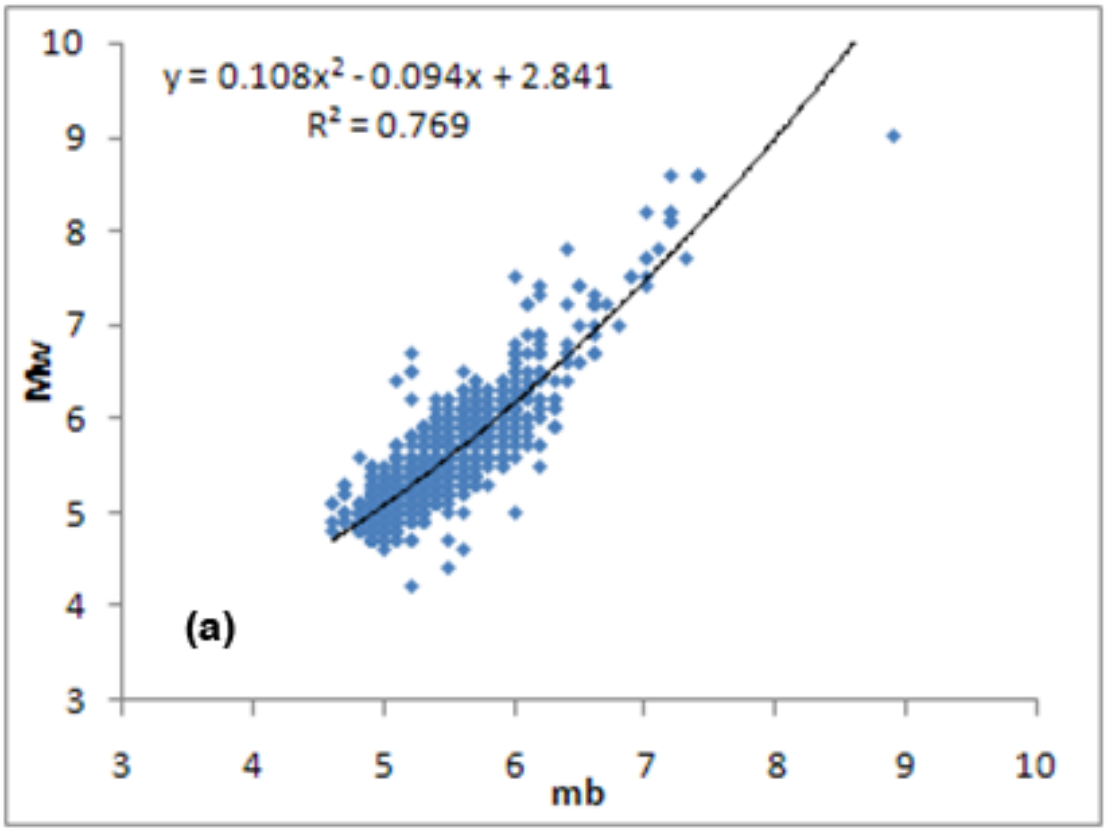

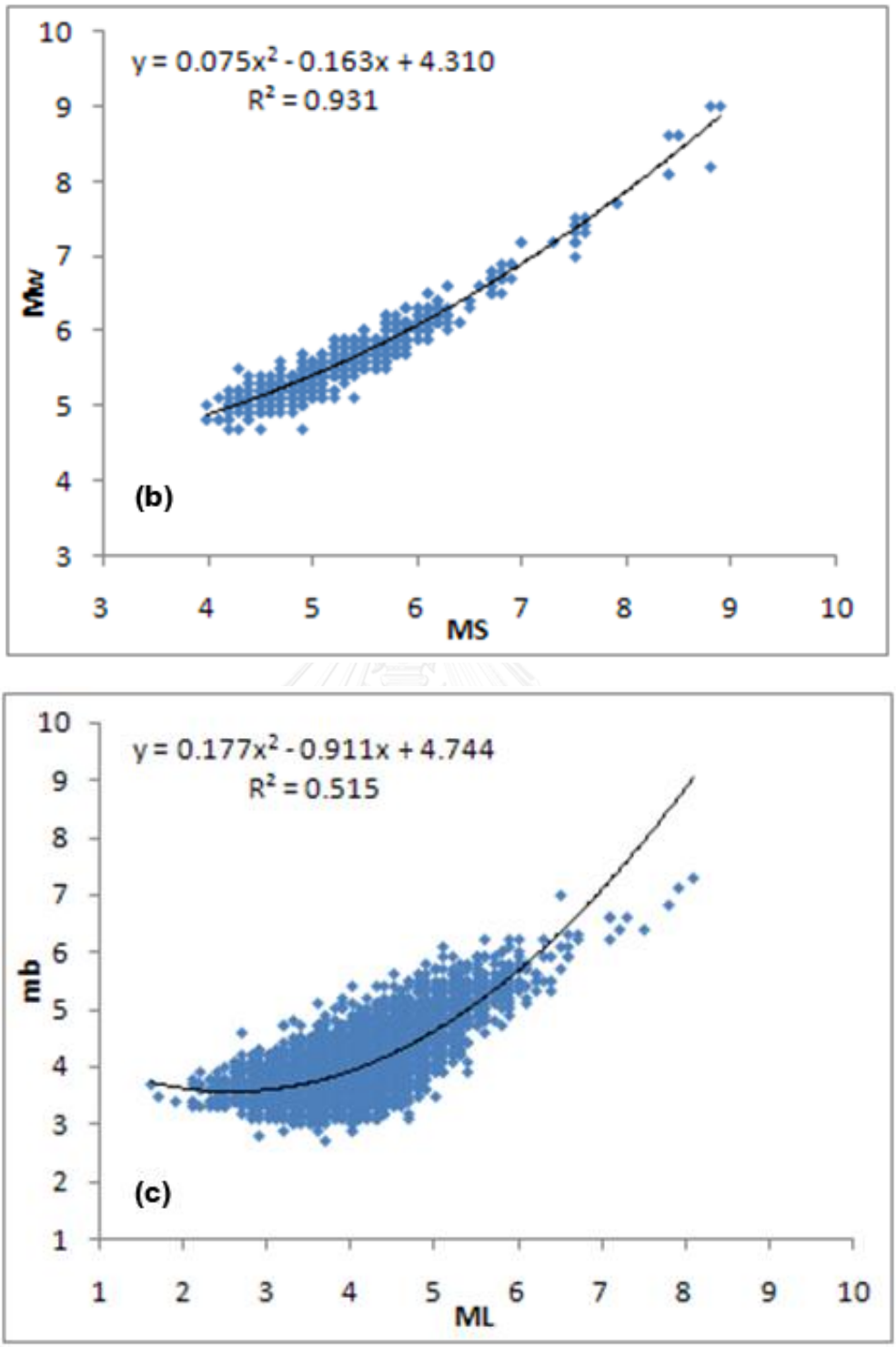

Figure 3.3. Empirical relationships between a) body wave magnitude (m_b) and moment magnitude (M_w), b) surface wave magnitude (M_s) and moment magnitude (M_w), and c) local magnitude (M_L) and body wave magnitude (m_b).

Due to the calibration curves as shown in Figure 3.3, the relationships of m_b and M_s to M_w are formulated as shown as equations 3.1 and 3.2. For M_L result, the empirical relationship between M_L and m_b (Equation 3.3) is applied in this study, and then re-convert m_b to M_w by using equation 3.1.

$$Mw = 0.108mb^2 - 0.094mb + 2.841 \quad ; mb \le 7.4 \qquad (3.1)$$

$$Mw = 0.075Ms^2 - 0.163Ms + 4.310 \quad ; Ms \le 8.9 \qquad (3.2)$$

$$mb = 0.177ML^2 - 0.911ML + 4.744 \quad ; ML \le 6.8 \qquad (3.3)$$

3.3 Earthquake Declustering

In nature, when any cluster of earthquakes occurs, the earthquake can classify temporally into 3 types; foreshock, main shock, and aftershock, relatively. Foreshocks are earthquakes which precede larger earthquakes in the same or nearby location, whereas aftershocks are smaller earthquakes which occur in the same general area during the days to years following a larger event or "main shock". Seismotectonically, the main shock refers directly to the released tectonic stress. Meanwhile, the foreshock and aftershock is a by-product according to the pre- and co-seismic stress change of the individual main shock (Felzer et al., 2004).

For instance, the time histogram and the cumulative number of earthquakes (Figure 3.4a) reveal a sudden increase in the seismicity from the end of 2004 after the M_w-9.0 Sumatra-Andaman earthquake was posed. This ensured the impaction of the aftershock sequences of the M_w-9.0 event and if not corrected, it would introduce bias into investigations in any related seismotectonic activities.

Therefore, before further seismotectonic investigation, the earthquake data obtained from the previous procedures need to be de-clustered by filtering main shocks from foreshocks and aftershocks in order to obtain a complete independent earthquake (i.e., only main shock) distribution.

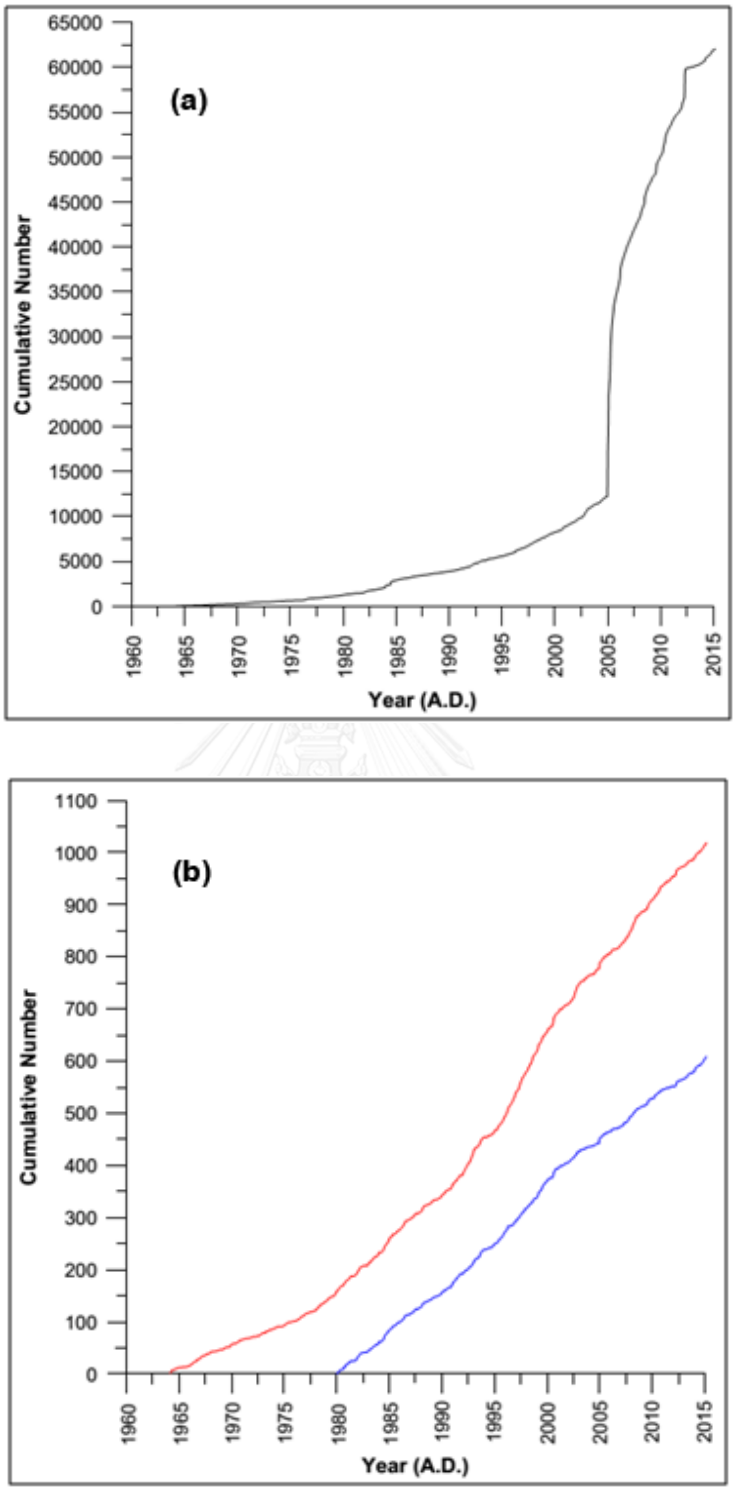

Figure 3.4. The cumulative number of earthquakes as a function of time for a) Non-declustered catalogue b) Declustered catalog, the red and blue lines indicate the incompleteness and completeness of the catalogue, respectively.

In the earthquake declustering, the empirical model proposed by Gardner and Knopoff (1974) is applied in this study similar to Petersen et al. (2004) who declustered the earthquake data in the Sumatra-Andaman subduction zone region. Windowing algorithms for cluster identification make use of a space and time windows around and following each event, whether it is a cluster event or not. Any earthquake occurring within the window is deemed a cluster event. The extension in time and in space of the window depends on the magnitude of the earthquake. The window is opened wider for stronger predecessor events (above the red lines in Figure 3.5).

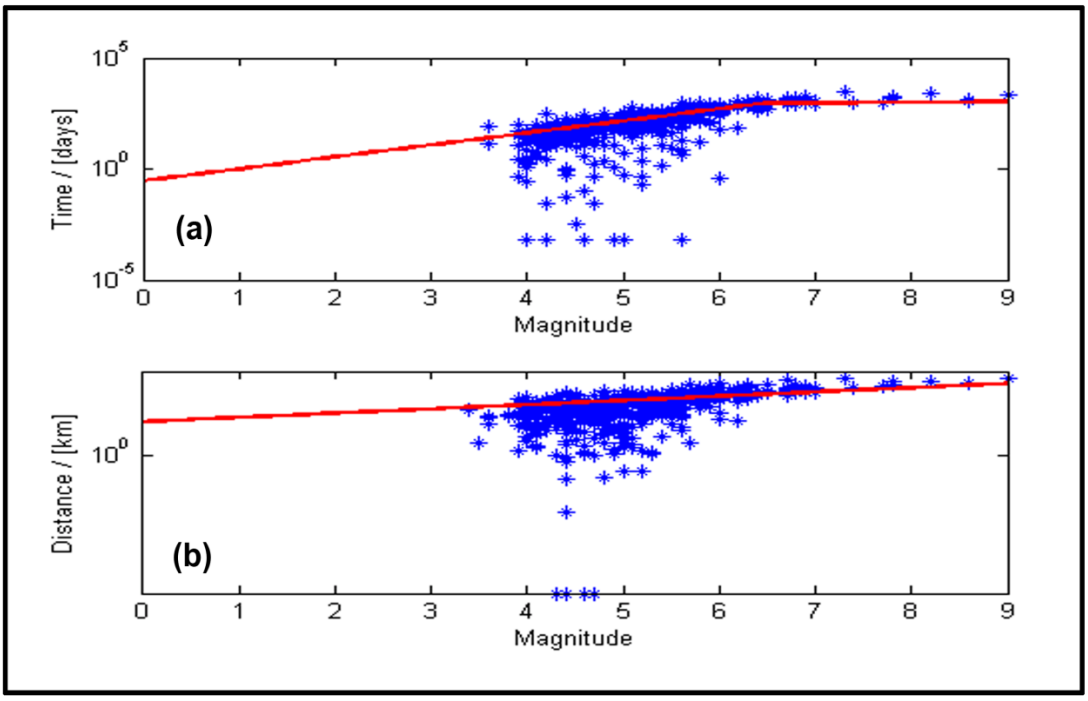

Figure 3.5. The parameters used to decluster and remove foreshocks and aftershocks according to the model of Gardner and Knopoff (1974). (a) time window and (b) space window. The earthquakes (blue stars) above the red lines of both time and space windows are identified as main-shock events.

According to the assumption of Gardner and Knopoff (1974) and as implemented in the ZMAP program (Wiemer, 2001). The declustering process distinguished 729 clusters from 73,583 earthquake events. Of these events, a total of

72,564 events (98%) was classified as foreshocks or aftershocks and, therefore, were eliminated. As a result, 1,019 main shock events, representing the seismotectonic activities were defined (Figure 3.6). The cumulative number of earthquakes after declustering did not show sudden increases, as shown by the red line in Figure 3.4b, and so this declustered subset of 1,019 main shock events was then used in all further analysis here (Figure 3.6).

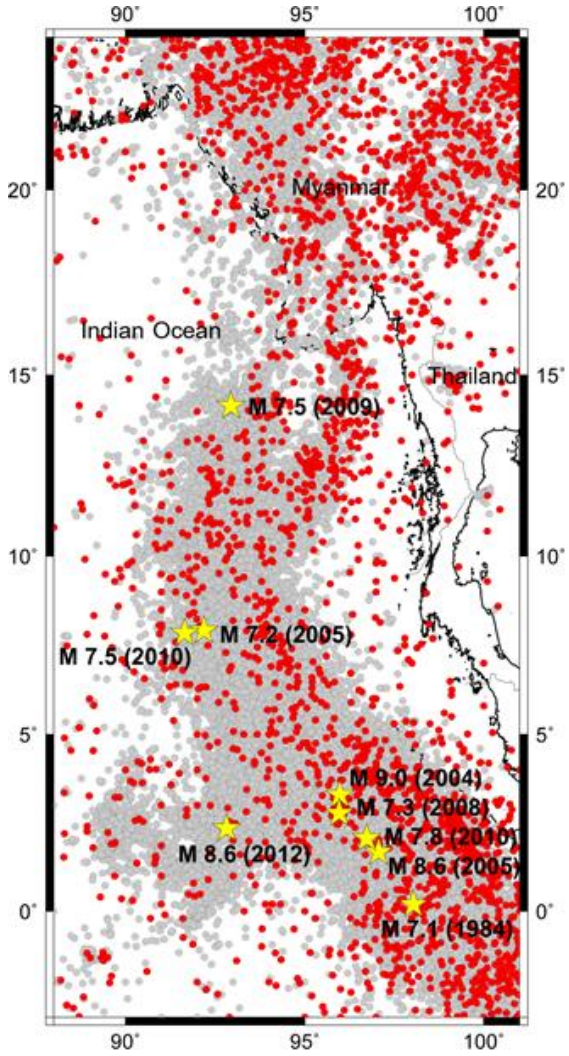

Figure 3.6. Map of Sumatra-Andaman Subduction Zone showing the epicentral distributions of earthquakes before (gray circles) and after (red circles) declustering with the algorithm according to Gardner and Knopoff (1974).

3.4 Man-Made Change Seismicity

Empirically, the apparent earthquake catalogue is normally contaminated by the varying operational procedures. As a result, biases and heterogeneity in the rate of reporting different magnitude earthquakes are present, which may distort the earthquake catalogue (Habermann and Wyss, 1984; Wyss, 1991; Zuniga et al., 2005). To avoid these artifacts in the reporting procedure, the statistical method called GENAS algorithm (Habermann, 1987; Habermann and Wyss, 1984) was employed in this study. Based on GENAS algorithm as implemented in ZMAP (Wiemer, 2001), the seismicity rate changes for a certain point in time for different magnitude bands are tested for difference by calculating the Z value (equation (2.1)).

Regarding to Figure 3.7, on the left side in the plot are the results for the magnitude bands “smaller than”plotted. The right side shows the results for the magnitude bands “greater than”. For each magnitude band and for each time point, GENAS calculates Z and determines its significance. If a value is significant, a marker is plotted. A circle stands for a negative Z-value, a cross for a positive z-value. The more significant the rate change, the larger the marker. If a rate change at a certain time appears in most of the magnitude bands “smaller than”, i.e., when the markers form a horizontal line starting at the left side, and in some of the magnitude bands “greater than”, i.e., the horizontal marker line from the left part of the figure is continued into the right part of the figure, it can be assumed that “something” has happened at that time.

Figure 3.7 shows the output of the GENAS algorithm as the times of significant rate changes. There are obvious rate changes in the reported events that can be identified, increases with $M_w < 4.5$ in 1977 and some minor changes in the earthquake records with a $M_w < 4.0$ throughout the 1990-2000. This does not coincide with any of the network expansion or upgrading events, implying no artificial-change impacted upon the composite catalogue with $M_w \geq 4.0$ throughout the 1980–2014 period, as shown in the red square of Figure 3.7, are deemed to be effective.

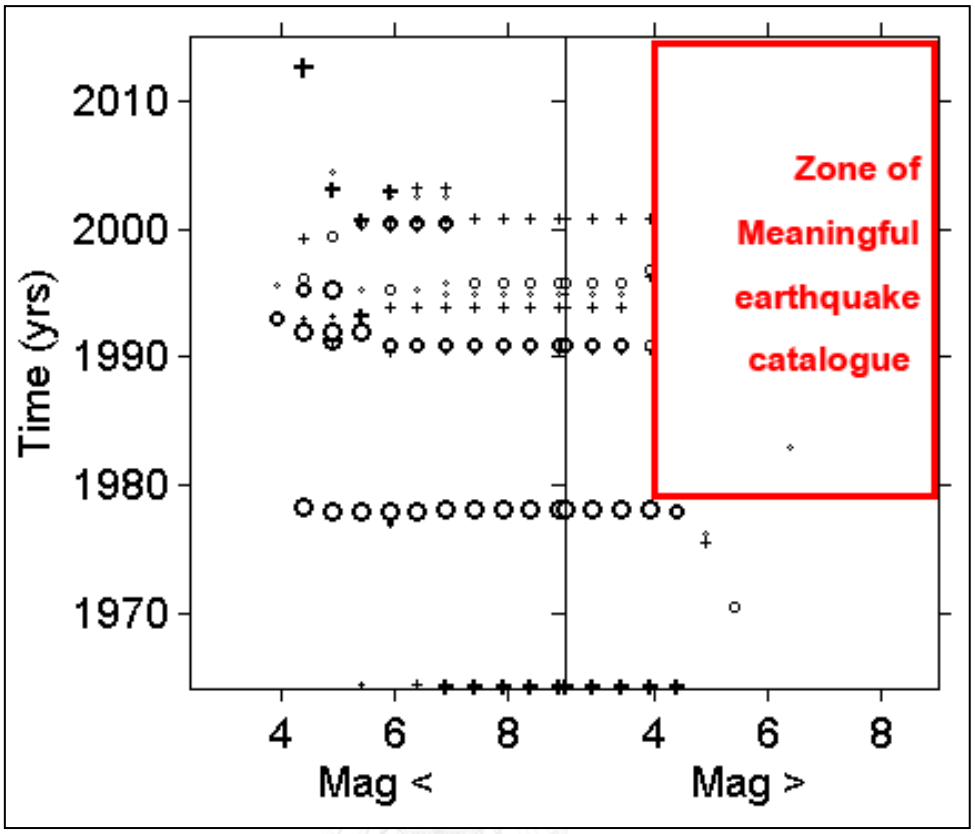

Figure 3.7. Rate changes as a function of time found by GENAS for the composite catalogue. The larger the markers, the larger the absolute z-value for the seismicity rate change at that time, and the more significant the change. Circles stand for increases in seismicity rates (negative z-values), crosses stand for decreases in seismicity rates (positive z-values). The left hand side of plot show the changes in seismicity rates for magnitudes “smaller than” and the right hand side displays them for magnitudes “greater than”.

3.5 Limitation of Earthquake Detection

Theoretically, in order to evaluate the location, time and magnitude of individual earthquake, the range of an earthquake signal must cover an area with at least four seismic recording stations. However, in practice, it lies in the nature of earthquake reporting that small earthquakes are more difficult to detect. Signals of small earthquakes do not travel far. The energy is quickly lost and the signal recorded by stations at a certain distance is weak. As a result, for every seismic recording network,

there exists a level above which all earthquakes that occur in the region, i.e. 100%, are actually reported. This limit is called the magnitude of completeness, Mc, which indicates the smallest magnitude earthquake that can be detected reliably by the existent seismic recording stations across that time period and so forms a complete record in both space and time (Rydelek and Sacks, 1989; Taylor et al., 1990; Wiemer and Wyss, 2000). For a certain space and time, a simple power-law can approximate the frequency-magnitude distribution (FMD). The FMD describes the relationship between the frequency of occurrence and the magnitude of earthquakes, as expressed in equation (3.4) (Gutenberg and Richter, 1944; Ishimoto and K., 1939);

$$\text{Log}(N) = a - bM, \tag{3.4}$$

where N is the cumulative number of earthquakes having magnitudes larger than M, and a and b are constants.

As shown in Figure 3.8, the FMD follows a straight line on a log-normal-diagram for the magnitude range in which all earthquakes are reported. Below a certain magnitude, the line flattens. For magnitudes smaller than the start of the curvature, not all earthquakes are reported. This point of flexing is Mc. Below Mc, the reporting homogeneity often varies and produces seismicity rate changes that are not of a natural origin. Cutting the earthquake catalog at the highest Mc in the whole data set rules out any seismicity rate changes introduced by changes in the network and in its ability to detect earthquakes. If an earthquake catalogue is cut at Mc, the incompletely reported earthquakes are simply ignored.

Therefore, in this study the Mc was estimated according to the Entire Magnitude Range method (EMR) (Woessner and Wiemer, 2005). Figure 3.8 illustrates the FMD plot, from which a is 5.13 and b is 0.512 ± 0.02. By the EMR method, the estimated Mc for the bulk data was found to be approximately 4.4 M_w that represents the level of the complete report.

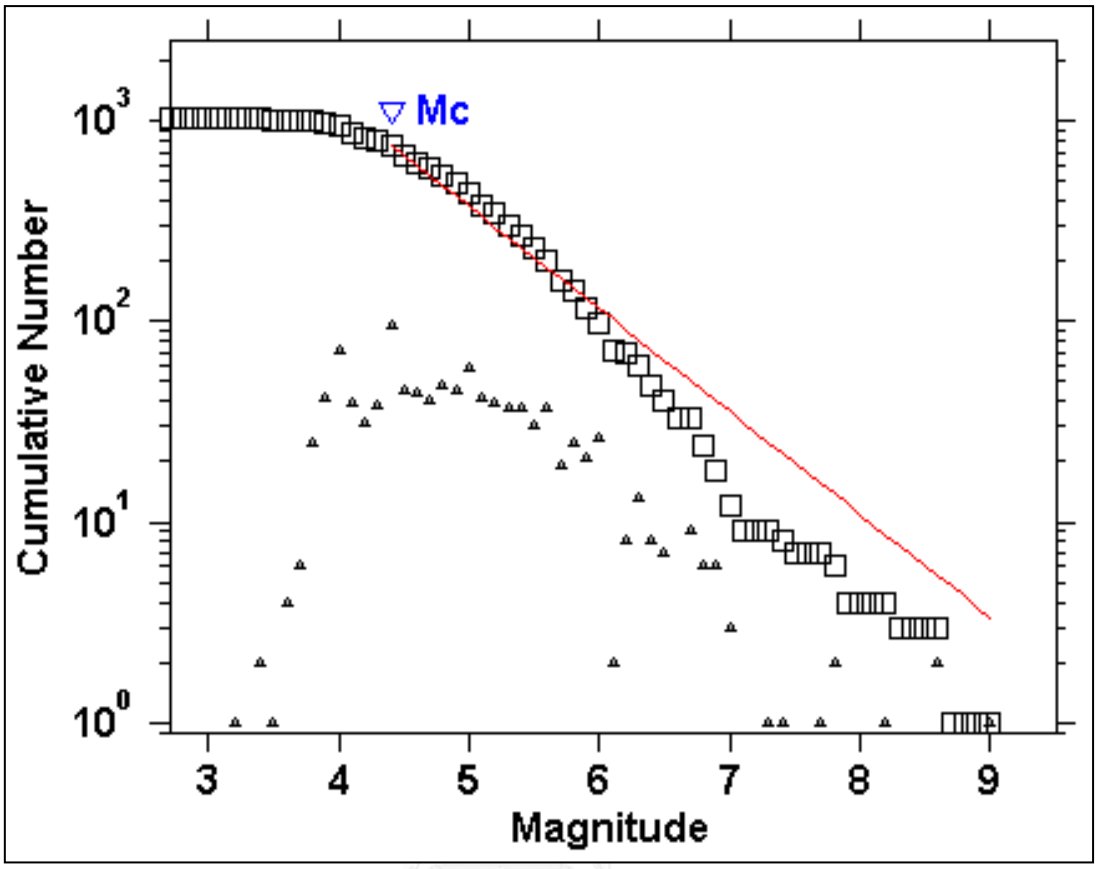

Figure 3.8. The FMD plot of the seismicity data recorded $M_w \geq 4.4$ during 1980-2014. Triangles indicate the number of earthquakes of each magnitude; squares represent the cumulative number of earthquakes equal to or larger than each magnitude. The solid line is the line of best fit according to Woessner and Wiemer (2005). Mc is defined as the magnitude of completeness.

3.6 Cross Section of Earthquake Distribution

Seismotectonically, the earthquakes' distribution, in particular for this subduction zone earthquake of the SASZ, was occupied by the two different seismotectonic settings, i.e., i) shallow crustal and ii) deep intraslab earthquakes. In order to separate the dataset according to these two seismotectonic regimes, three lines of cross-section were established perpendicular the strike of SASZ, as shown in Figure 3.9a. The earthquake distributions in each cross-section point of view illustrated clearly that the Indo-Australian plate is subducting underneath the Eurasian plate (Figure 3.9a-c).

Crustal earthquakes were generated in the depth range of 0–45 km while the slab dips northwards with a dip angle of about 40–45°. Therefore, in order to focus only the interplate and intraplate earthquake that might generate the tsunami hazard, the completeness earthquake data were separated into shallow crustal earthquakes with a focal depth range between 0–45 km, meanwhile the deep intraslab earthquakes from the slab down to 200 km underneath the Eurasian plate were excluded (Figure 3.9).

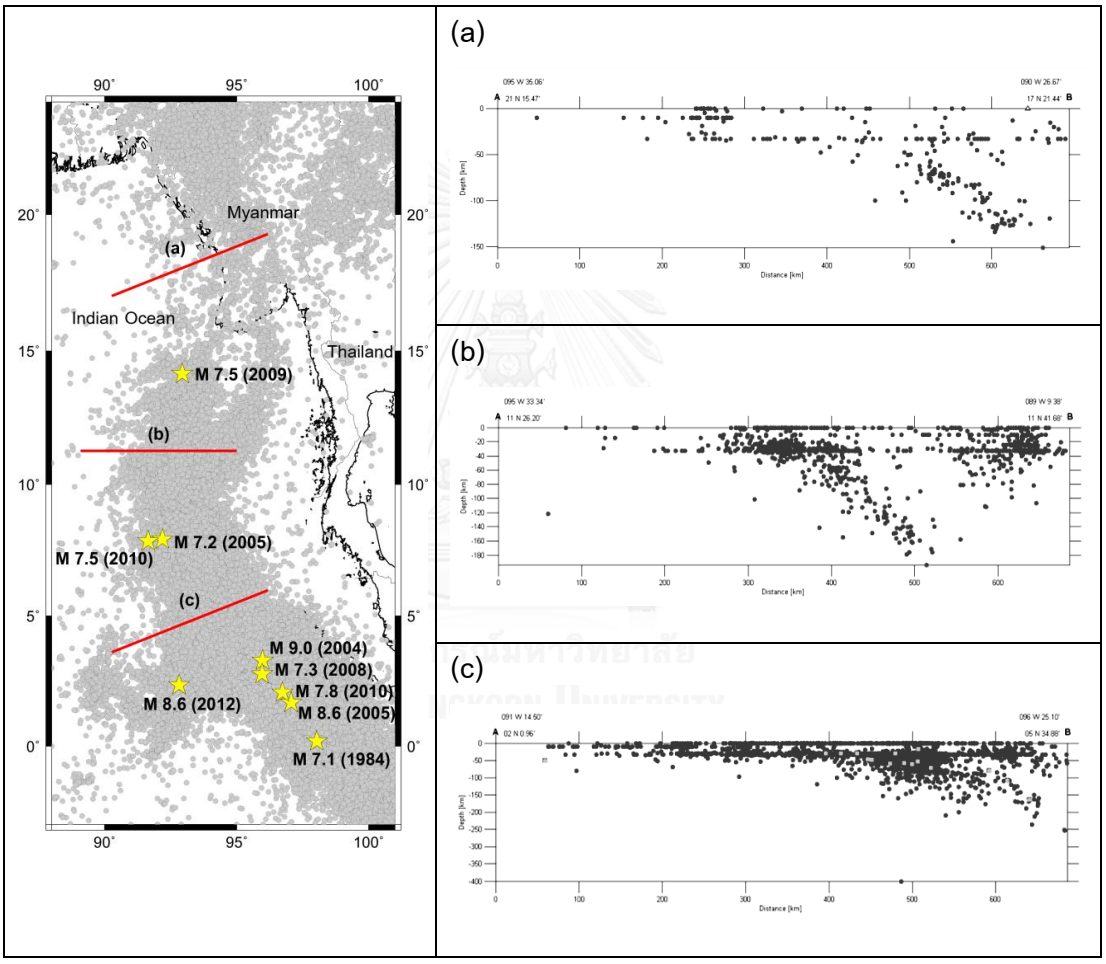

Figure 3.9. (a) Map of the SASZ showing cross section line of earthquake distribution as shown in Figures a-c.

CHAPTER IV
SEISMICITY RATE CHANGE INVESTIGATION

Practically in order to investigate the Z value, the N numbers of earthquake data, closest to any site of interest, were selected and plot the cumulative number of earthquake versus time. Thereafter, the Z value was estimated temporally by moving a short time window, T, moved step by step forward through the time series of considered earthquake data. The factors of both N and T are therefore variable depending on the specific time and region of interest.

Therefore, after synthesizing the completeness of the utilized earthquake data, the obtained earthquake catalogue was used, in this chapter, to test retrospectively in both spatial and temporal aspects using the seismicity rate changes (Z-value). To satisfy this, the seismic precursors were investigated before the occurrences of 8 major earthquakes ($M_w \geq 7.0$) which occurred along the SASZ (88–100°E and 2°S–24°N) (Table 4.1). In an individual earthquake case study listed in Table 1, the factor N was varied between 50 and 200 events with a 25 events interval, whereas T was investigated from 1 and 15 year with a 0.5-year stepping time window. Thus, in each case study, totally 210 (7 x 30) conditions of pair factors were tested iteratively.

Chulalongkorn University

Table 4.1. Case study of major earthquakes, i.e., $M_w \geq 7$, used for the retrospective test.

Case	Year	Month	Date	Origin time H Min Sec	Latitude (°)	Longitude (°)	Depth (km)	M_w
1	2004	12	26	00 58 53	1.75	95.60	30	9.0
2	2005	3	28	16 10 31	1.67	97.07	26	8.6
3	2005	7	24	15 42 06	7.92	92.19	16	7.2
4	2008	2	20	08 08 30	2.76	95.96	26	7.3
5	2009	8	10	19 56 05	14.16	92.94	22	7.5
6	2010	4	6	22 15 18	2.07	96.74	18	7.8
7	2010	6	12	19 26 59	7.85	91.65	33	7.5
8	2012	4	11	08 39 31	2.35	92.82	45	8.6

4.1 Temporal Investigation

In each condition of free parameters, the Z values were evaluated temporally in steps of 0.04 years (~14 days) through the time series starting at the available completeness data, i.e., 1980 and ending at the occurrence time of each earthquake considered. After iterative tests, it is revealed that if take N = 50 events and T= 2 year, all 8 earthquake case studies were preceded by the seismic quiescence. Figure 4.1 illustrates histograms of cumulative number of earthquakes and Z values calculated at individual 8 epicenters which the major earthquake is generated. The maximum of Z is in the range of 6.7-7.0 imply that the anomalous quiescence obtained in this study is obvious (see also Table 4.2). The explanations of temporal variation can be described as follows;

Table 4.2. List of large earthquake ($M_w \geq 7.0$) calculated by using Z parameter N = 50 and T_w = 2. The parameters Zmax, Ts, and Duration indicate a maximum of Z values at the epicenter of the earthquake, starting time of seismic quiescence, and the duration between the starting time of seismic quiescence and the occurrence time of main shock, respectively.

Case	Sample Size, N	Window Length, T_w (years)	Zmax	Start Date, Ts	Duration (years)
1	50	2	7.0	1999.68	5.3
2	50	2	6.9	1999.68	5.6
3	50	2	6.7	2001.48	4.1
4	50	2	6.8	2005.24	2.9
5	50	2	6.8	2002.44	7.2
6	50	2	6.9	2005.24	5.0
7	50	2	6.8	2008.31	2.1
8	50	2	6.9	2005.01	7.3

i) In Figure 4.1a, before the December 26, 2004 M_w-9.0 earthquake (the Sumatra-Andaman earthquake), the calculated Zmax = 7.0 was found in 1999.68 at latitude 1.75°N longitude 95.60°E (around the epicenter of the earthquake). This value of the maximum Z represents directly the anomalous decreasing of the seismicity rate. The time span between the mentioned quiescence and the corresponding earthquake occurred are around 5.3.

ii) Quite similar to Figure 4.1a, the temporal variation of Z as shown in Figure 4.1b revealed the prominent Zmax = 6.9 in 1999.68. After that around 4 years later, the M_w-8.6 earthquake posed at the same location at latitude 1.75°N longitude 95.60°E on March 28, 2005. As this event occurred after the 2004 Sumatra-Andaman earthquake about 3 months and 163 km away from the epicenter, the anomaly of decreasing of the seismicity rate was detected at the same time and in the same area before both major earthquakes occurred (see also Figures 4.1a and b).

iii) Regarding to Figure 4.1c, there is only one prominent time span from 2001.48 to 2002.59 showing the anomalously high Z, i.e., Zmax = 6.7. After that around 4.1 years after the end of high Z mentioned, the earthquake with M_w 7.2 was posed in July 24, 2005 in the vicinity of the mentioned anomalies, i.e., at the latitude 8.50°N longitude 92.35°E.

iv) According to Figures 4.1d and 4.1e, before the February 20, 2008 M_w-7.3 earthquake and the August 10, 2009 M_w-7.5 earthquake, the Zmax = 6.8 was found far away from the epicenter about 155 km posed in 2005.24 and 383 km posed in 2002.44, respectively. These represent the anomalies of decreasing of the seismicity rate before the major earthquakes occurred about 2.9 and 7.2 years near the epicenter of the earthquakes.

v) Based on Figure 4.1f, before the April 6, 2010 M_w-7.8 earthquake, the Zmax = 6.9 was found at latitude 1.75°N longitude 97.26°E far away from the epicenter about 68 km posed in 2005.24. This represents the anomaly of decreasing of the seismicity rate before the major earthquake occurred about 5 years near the epicenter of the

earthquake and also related to the constant or a flat cumulative number of earthquakes (blue line in Figure 4.1f).

vi) Regarding to Figure 4.1g, before the June 12, 2010 M_w-7.5 earthquake, the Zmax = 6.8 was found at latitude 9.50°N longitude 92.25°E far away from the epicenter about 195 km posed in 2008.31. This represents the anomaly of decreasing of the seismicity rate before the major earthquake occurred about 2.1 years near the epicenter of the earthquake. In addition, the Zmax = 6.8 was found in 2002.44 and followed the 2005 M_w-7.2 earthquake indicate the anomaly of decreasing of the seismicity rate before the major earthquake occurred about 3.1 years.

vii) Different from the other case studies described above, there are 2 anomalies of the comparatively high Z that can be detected in the Figure 4.1h. The Zmax is estimated around 6.9 in the 1982.15 to 1983.76 and 2005.01 (see Table 4.1h). After that at the same location of latitude 4.50°N longitude 92.01°E the earthquake with magnitude 8.6 M_w were posed on April 11, 2012. Regarding to the queiscence of 1982.15, the previous researches mentioned that this is normally caused by the initial improvement of the seismic recording network leading to the incompleteness of earthquake catalogue. This may result in high Z value during that period. Regarding to the last quiescence mentioned in 2005.01, there is no evidence of any man-made change of seismicity. Therefore, the time span between the quiescence and the occurrence time of the following earthquake is estimated around 7.3 years.

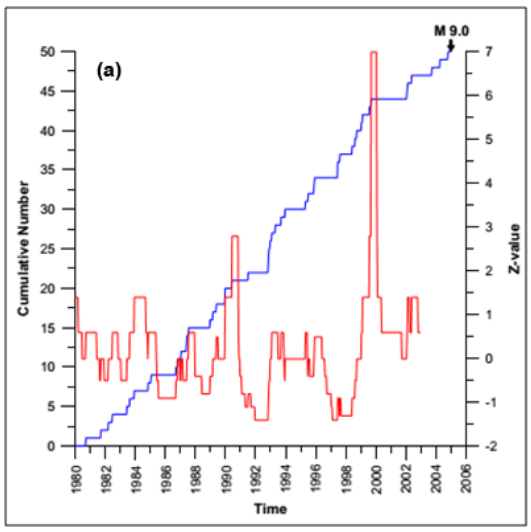

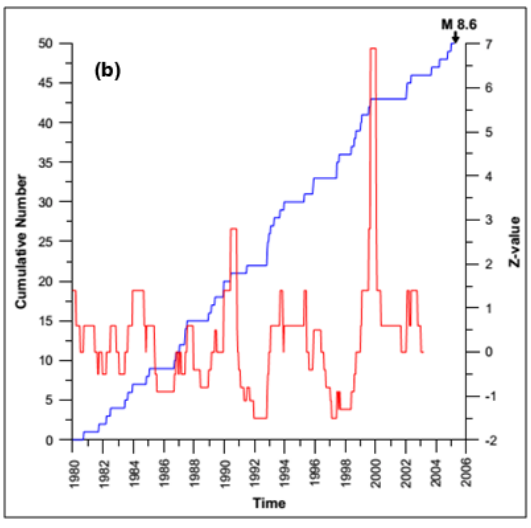

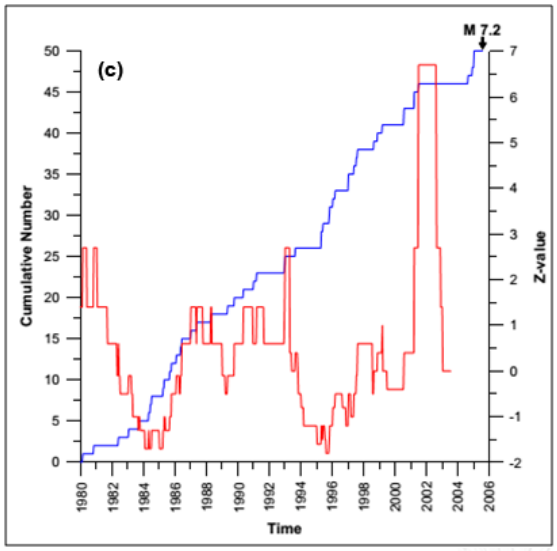
(c)
M 7.2
Cumulative Number
Z-value
Time

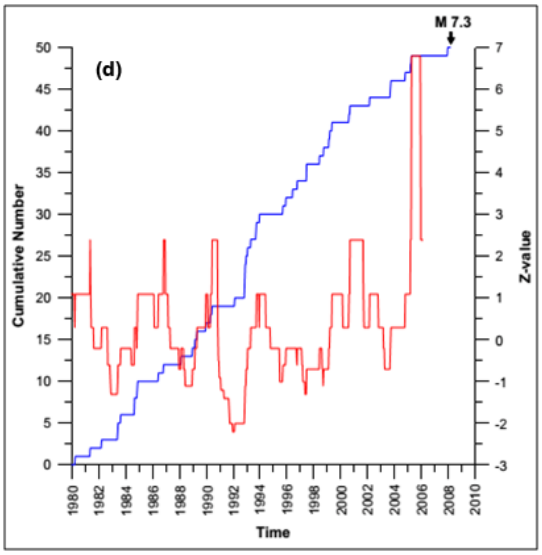
(d)
M 7.3
Cumulative Number
Z-value
Time

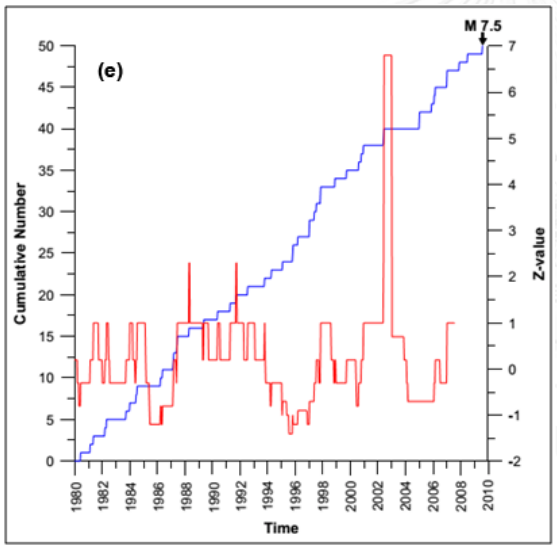
(e)
M 7.5
Cumulative Number
Z-value
Time

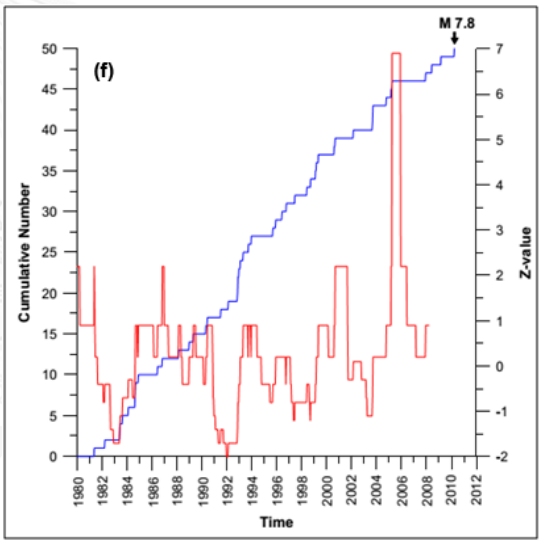
(f)
M 7.8
Cumulative Number
Z-value
Time

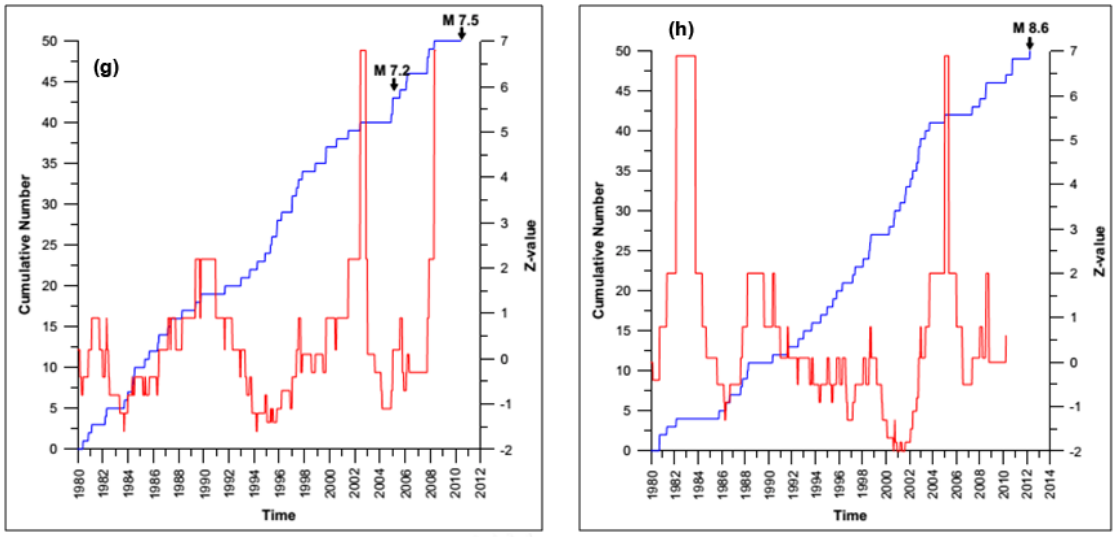

Figure 4.1. Cumulative number of earthquake (blue line) and Z value (red line) plot versus time interval of the (a) December 26, 2004 M_w-9.0 earthquake (95.6˚E, 1.75˚N), (b) March 28, 2005 M_w-8.6 earthquake (95.6˚E, 1.75˚N), (c) July 24, 2005 M_w-7.2 earthquake (92.35˚E, 8.5˚N), (d) February 20, 2008 M_w-7.3 earthquake (97.26˚E, 2.25˚N), (e) August 10, 2009 M_w-7.5 earthquake (91.51˚E, 11˚N), (f) April 6, 2010 M_w-7.8 earthquake (97.26˚E, 1.75˚N), (g) June 12, 2010 M_w-7.5 earthquake (92.26˚E, 9.5˚N), (h) April 11, 2012 M_w-8.6 earthquake (92.01˚E, 4.5˚N).

จุฬาลงกรณ์มหาวิทยาลัย
Chulalongkorn University

4.2 Spatial Investigation

In order to constrain the potential of the Z value for detecting the earthquake precursor along the SASZ, this work applied also spatial investigation to investigate the upcoming major earthquake in this area. At first, the study areas were divided by a grid from latitude 2°S- 24°N and longitude 88-100°E, with an interval of 0.25˚ gridded spacing. Thus, the total number of nodes is 4,992. In each grid node, a circle is drawn around by radius (r) that it was increased until it includes a total of earthquake number (N) = 50 events. However, in this study the limit of radius r = 250 km was fixed. The radius more than 250 km will be cut-off because this area lack of the seismicity data, for preventing the meaningless anomaly.

Afterward, the cumulative number of earthquakes event versus time is plotted for every grid node the same as what have been done previously in temporal investigation, starting at a time t_0 (January 1, 1980) and ending at a time t_e (before the occurrence time of considered earthquake case study). A time window is placed, starting at T_s and ending at $T_s + T_w$, where $t_0 \leq T_s \leq T_s + T_w \leq t_e$. T_w value of 2 years is used here, and T_s is moved forward in steps period of 0.04 years (~14 days). Then, in each interval position the Z value is calculated, generating the Long Time Average (LTA) function defined by Wiemer and Wyss (1994), which measures the significance of the difference between the mean seismicity rate and the background rate which is defined in the equation (2.1). As the number of effective grid nodes is 4,992 for each time slice, and since there are more than 900 time slices, the total number of effective grid nodes, where Z value was calculated, are more than 4,555,200.

According to the temporal variation of Z in the individual grid node, the Z value of every node was selected systematically at the time span mentioned in Figure 4.1. Thereafter, the obtained series of Z values were then contoured and mapped as shown in Figure 4.2. As shown in Figure 4.2, the Z value in each time slice indicates the spatial distribution of the seismicity rate of each case study of the major earthquakes. Positive and negative Z values represent that the seismicity rate is lower, and higher, than the mean rate, respectively. Seismically, the positive of Z value represents the decreasing of earthquake in the study area (seismic quiescence). The results of spatial investigation at the starting time of seismicity quiescence indicated as follows (see also Figure 4.2);

i) For instance, in Figures 4.2a and 4.2b, these Z value maps show the obvious area of quiescence after 1999.68, near the epicenter of the Mw-9.0 and Mw-8.6 earthquakes posed in 2004 and 2005, with Z value ranged between +6.4 and +7.0, respectively, cover latitude 1.25-4.5^{o}N longitude 95.35-96.6^{o}E (red areas). After that around 5.3 and 5.6 year, the earthquakes of M_w 9.0 and 8.6 mentioned above posed, respectively.

ii) In addition, in Figure 4.2c, the comparative high Z value, i.e., between +6.2 and +6.9 , defined in 2001.48 at off coast between Nicobar and Aceh cities is quite

conform to the epicenter of the M_w-7.2 earthquake posed 4.1 years later in July 4th, 2005 (Figure 4c).

iii) According to Figure 4.2d and 4.2f, this quiescence of the west coast of Sumatra Island were grouped into the same quiescence because the two quiescences are located very close and they start almost simultaneously. Thereafter, the quiescence mentioned was also followed by the major earthquakes with M_w 6.8 and 6.9, respectively.

iv) As noticeable in Figures 4.2e, another seismic quiescence was posed in the Nicobar Islands, since 2002.44-2005.24. Four years later, the earthquake with M_w 7.5 posed in August 10th, 2009.

v) Regarding to Figure 4.2g, before the June 12, 2010 M_w-7.5 earthquake, Z value between +5.6 and +6.7 was found cover the latitude 8.75–11.25^{o}N longitude 92.01-94.01^{o}E in 2008.31. This represents the anomaly of decreasing of seismicity rate cover far away from the epicenter about 182 km before the major earthquake occurred about 2.1 years.

vi) Although Figure 4.2h shows sparsely the quiescence distribution, the following earthquake with 8.6 M_w posed a in April 11th, 2012 (Figure 4.2h).

Therefore, it appears that by using N = 50 events and T = 2 years, results and methodology in this study enabled to map the anomalous high Z implying the seismic quiescence with a reasonable accuracy, the precursory seismicity patterns associated with the impending earthquake might generated along the SASZ.

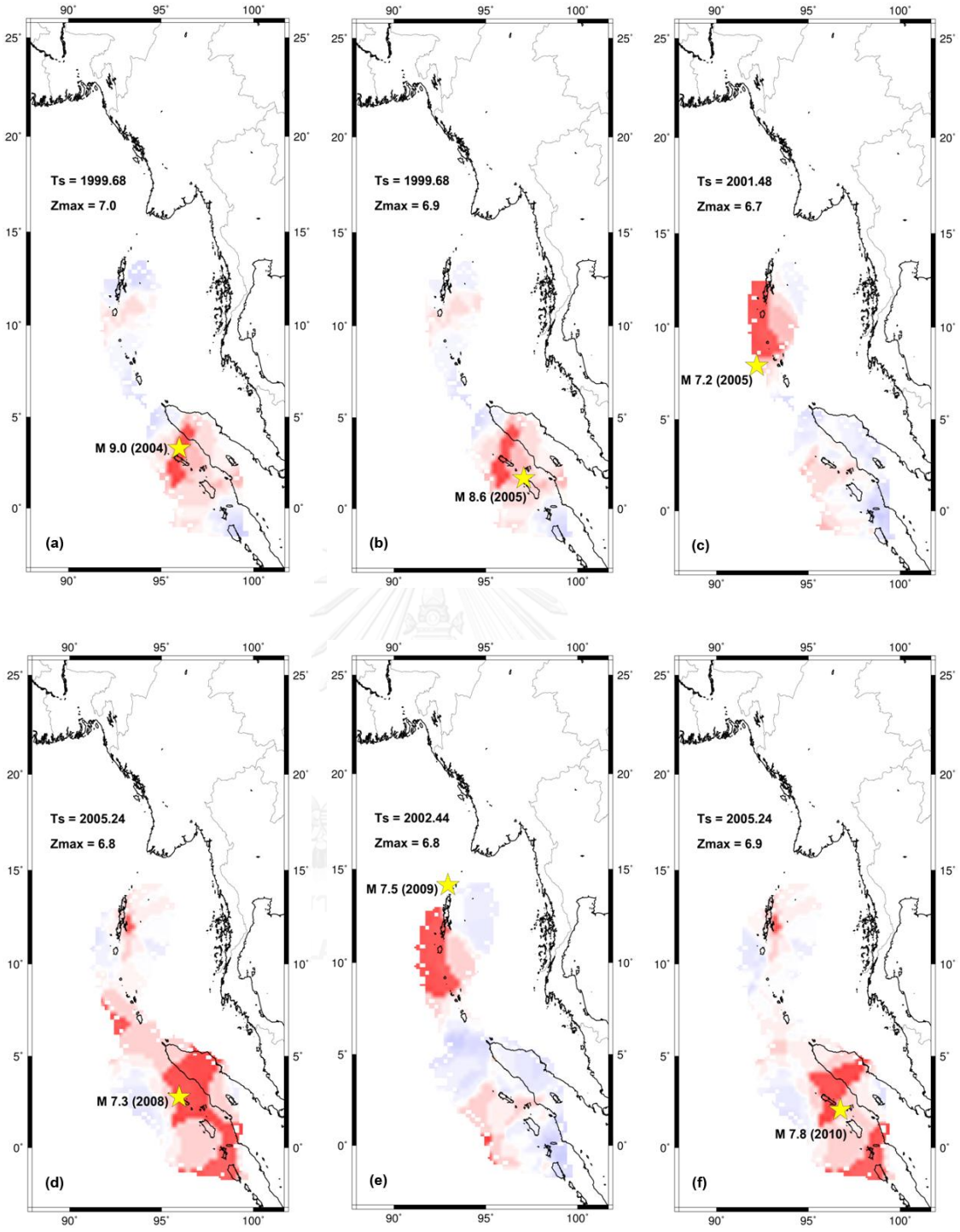
Ts = 1999.68
Zmax = 7.0
M 9.0 (2004)
(a)
Ts = 1999.68
Zmax = 6.9
M 8.6 (2005)
(b)
Ts = 2001.48
Zmax = 6.7
M 7.2 (2005)
(c)
Ts = 2005.24
Zmax = 6.8
M 7.3 (2008)
(d)
Ts = 2002.44
Zmax = 6.8
M 7.5 (2009)
(e)
Ts = 2005.24
Zmax = 6.9
M 7.8 (2010)
(f)
90°
95°
100°
25°
20°
15°
10°
5°
0°

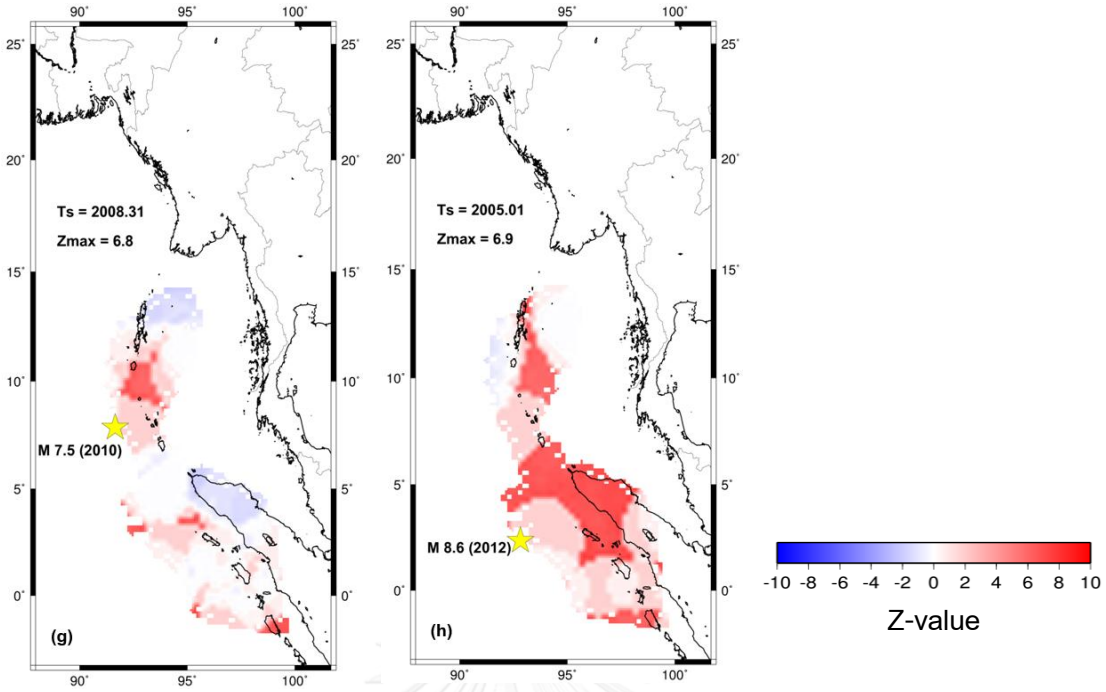

Figure 4.2. Map showing spatial distribution of Z values, at the starting time of quiescence of the (a) December 26, 2004 M_w-9.0 earthquake (95.6˚E, 1.75˚N), (b) March 28, 2005 M_w-8.6 earthquake (95.6˚E, 1.75˚N), (c) July 24, 2005 M_w-7.2 earthquake (92.35˚E, 8.5˚N), (d) February 20, 2008 M_w-7.3 earthquake (97.26˚E, 2.25˚N), (e) August 10, 2009 M_w-7.5 earthquake (91.51˚E, 11˚N), (f) April 6, 2010 M_w-7.8 earthquake (97.26˚E, 1.75˚N), (g) June 12, 2010 M_w-7.5 earthquake (92.26˚E, 9.5˚N), (h) April 11, 2012 M_w-8.6 earthquake (92.01˚E, 4.5˚N). The anomalous zone is indicated as shaded area and the epicenter is shown as yellow star.

4.3 Present-day Seismic Quiescence

Beside retrospective test constraining the possibility of earthquake forecasting with Z value, the investigations of the present-day seismic quiescence are also the main aim of this study. By using the suitable factors of N = 50 event and T = 2 year, spatial distributions of Z values were evaluated for every 14 days during 1980-2014. Based on 144 time slice of Z map, 1 specific areas showing anomalous Z can be defined by the maximum of Z = 6.5, i.e., Nicobar Islands (Figures 4.3).

For instance in the Nicobar Islands, the Z value peaked with 6.5 at 2007.89-2014.99 (Figures 4.3). Thus, it can be observed that the duration of quiescence is 5 years.

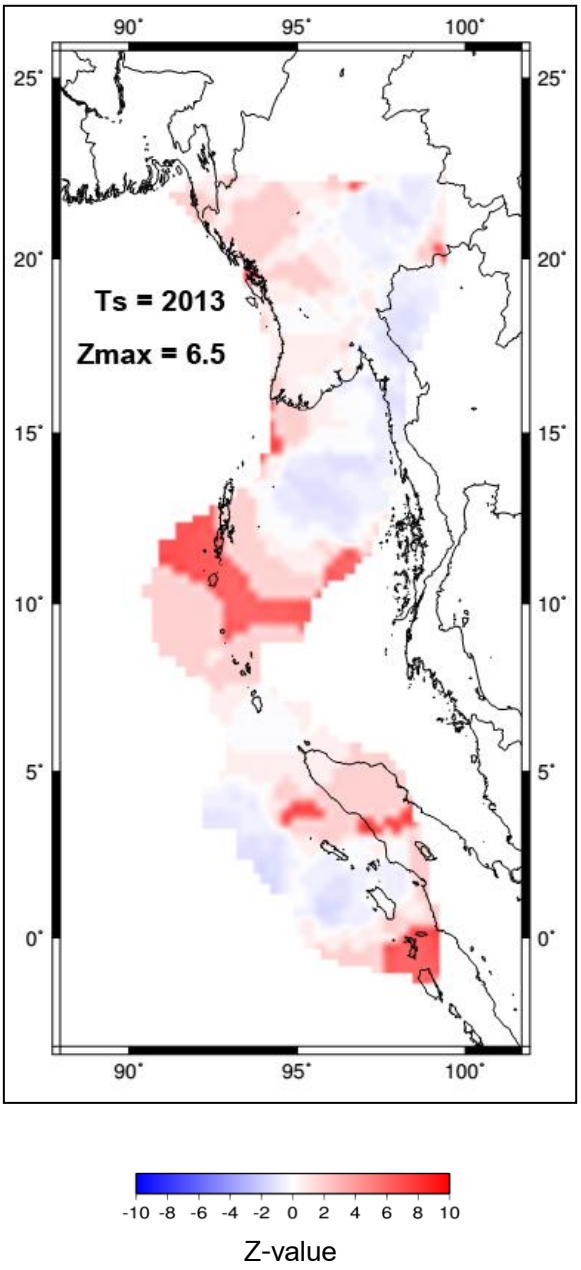

Figure 4.3. Map of SASZ showing distribution of Z values.

CHAPTER V
REGION-TIME-LENGTH ALGORITHM INVESTIGATION

Beside the Z value utilized in the previous chapter, the Region-Time-Length algorithm (RTL) is also used in this chapter to investigate the significance of rate changes in space and time. In order to (i) test the potential of the RTL algorithm as a reliable marker of an earthquake precursor and (ii) find out the suitable RTL characteristics of r_0 and t_0 corresponding to R_{max} and T_{max}, eight major earthquakes that occurred along the SASZ (88–100°E and 2°S–24°N) during 1980–2014 (Table 4.1) were investigated retrospectively using the RTL algorithm. The parameter R_{max} was varied between 25 and 250 km with a 25-km space window, while T_{max} was evaluated between 0.5 and 15 year with a 0.5-year time window. Thus, in total 300 (10 x 30) characteristic conditions were tested iteratively.

5.1 Temporal investigation

In each epicenter of the demonstrated earthquake (Table 4.1), the RTL score was calculated every 14 days starting from 1980 up to the recorded occurrence of the earthquake. According to these iterative tests, values of R_{max}=200 km and T_{max}=2.5 year, i.e., r_0 = 100 km and t_0 = 1.25 years, allowed detection of the anomalous drop in the RTL score prior to the occurrence of all recognized earthquakes (Table 5.1 and Figure 5.1).

After the seismicity change calculation, the results of the retrospective temporal investigation found 8 seismicity precursors from 8 major earthquake events (100%). In the overview, the minimum RTL score varied between -0.3 and -0.6. This indicates that the anomalous drop in the RTL score was fairly obvious as a quiescence precursor. However, in this study, no prominent evidence of the activation stage was found, as has also been mentioned previously for the M_w-7.2 Kobe earthquake, Japan (Huang et al., 2001), M_w-6.8 Nemuro earthquake, Japan (Huang and Sobolev, 2002) and M_w-7.3 Chi-Chi earthquake, Taiwan (Chen and Wu, 2006). For detail explanation, the temporal variation of RTL can be described as follows;

Table 5.1. List of major earthquakes ($M_w \geq 7.0$) calculated by using RTL parameter Rmax = 200 and Tmax = 2.5. The parameters RTLmin, Ts, and Duration indicate a minimum of RTL score at the epicenter of the earthquake, starting time of seismic quiescence, and the duration between the starting time of seismic quiescence and the occurrence time of main shock, respectively.

Case	Rmax (km)	Tmax (years)	RTLmin	Start Date, Ts	Duration (years)
1	200	2.5	-0.3	2001.94	3.0
2	200	2.5	-0.3	2001.94	3.3
3	200	2.5	-0.6	2004.59	1.0
4	200	2.5	-0.4	2007.81	0.3
5	200	2.5	-0.4	2004.90	4.7
6	200	2.5	-0.5	2007.89	2.4
7	200	2.5	-0.4	2004.78	5.7
8	200	2.5	-0.3	2007.12	5.2

i) As illustrated in Figure 5.1c, In the case of the devastating M_w-9.0 earthquake at the end of 2004, the quiescence stage was evident from 2001 at latitude 1.75°N longitude 95.60°E. The RTL score reached its minimum RTL value = (-0.3) in 2001.94. After that around 3 years later, a M_w-9.0 earthquake occurred in December 26, 2004 (Figue 5.1c).

ii) Based on Figure 5.1b, before the March 28, 2005 M_w-8.6 earthquake, the RTLmin = -0.3 was found in 2001.94 in the vicinity of the earthquake epicenter. As this event occurred about 3 months after the 2004 Sumatra earthquake and 163 km away from the 2004 epicenter, the seismic quiescence was detected at the same time and in the same area before the major earthquake occurred about 3.3 years.

iii) According to Figure 5.1c, during 2004.59, the RTLmin = -0.6 was found at latitude 8.50°N longitude 92.35°E. After that, only 1 year later, a M_w-7.2 earthquake occurred in July 24, 2005.

iv) According to Figure 5.1d before the February 20, 2008 M_w-7.3 earthquake, the RTLmin = -0.4 was found far away from the epicenter about 155 km, occurred in 2007.81. This represents the seismic quiescence before the major earthquake occurred about 0.3 years near the epicenter of the earthquake. However, variation pattern of RTL is not complete which decreases quickly from 0 and there is no evident turning. The major earthquake occurs in the short period around the peak RTL, in which RTLmin was found after Zmax about 2.6 years.

v) According to Figure 5.1e, before the August 10, 2009 M_w-7.5 earthquake, the RTLmin = -0.4 was found far away from the epicenter about 383 km occurred in 2004.90. This represents the seismic quiescence before the major earthquake occurred about 4.7 years near the epicenter of the earthquake. Moreover, variation pattern of RTL is complete which decreases from 0 and turning and rising, indicate seismic quiescence followed by seismic activation before the major earthquake.

vi) Based on Figure 5.1f, before the April 6, 2010 M_w-7.8 earthquake, the RTLmin = -0.5 was found at latitude 1.75°N longitude 97.26°E away from the epicenter about 68 km occurred in 2007.89. This represents the anomaly of decreasing of the seismicity rate before the major earthquake occurred about 2.4 years near the epicenter of the earthquake. In addition, variation pattern of RTL is complete and show dropping from 0 and turning before the major earthquake, and RTLmin was found after Zmax about 2.6 years.

vii) Regarding to Figure 5.1g, before the June 12, 2010 M_w-7.5 earthquake, the RTLmin = -0.4 was found at latitude 9.50°N longitude 92.25°E away from the epicenter about 195 km occurred in 2004.78. This represents the seismic quiescence before the major earthquake occurred about 5.7 years near the epicenter of the earthquake. However, Only this case that RTLmin was found before Zmax about 3.6 years.

viii) In the final case in Figure 4.1h, before the April 11, 2012 M_w-8.6 earthquake, the RTLmin = -0.3 was found at latitude 4.50°N longitude 92.01°E away from the epicenter about 255 km occurred in 2007.12. This represents the seismic quiescence before the major earthquake occurred about 5.2 years near the epicenter of the

earthquake. However, variation pattern of RTL is complete which decreases from 0 and turning and rising indicate seismic quiescence followed by seismic activation before the major earthquake. In addition, also the RTL = -0.3 was found from 1984.38 to 1985.14 that initial of earthquake catalogue. The previous researches found initial of earthquake catalogue are not completeness. This may result in low RTL during that period.

Regarding the time span between the occurrences of an anomalous RTL score and subsequent major earthquakes (see also Table 1), most case studies illustrated a short time period of 0.3–5.7 years (Figure 5.1a–h). This indicates that monitoring of the RTL measurements with r_0 = 100 km and t_0 = 2 years may be useful for the intermediate-term (months, years) earthquake forecasting along the SASZ.

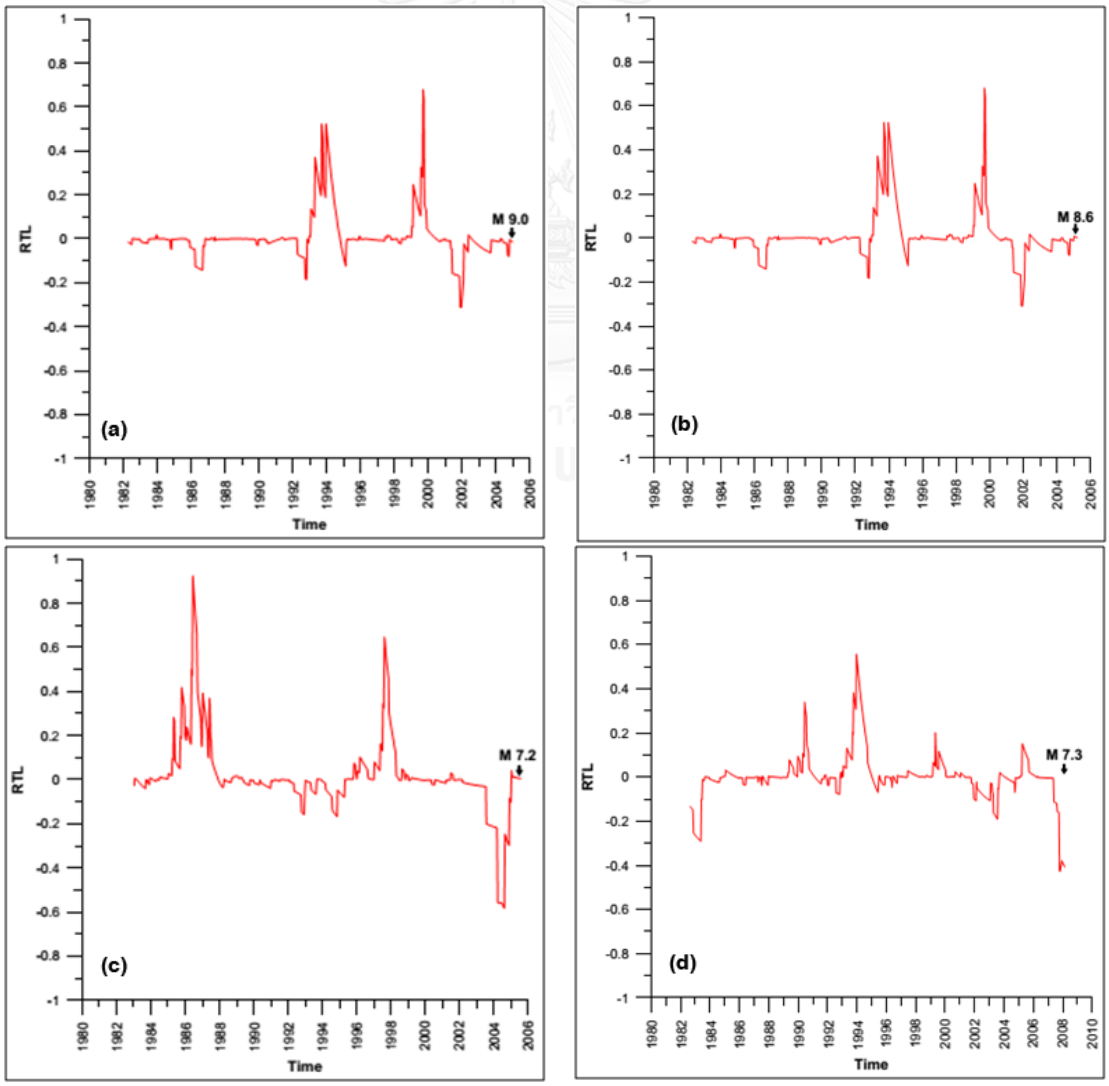

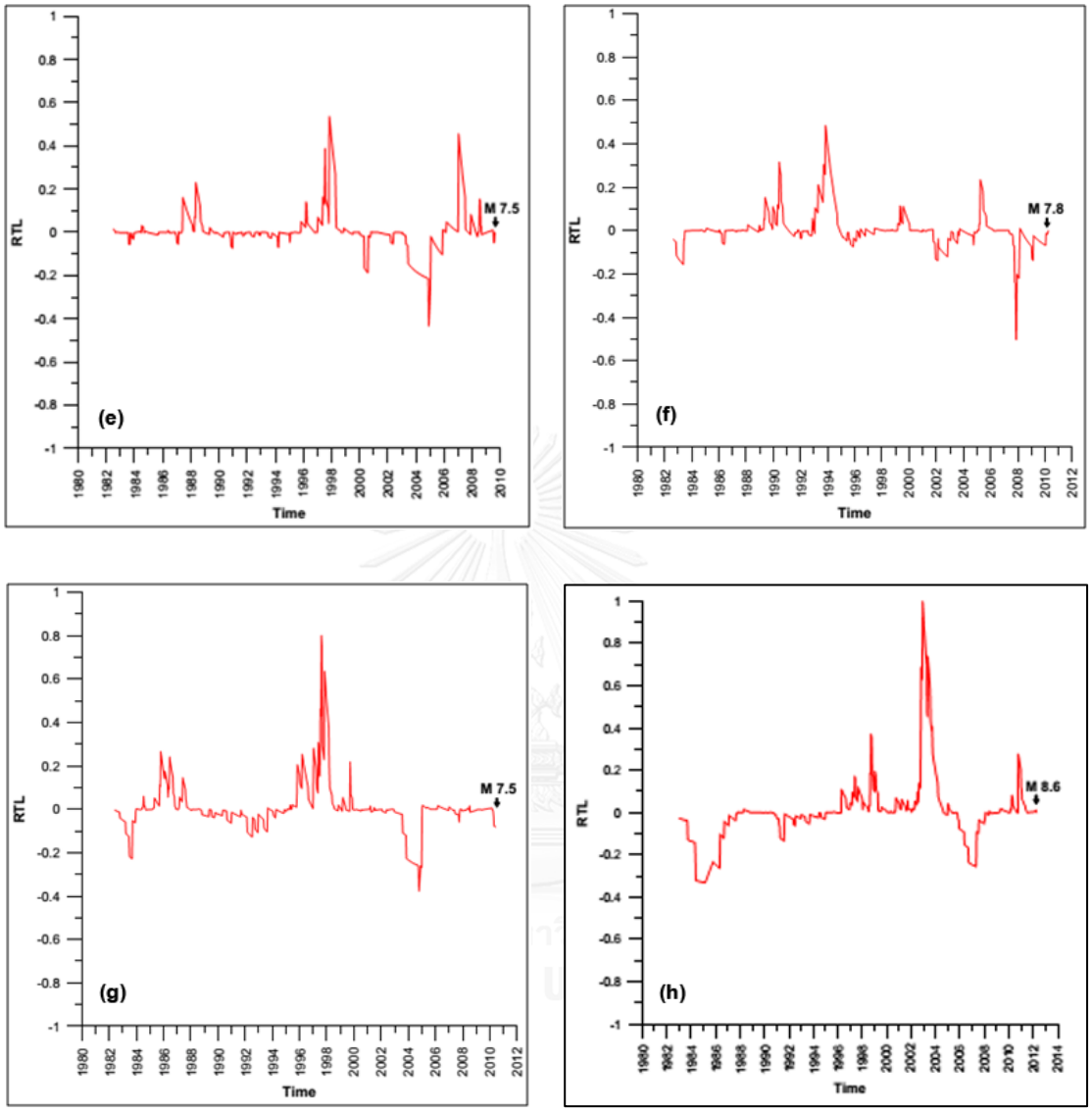

Figure 5.1. Temporal variation of the RTL parameter of the (a) December 26, 2004 M_w-9.0 earthquake (95.6˚E, 1.75˚N), (b) March 28, 2005 M_w-8.6 earthquake (95.6˚E, 1.75˚N), (c) July 24, 2005 M_w-7.2 earthquake (92.35˚E, 8.5˚N), (d) February 20, 2008 M_w-7.3 earthquake (97.26˚E, 2.25˚N), (e) August 10, 2009 M_w-7.5 earthquake (91.51˚E, 11˚N), (f) April 6, 2010 M_w-7.8 earthquake (97.26˚E, 1.75˚N), (g) June 12, 2010 M_w-7.5 earthquake (92.26˚E, 9.5˚N), (h) April 11, 2012 M_w-8.6 earthquake (92.01˚E, 4.5˚N).

5.2 Spatial Investigation

In order to constrain the potential of the RTL algorithm for intermediate-term earthquake forecasting, the spatial distribution of the RTL score was also evaluated in this study. At first, the area in the vicinity of SASZ was gridded with a 0.25^{o} x 0.25^{o} spacing and the temporal variations of RTL scores were evaluated at each grid node. As the number of effective grid nodes is 4,992 for each time slice, and since there are more than 900 time slices, the total number of effective grid nodes, where RTL values were calculated, are more than 4,555,200. Thereafter, an average of the RTL score ($Q(x,y,z,t_1,t_2)$) at each grid node (x,y,z) over the time span of interest (t_1,t_2) was determined systematically as reported (Huang et al., 2002) according to Equation (2.6). According to Figure 5.2, the spatial distribution of the average RTL score in the individual time spans of interest in the eight major earthquakes revealed that all these earthquakes were generated in the vicinity of a comparatively low RTL score. The detailed results of spatial investigation between the duration of seismicity quiescence stage indicated as follows;

i) For example, based on both Figures 5.2a and 5.2b, prior to the M_w-9.0 earthquake of December 26, 2004 and the March 28, 2005 M_w-8.6 earthquake on the offshore western Sumatra Island an anomalous RTL score, i.e., between -0.05 and -0.3, was evident 0.15 y during 2001.41-2002.06 (Figures 5a and 5b).

ii) Regarding to Figure 5.2c, RTL score between -0.05 and -0.6 was found during 2003.55-2004.97 in the southern part of Nicobar Islands cover latitude 1.00-12.75^{o}N longitude 92.01-96.01^{o}E. This represents the seismic quiescence of the earthquake with M_w 7.2 posed in July 24, 2005.

iii) As well as Figures 5.2a and 5.2b, the RTL anomalies, ranged -0.05 to -0.4, exposed again during in the vicinity of the west coast of Sumatra Island during 2007.39-2008.12 (Figures 5.2d and 5.2f). After that around 0.3-2.4 years, the M_w-7.3 earthquake posed in February 20, 2008 including the M_w-7.8 earthquake generated on April 6, 2010.

iv) During 2003.44-2005.01, the RTL score between -0.05 and -0.4 was detected cover the latitude 7.5-12.5°N longitude 91.51-94.26°E (Nicobar Island). Thereafter, about 4.7 years later, the M_w-7.5 earthquake was posed in August 10, 2009.

v) Regarding to Figure 5.2g, before the June 12, 2010 M_w-7.5 earthquake, RTL score between -0.05 and -0.4 was found cover the latitude 7.75–12.00°N longitude 92.01-93.76°E posed during 2003.59-2004.97. This represents the quiescence cover far away from the epicenter about 95 km before the major earthquake occurred about 5.7 years. However, RTL anomaly was closer to the epicenter of earthquake than Z anomaly (Figure 4.2g).

vi) In final case of Figure 5.2h, before the April 11, 2012 M_w-8.6 earthquake, an RTL score between -0.05 and -0.4 was found covered two areas of latitude 12.00–7.75°N longitude 92.01-93.76°E and latitude 12.25–13.50°N longitude 92.76-94.76°E posed in 2003.59-2004.97. This represents the seismic quiescence cover far away from the epicenter about 113 km before the major earthquake occurred about 5.2 years. Furthermore, distribution of RTL anomaly was similar to Z anomaly before the major earthquake (Figure 4.2h).

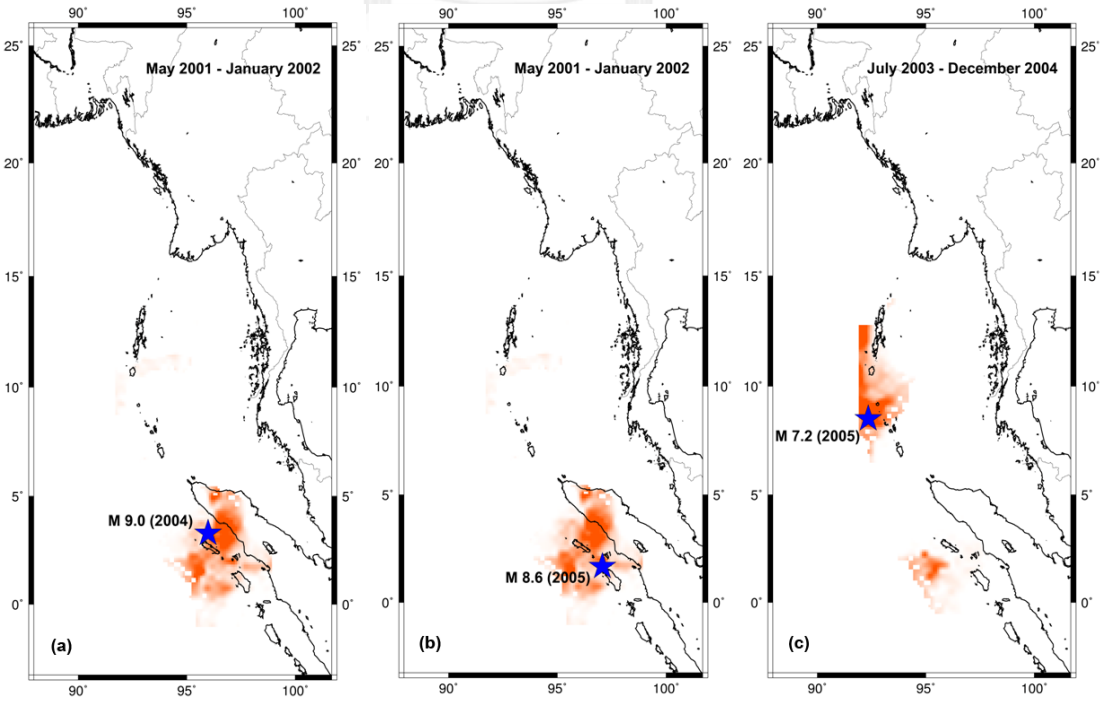

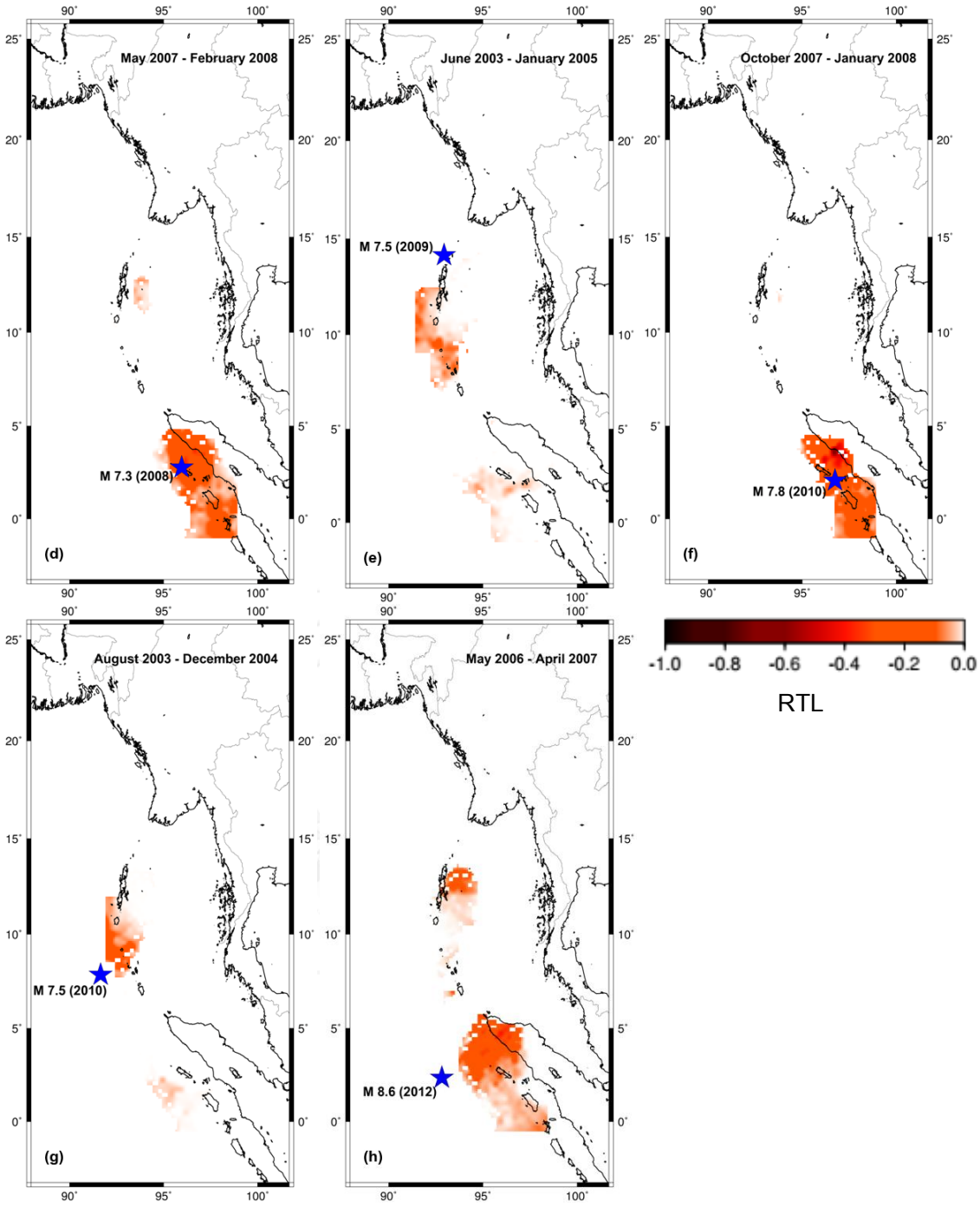

Figure 5.2. Map of the SASZ showing spatial distribution of RTL score, at the starting time of quiescence of the (a) December 26, 2004 M_w-9.0 earthquake (95.6˚E, 1.75˚N), (b) March 28, 2005 M_w-8.6 earthquake (95.6˚E, 1.75˚N), (c) July 24, 2005 M_w-7.2 earthquake (92.35˚E, 8.5˚N), (d) February 20, 2008 M_w-7.3 earthquake (97.26˚E, 2.25˚N), (e) August 10, 2009 M_w-7.5 earthquake (91.51˚E, 11˚N), (f) April 6, 2010 M_w-7.8 earthquake (97.26˚E, 1.75˚N), (g)

June 12, 2010 M_w-7.5 earthquake (92.26°E, 9.5°N), (h) April 11, 2012 M_w-8.6 earthquake (92.01°E, 4.5°N). The anomalous zone indicated as shaded area and the epicenter is shown as blue star.

5.3 Present-day Investigation

Based on the suitable values of r_0 and t_0 obtained from the retrospective test, the spatial distribution of the RTL anomalies were also investigated carefully in this study with the most up-to-date seismicity data. As a result, one areas showed noticeable RTL anomalies were detected around northern Nicobar Islands, the anomalies existed for almost 2 year during 2008.54–2013.45 (Figures 5.3).

No significant earthquakes have been reported in the vicinity of this region since 2012, and so this region is additionally proposed as being high seismic risk areas that are likely to experience an earthquake in the near future.

จุฬาลงกรณ์มหาวิทยาลัย
Chulalongkorn University

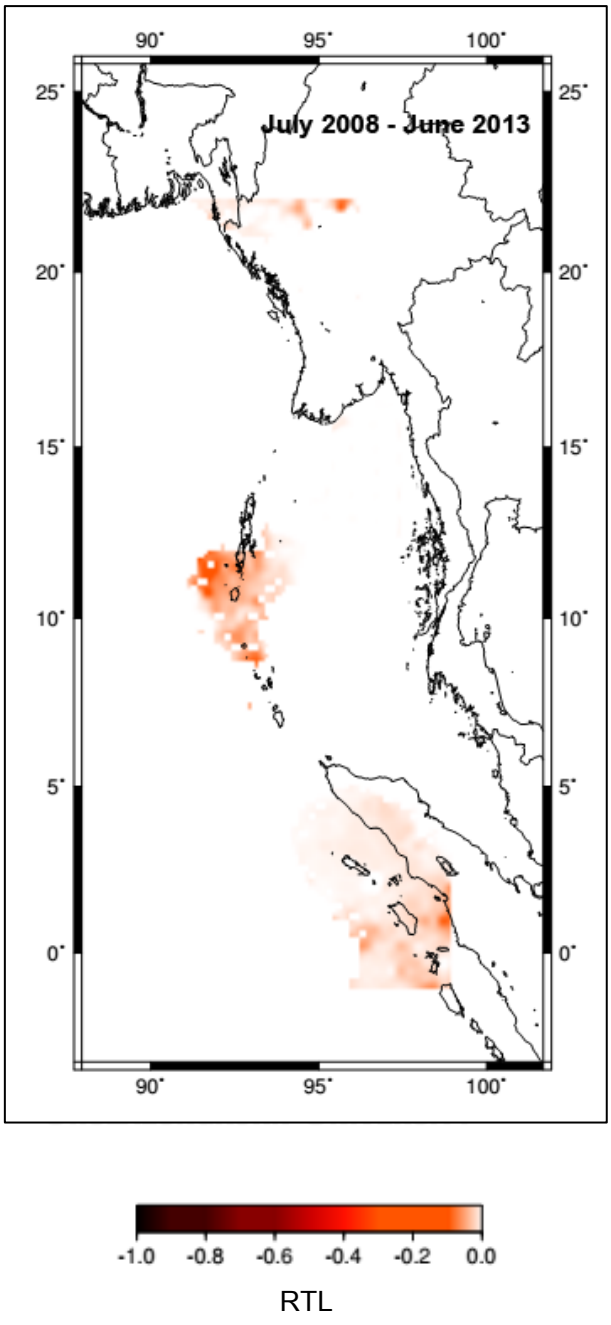

Figure 5.3. Spatial distributions of the average RTL scores determined during 2008–2013.

CHAPTER VI
DISCUSSION

In order to constrain that the seismicity rate change (Z value) and RTL algorithm can utilized as earthquake forecaster tools along the SASZ. In this chapter, the results in previous chapters were considered with each other and comparing with the previous researches which corresponded to this study. The comparison of rational results is described below.

6.1 Completeness of Earthquake Data

Due to the seismicity data which applied in the statistical seismology should have homogeneous database, the existing seismicity catalogues after the procedures of earthquake data improvement should imply only the main shock which directly related to tectonic activities (excluding foreshock, aftershock, man-made earthquake, and the maximum magnitude which seismic instrument cannot recorded 100%). In order to constrain the results of completeness of seismicity data, several works were attempted to observe the relationships of cumulative number of earthquakes against time. The results indicated that the trend line of cumulative number versus time or magnitude scales more smoothly and reformed to the straight line after the process such as earthquake declustering, man-made cut-off, magnitude of completeness (Chouliaras, 2009; Katsumata, 2011a; Katsumata and Sakai, 2013; Rudolf-Navarro et al., 2010). Therefore, this work also observed the cumulative number of earthquakes against time in each procedure of completeness seismicity data. At first, the curve of cumulative number of the total seismicity data represents the flat trend line between 1960 and 1980. After that, the cumulative curve raised gradually until 2004, then the curve suddenly rose until the end of the data.

Secondly, the cumulative number curve after declustering indicates the flat trend line during 1960 and 1980. Afterward, the cumulative curve developed gradually until the end of the data. The overall trend line of declustered seismicity catalogue seems to

be straighter than before. The cumulative number curve after removing the man-made earthquake do not show the flat trend line. Moreover, the cumulative number curve increased gradually as a straight line during the time span. Finally, the cumulative number rate of the earthquake data with magnitude scales ≥ 4.4 indicate the trend of straight line also formed, smoothly along the function of time (Figure 6.1c). Consequently, the seismicity data improvement in each procedure in Chapter III can improve earthquake catalogue along the SASZ. Then, it can mention that the seismicity catalogue before applying to Z value and RTL algorithm investigation here are the reliable earthquake catalogues.

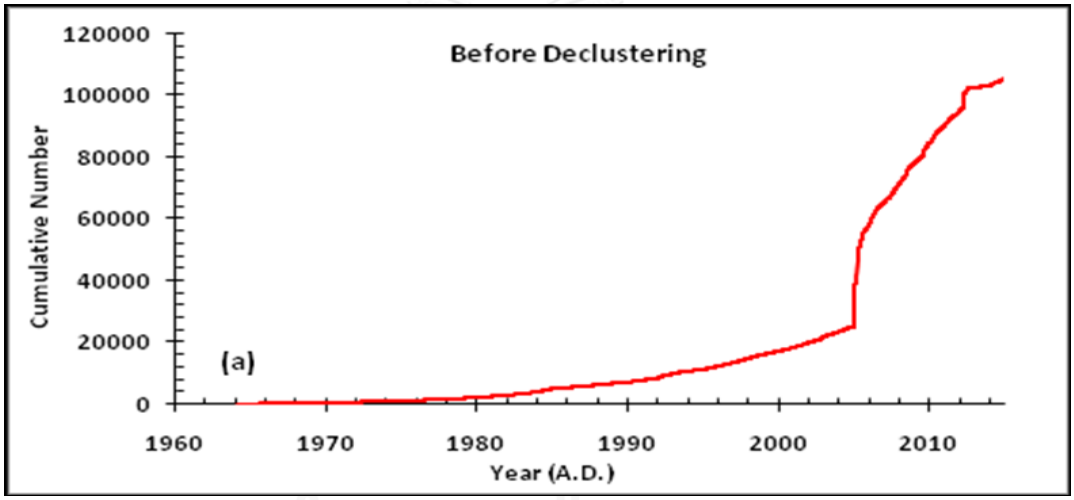

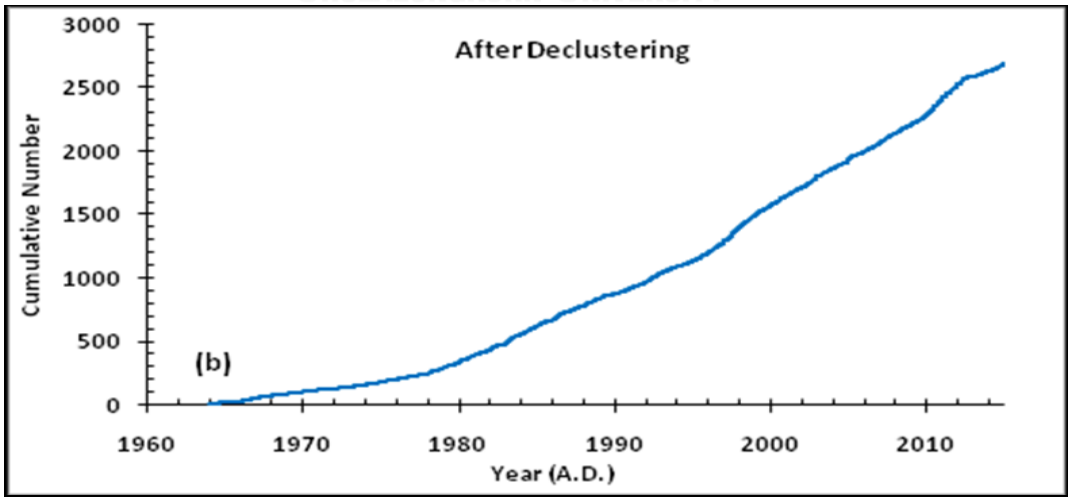

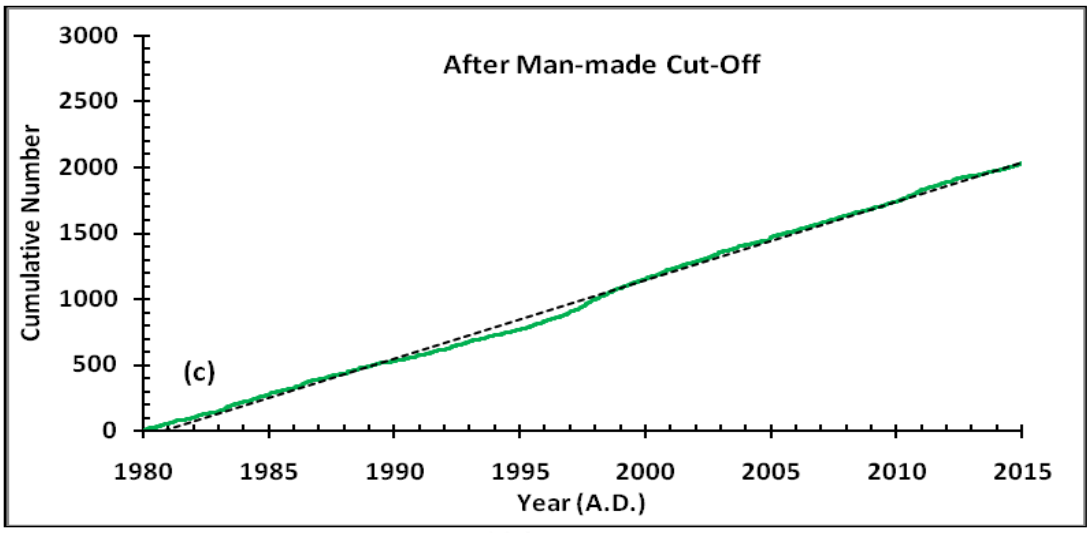

Figure 6.1. The cumulative number of earthquakes along the SASZ plotted against time. a) Before declustering. b) After declustering. c) After man-made cut-off. Dash lines indicate the linear trend line.

6.2 The Precursor Parameters Comparison

In addition to constrain the results of both methods, this work attempt to compare the characteristic parameters of both methods with previous researches as well. The previous studies indicated the maximum Z value (Zmax) before main shock varied between Z = 2.5 and Z = 7.4, while the results of Zmax before a major earthquake of this work showed the Z value in the ranged of that the previous work proposed. Although both tectonic and geologic setting are different in individual areas, i.e., previous work and this study area, it is reveal that the trend of Zmax in this study ($Z \geq 6.7$) were higher than several previous researches indicate anomaly of decreasing of seismicity rate before major earthquake along the SASZ are very clear comparing with the previous works (Figure 6.2).Therefore, it can mention that the Z-value investigation along the SASZ by using Z parameter N = 50 earthquake events and T_w = 2 years can generate the Zmax around the epicenter of major earthquake clearly and all of Z values in this work are reliable.

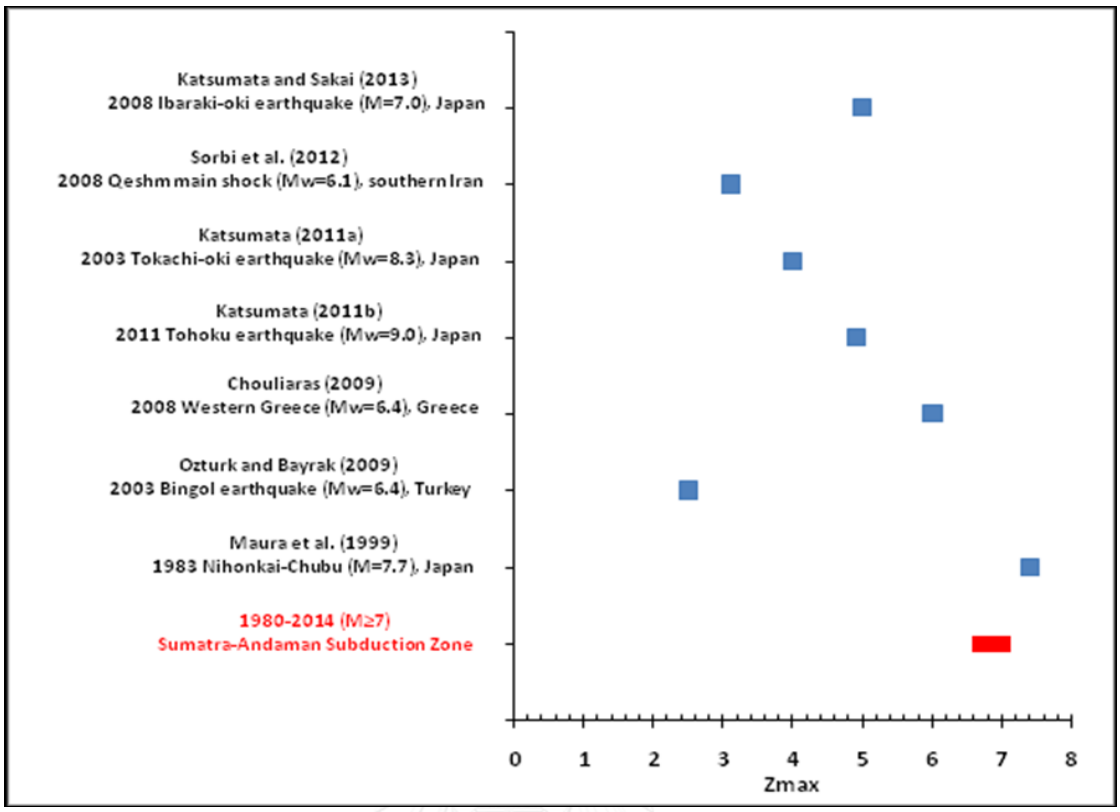

Figure 6.2. The Z value comparisons between this study and previous research works. Blue squares indicated Z value of previous works. The rang of Z value obtained from this study according to the retrospective test of 8 case study of major earthquakes is illustrated as red squares.

จุฬาลงกรณ์มหาวิทยาลัย
Chulalongkorn University

Regarding to RTL algorithm, the minimum RTL value (RTLmin) obtained in this study cannot compare with the previous works because several previous studies did not normalize the RTL values. However, the RTL curve of retrospective temporal investigation indicated the similar results as previous works (some events are better). Hence, it can conclude that the RTL investigation along the SASZ by using characteristic parameter r_0 = 100 km and t_0 = 1.25 year can generate anomaly of the RTL value before major earthquakes in particular for the region of SASZ.

6.3 The Starting Time of Seismic Quiescence

In order to check if the Z value and RTL algorithm investigation are effective or not to evaluate precursory seismicity pattern changes in the short-term and intermediate-term, this work also compared the duration time between the starting time of seismic quiescence and the occurrence time of the main shock (Q-time) from both techniques with the previous researches. At the beginning, after review the previous researches of Z value, the Z value investigation can categorize the forecasting duration in 2 groups. The first group is the intermediate-term investigation (months - 10 years) because most previous studies indicated the duration of Q-time varied in the range of 1 – 7 years (Chouliaras, 2009; Katsumata, 2011a; Katsumata and Sakai, 2013; Murru et al., 1999; Ozturk and Bayrak, 2009; Sorbi et al., 2012). The second group is the long-term investigation (more than 10 years) because there is one research indicate the quiescence detection more than 20 years (Katsumata, 2011b). However, the results after calculating Z value along the SASZ indicate the detection time of quiescence varies in the zone of intermediate-term, the quiescence detection time before major earthquake of this work is inside the Q-time range of previous surveys. Therefore, according to the reasons mentioned above, the quiescence detection time of this work which is calculated by Z-value investigations are effective in particular for the intermediate-term earthquake forecasting (Figure 6.3).

Secondly, after review the previous researches of RTL algorithm, all previous research reported the RTL investigation can classify the forecasting duration as short-term and intermediate-term (Chen and Wu, 2006; Gambino et al., 2014; Gentili., 2010; Huang, 2004; Huang, 2005; Huang and Sobolev, 2002; Sobolev and Tyupkin, 1997). These previous studies indicated the detection of quiescence time, which was calculated by RTL algorithm varied between 0 and 3 years. In the same way as mentioned works, the duration time between starting time of seismic quiescence and the occurrence time of the main shock for M_w-9.0 earthquake on December 26, 2004, M_w-8.6 earthquake on March 28, 2005, M_w-7.2 earthquake on July 24, 2005, M_w-7.3 earthquake on February 20, 2008 and M_w-7.8 earthquake on April 6, 2010 developed in the same

term of previous studies. However, the quiescence detection time of M_w-7.5 earthquake on August 10, 2009, M_w-7.5 earthquake on June 12, 2010 and M_w-8.6 earthquake on April 11, 2012 also found in the duration of intermediate-term forecasting. Then, regarding to the rationale mentioned above, the quiescence detection time of this work which calculated by RTL algorithm is also reliable as the intermediate-term earthquake forecastor (Figure 6.4).

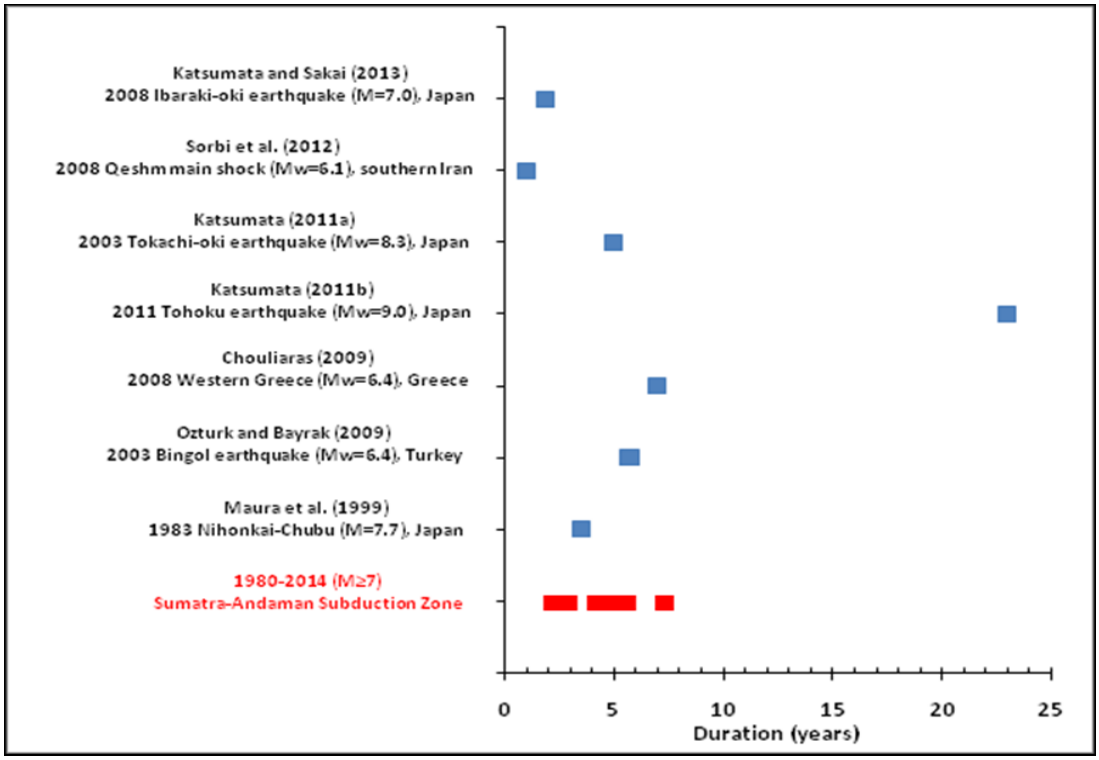

Figure 6.3. The duration time between starting time of seismic quiescence and the occurrence time of the main shock (Q-time), calculated by Z-value investigation. Blue squares indicate seismic quiescence detection time of previous works in intermediate-term and long-term forecasting. Meanwhile, the quiescence detection times obtained in this study are shown in red squares.

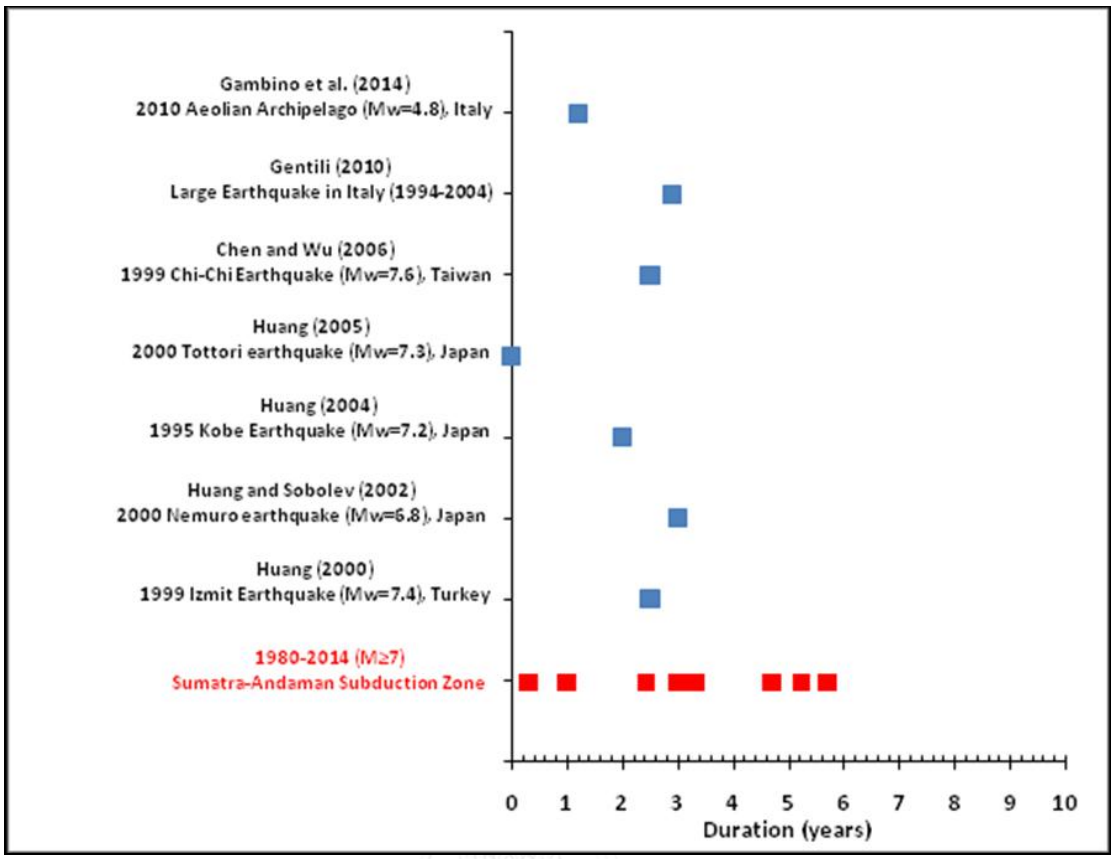

Figure 6.4. The duration time between the starting time of seismic quiescence and the occurrence time of the main shock (Q-time), investigated by RTL algorithm. Blue squares indicate seismic quiescence detection time of previous works, whereas the results of this study are expressed as red squares.

Chulalongkorn University

6.4 The Relationship of Precursor and Magnitude of Major Earthquake along the SASZ.

Regarding to the Zmax and RTLmin represented the seismic quiescence before major earthquake, previous researches were not clear about the relationship of levels of seismic quiescence and magnitude of a major earthquake. In this work, it is noticeable from the obtained results that the higher Zmax were found before larger earthquake (Figure 6.5). However, for the RTLmin, this work show the lower RTLmin were found before smaller earthquake (Figure 6.6), but it is not clear about relationships of precursor and magnitude of the major earthquake along the SASZ.

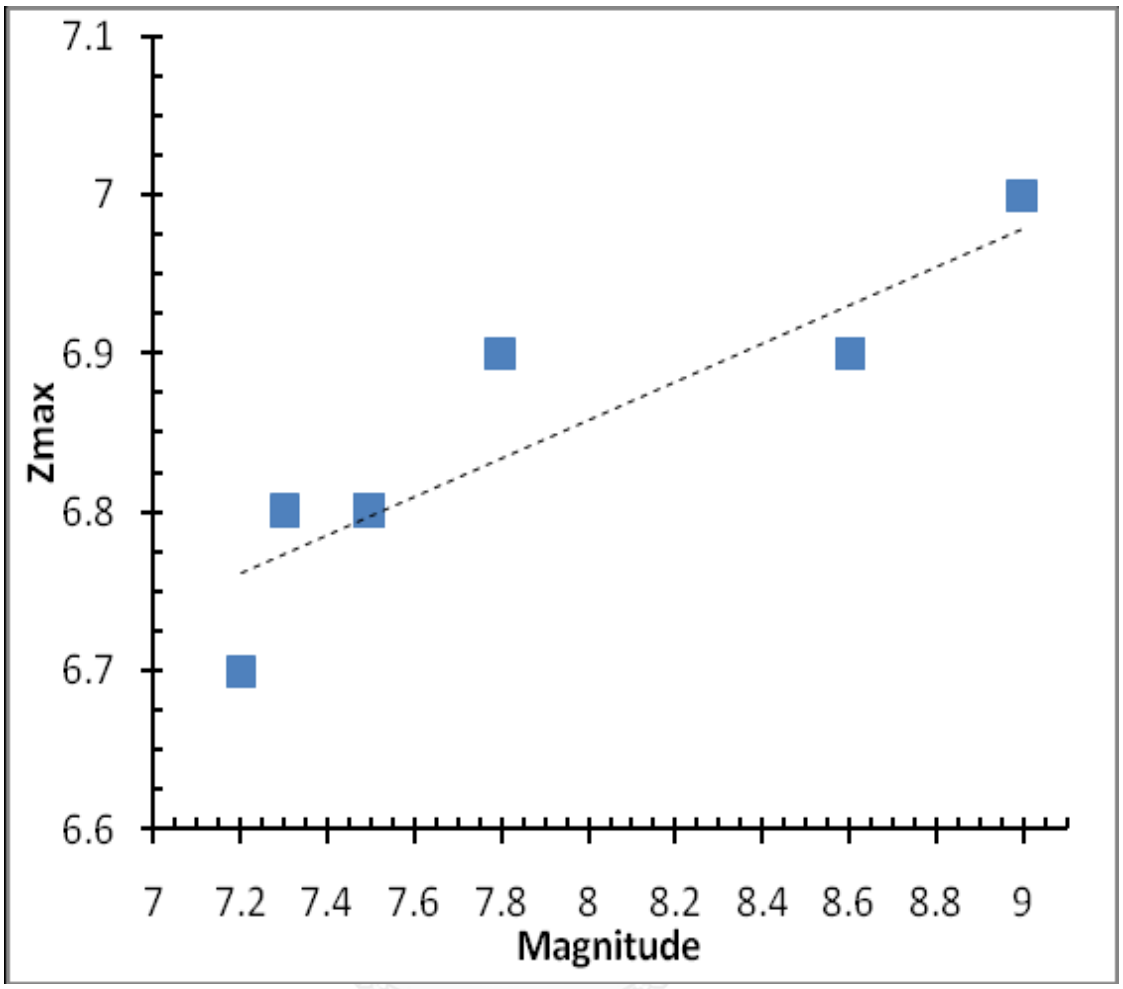

Figure 6.5. The relationship of Zmax and the earthquake magnitude of various case studies of retrospective test in this study. Dash lines indicate the linear trend line.

จุฬาลงกรณ์มหาวิทยาลัย
Chulalongkorn University

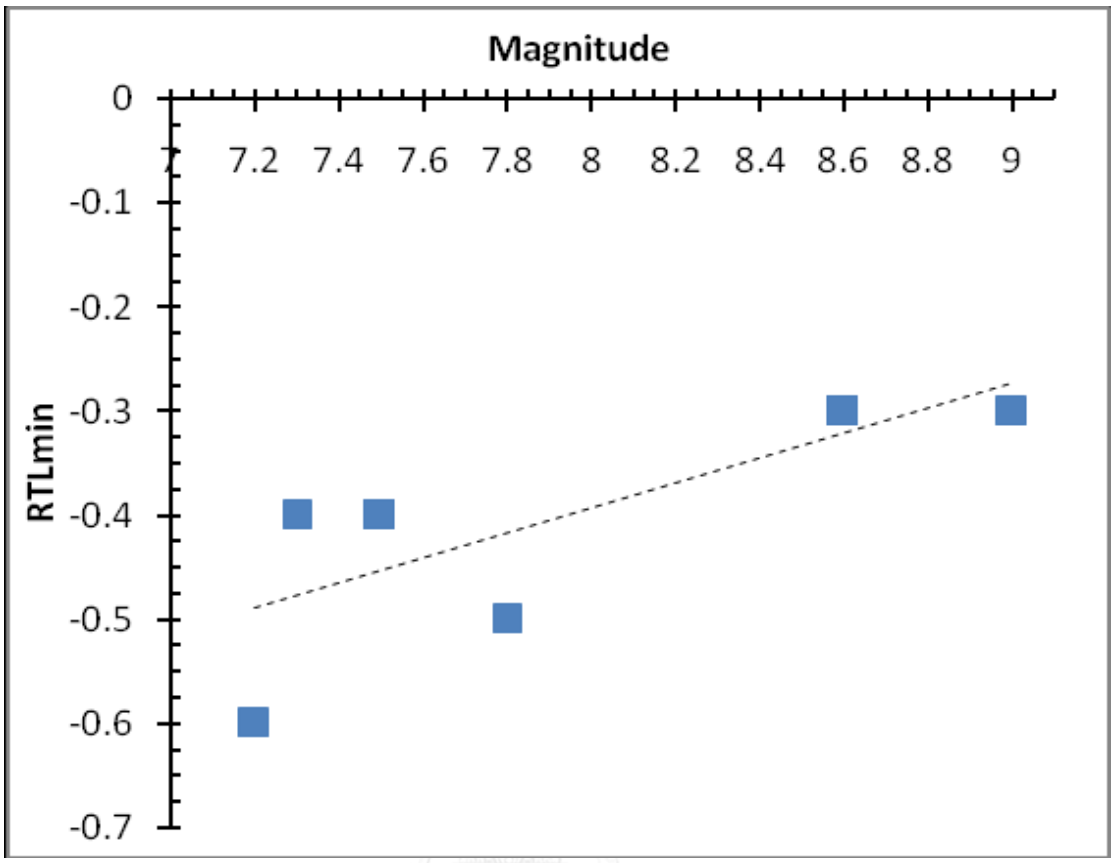

Figure 6.6. The relationship of RTLmin and the earthquake magnitude of various case studies of retrospective test in this study. Dash lines indicate the linear trend line.

จุฬาลงกรณ์มหาวิทยาลัย
Chulalongkorn University

6.5 Comparison between Temporal Variation of Z and RTL values.

Regarding to the results of the temporal variation of Z and RTL values, there are 7 of 8 events that Z-value anomalies were found before major earthquakes and followed by the anomalies of RTL after 1-2 years. However, before M_w-7.5 earthquake on June 12, 2010 anomalies of RTL and Z were found in 2003 and 2007, respectively (Figure 6.7g). Therefore, regarding to the technical aspect, it is implied that whenever the RTL anomalies was found, the effective mitigation plan should be contributed urgently. Meanwhile, if the anomalies are obtained from the Z-value investigation, there are some more time span for mitigation plan.

(a) Mw-9.0 earthquake on December 26, 2004

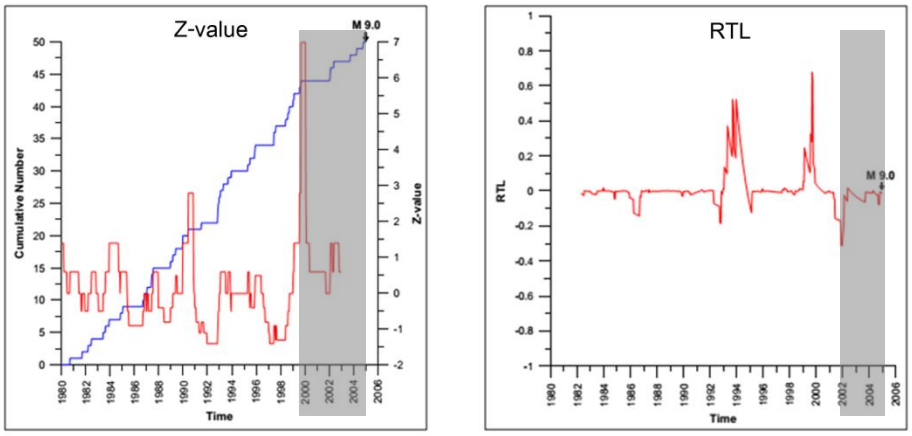

(b) Mw-8.6 earthquake on March 28, 2005

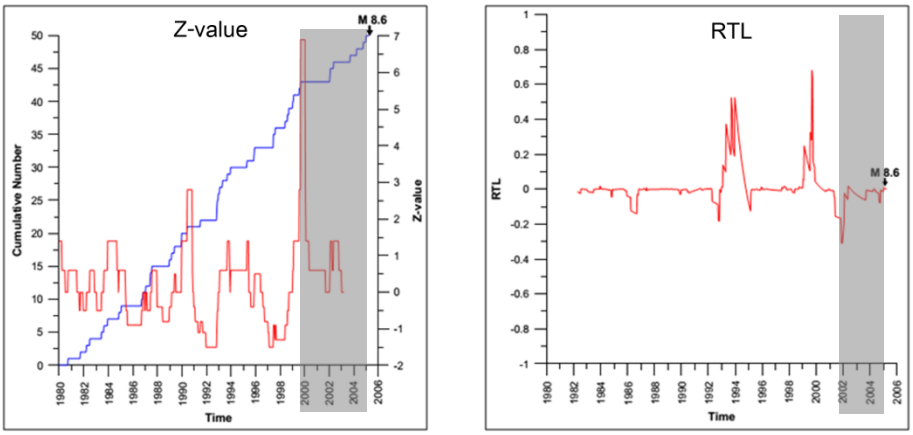

(c) Mw-7.2 earthquake on July 24, 2005

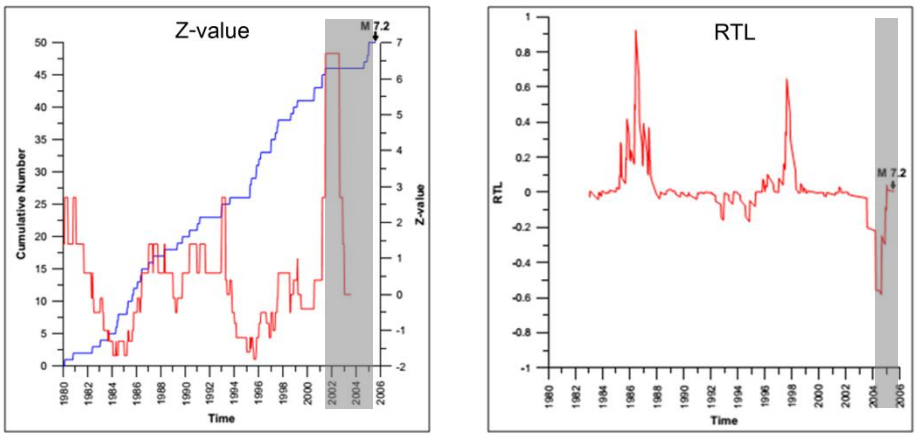

(d) Mw-7.3 earthquake on February 20, 2008

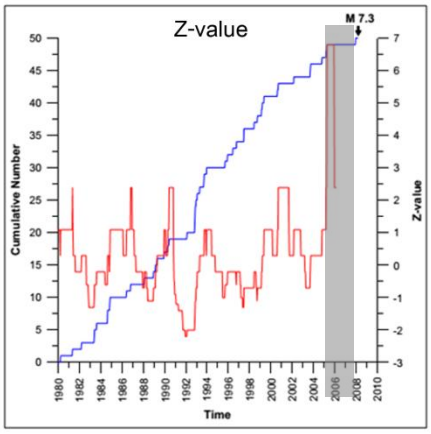

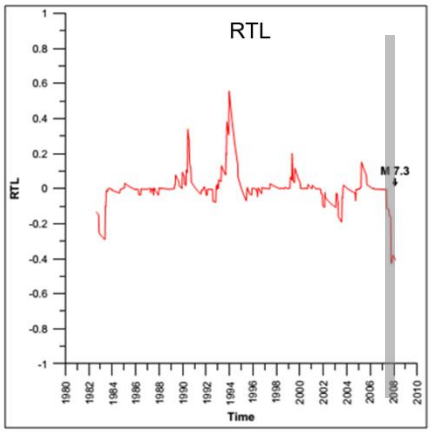

(e) Mw-7.5 earthquake on August 10, 2009

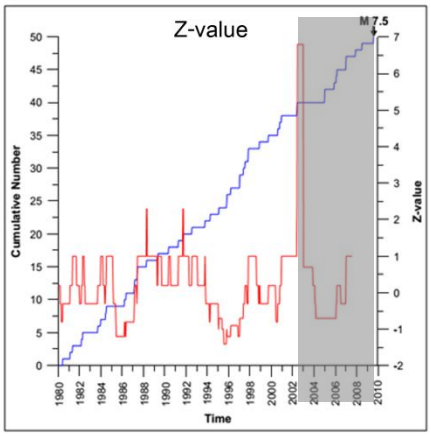

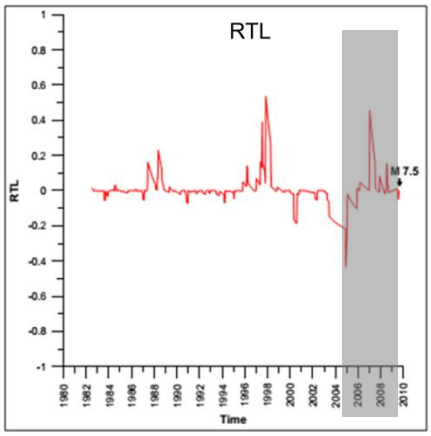

(f) Mw-7.8 earthquake on April 6, 2010

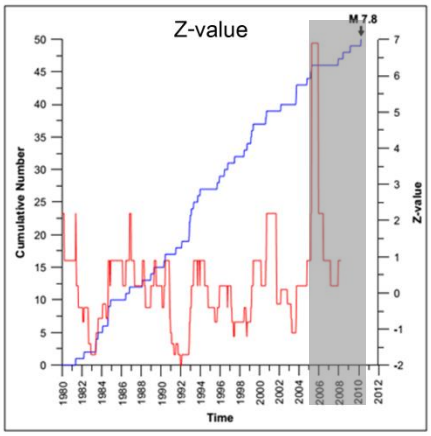

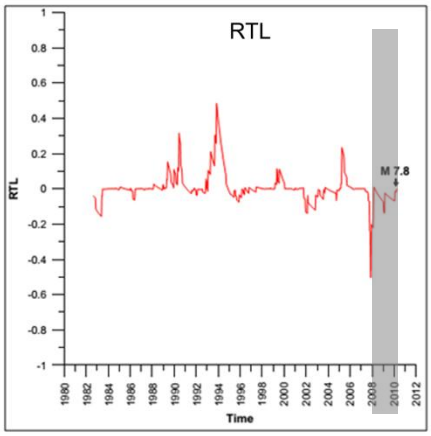

(g) Mw-7.5 earthquake on June 12, 2010

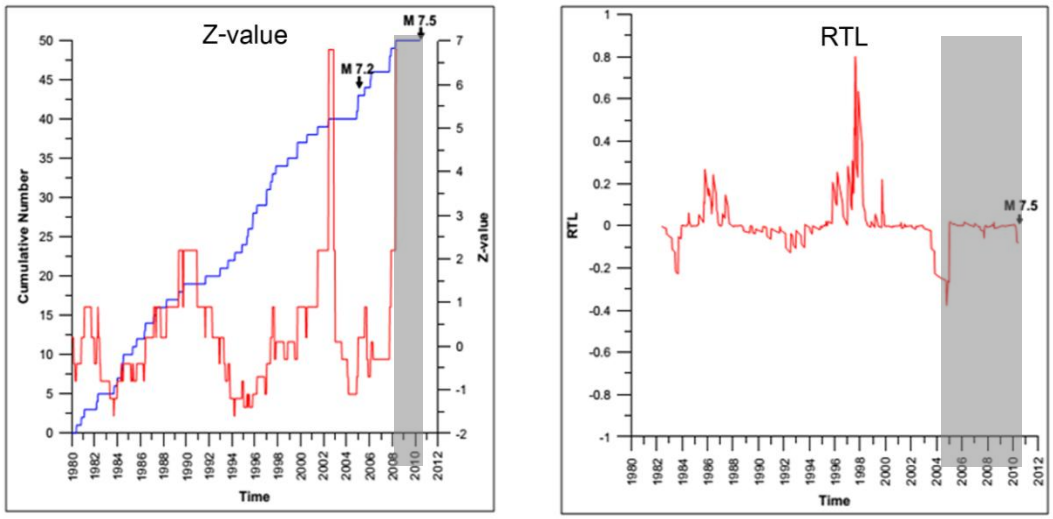

(h) Mw-8.6 earthquake on April 11, 2012

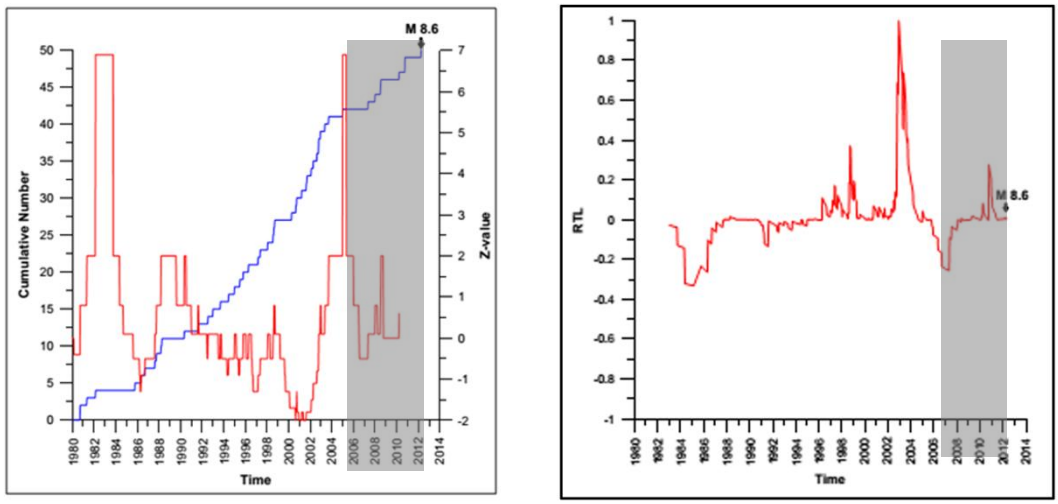

Figure 6.7. Comparing between the temporal variations of Z and RTL values evaluated from various earthquake case studies considered in this study. Grey shaded area shows duration time between the starting time of seismic quiescence and the occurrence time of the main shock.

6.6 Comparison between Spatial Distribution of Z and RTL values

In addition, regarding spatial investigation of Z and RTL values, the both quiescences locate in the vicinity of the epicenters of major earthquakes generated previously along the SASZ (Figure 6.8). Due to no evidence of man-made seismicity, both temporal and spatial Z anomalies obtained in this study, therefore, imply empirically the precursor of the earthquakes.

(a) M_w-9.0 earthquake on December 26, 2004

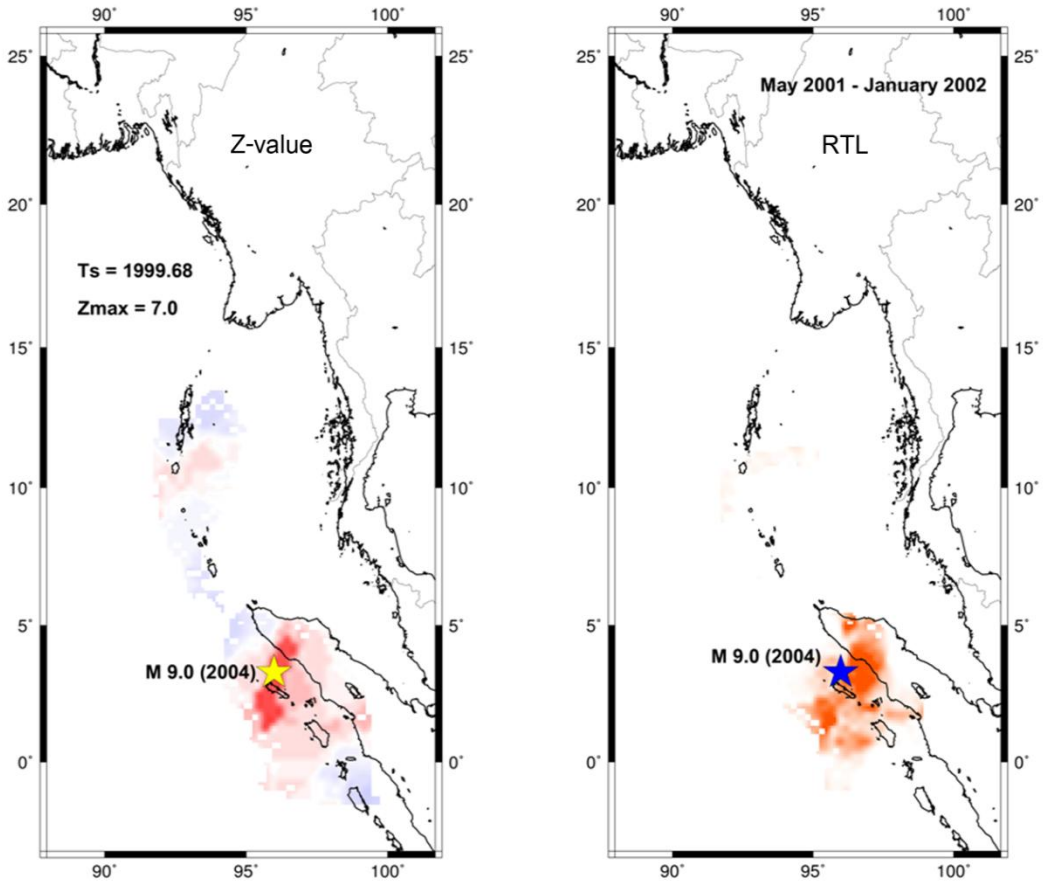

(b) M_w-8.6 earthquake on March 28, 2005

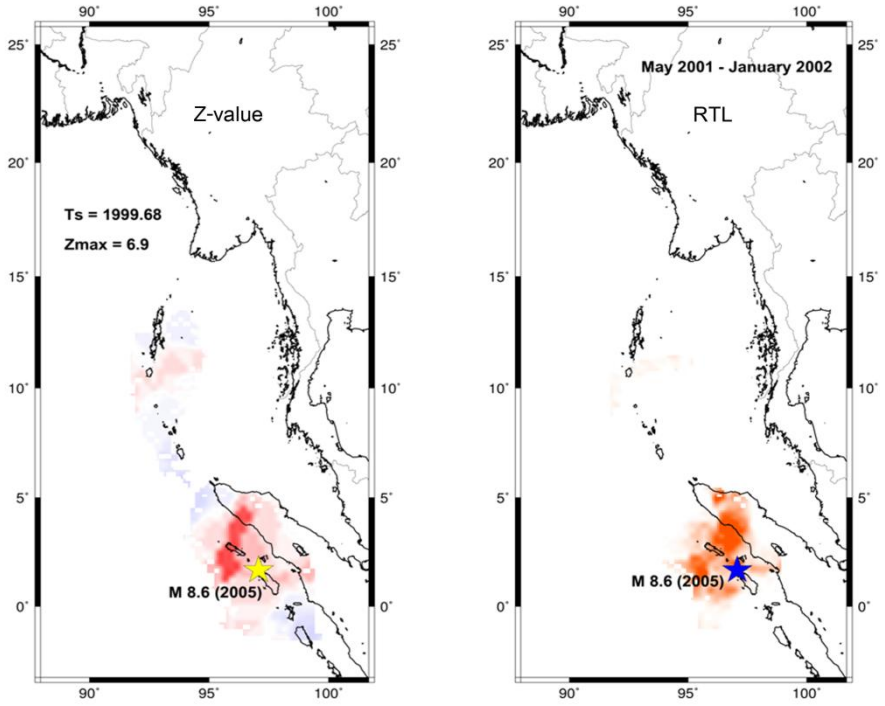

(c) M_w-7.2 earthquake on July 24, 2005

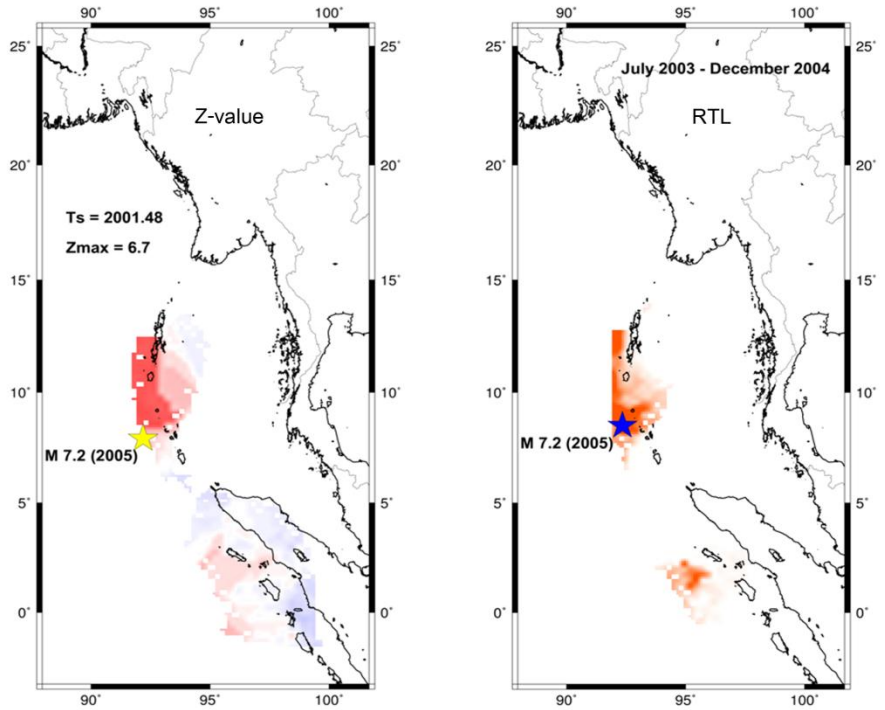

(d) M_w-7.3 earthquake on February 20, 2008

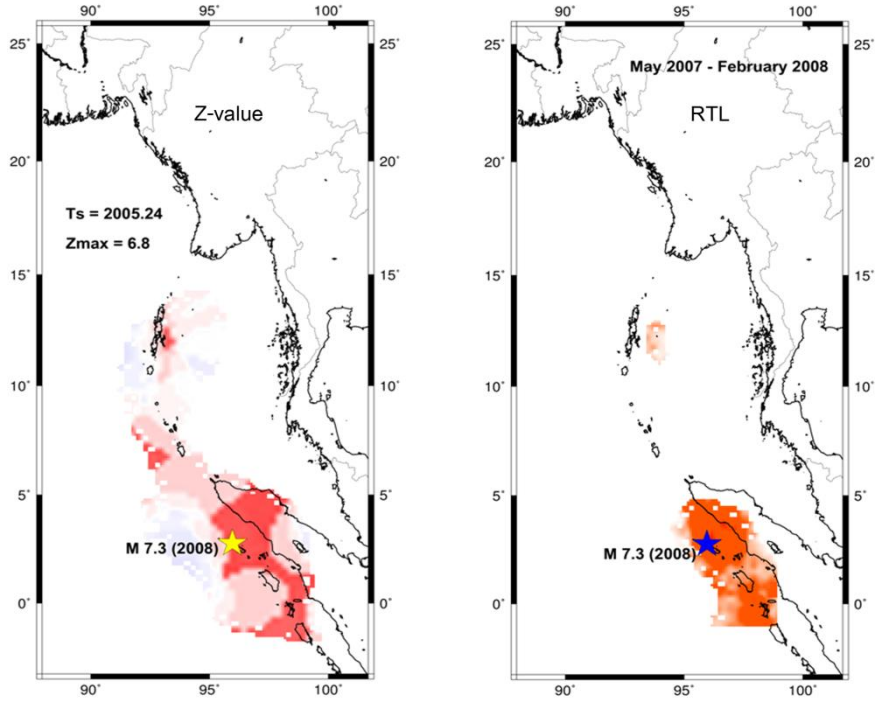

(e) M_w-7.5 earthquake on August 10, 2009

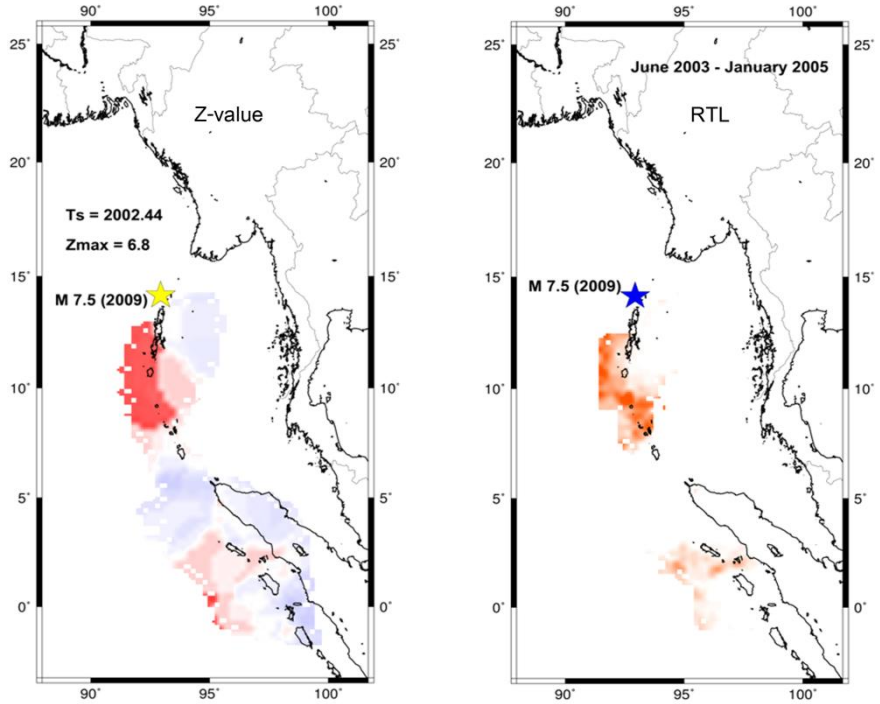

(f) M_w-7.8 earthquake on April 6, 2010

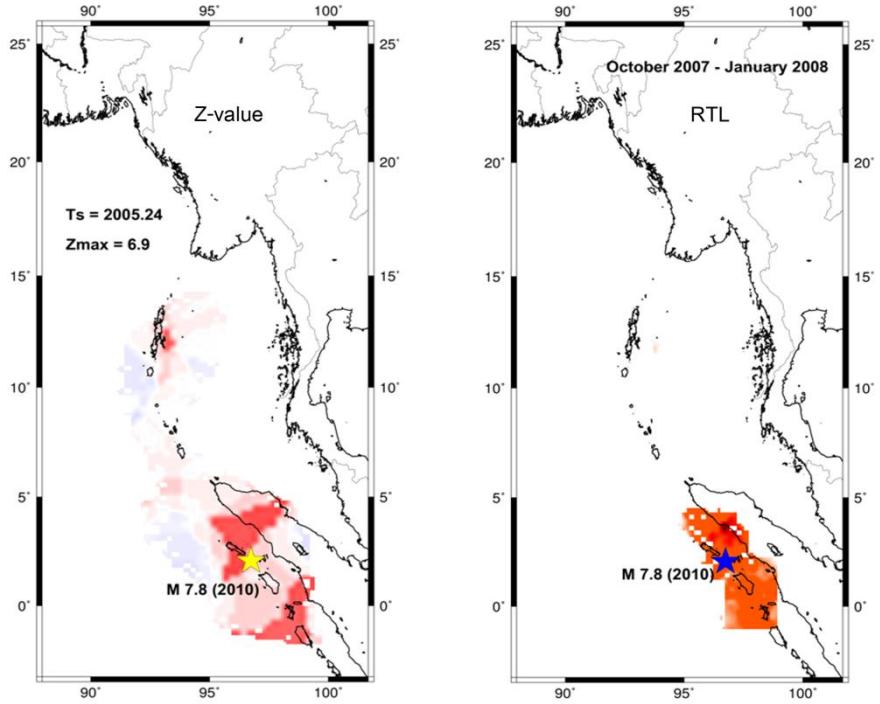

(g) M_w-7.5 earthquake on June 12, 2010

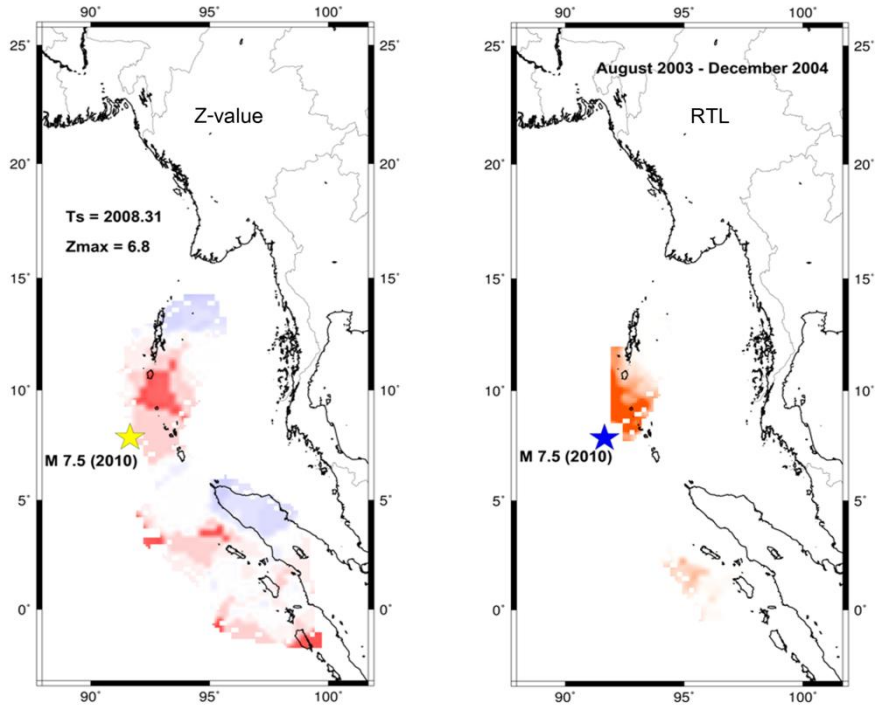

(h) M_w-8.6 earthquake on April 11, 2012

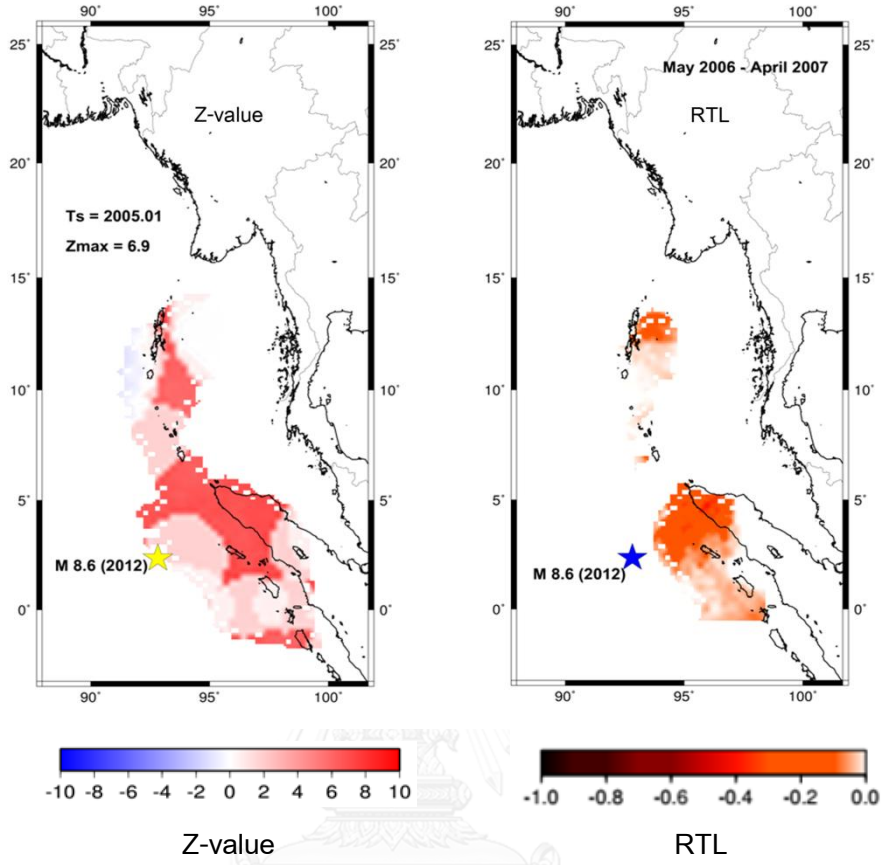

Figure 6.8. The Spatial distribution of Z and RTL value before a number of retrospective case study recognized in this study. Stars indicate epicenter of main shocks.

6.7 Pattern of Seismicity before major earthquake along the SASZ.

Regarding to the results of the temporal variation of RTL along the SASZ, the anomalies show the short or intermediate-terms that there are four types of RTL patterns before the main shock. For the I-type, the variation pattern of the RTL is complete and dropping from 0 and turning to the background level before the main shock (Figure 6.9). For the II-type, similar to the I-type is dropping from 0 turning to the background level of the main shock (Figure 6.10a). For the III-type, dropping from 0 and turning to the background level and rising before the main shock (Figure 6.11). For the IV-type, the variation pattern of RTL is not complete, which decreases quickly from 0 and there is no

evident turning, the main shock occurs in the short period around the peak RTL (Figure 6.10b). Furthermore, in this work indicate before major earthquake were found the most variation pattern of the RTL are Type I, i.e., the variation pattern of the RTL is complete and dropping from 0 and turning to the background level before main shock.

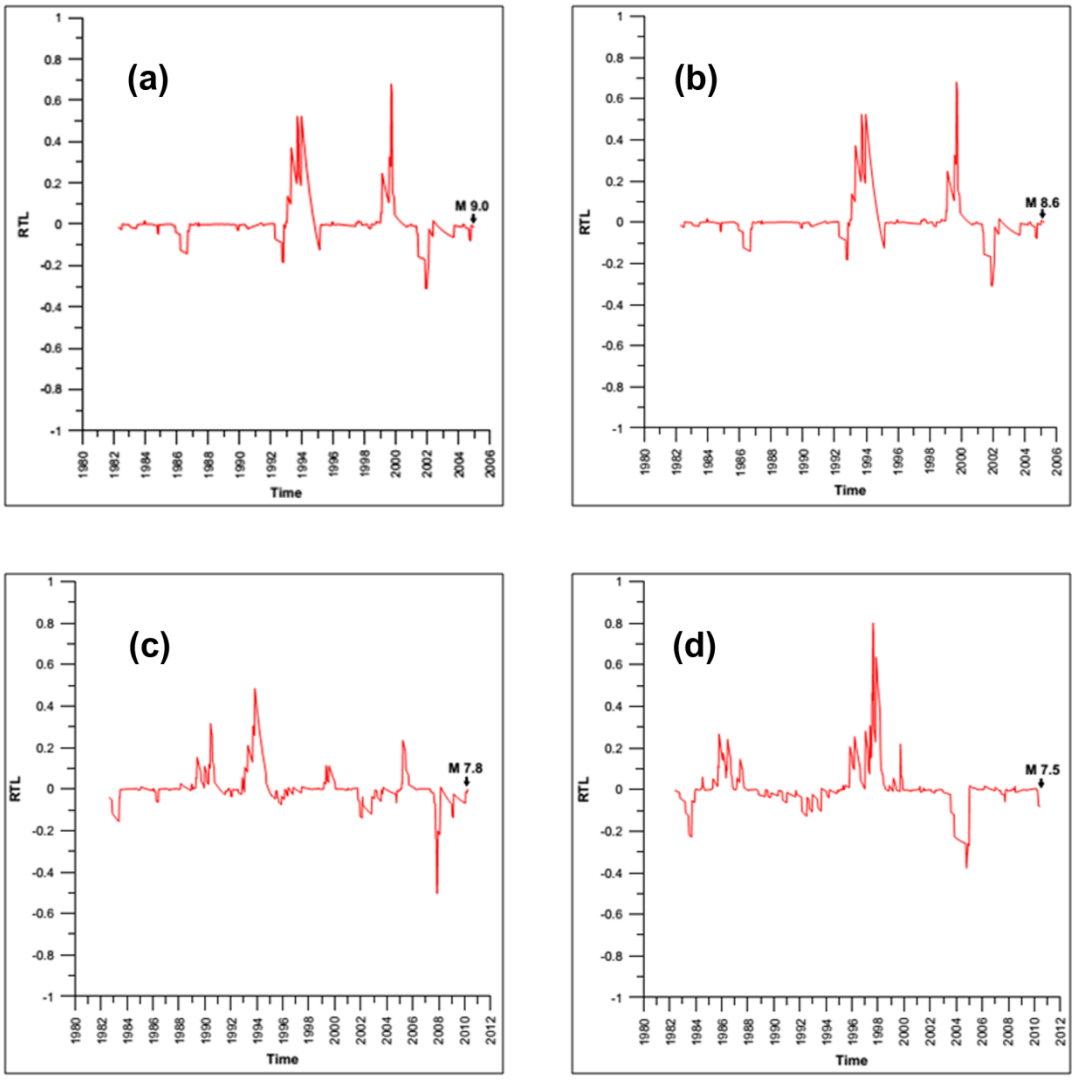

Figure 6.9. The variation pattern of RTL in I-Type before (a) M_w-9.0 earthquake on December 26, 2004, (b) M_w-8.6 earthquake on March 28, 2005 (c) M_w-7.8 earthquake on April 6, 2010, and (d) M_w-7.5 earthquake on June 12, 2010.

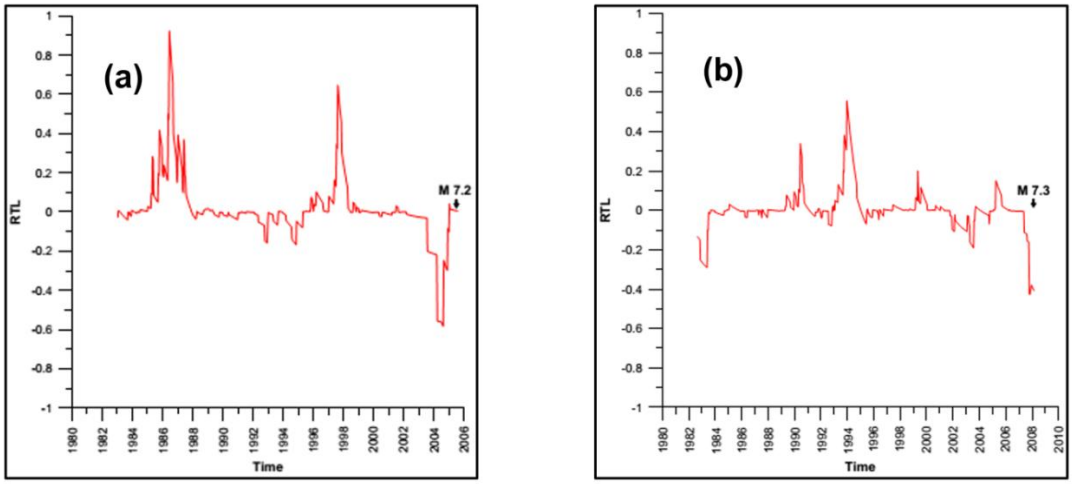

Figure 6.10. The variation pattern of RTL in II-type and IV-type before (a) M_w-7.2 earthquake on July 24, 2005 and (b) M_w-7.3 earthquake on February 20, 2008, respectively.

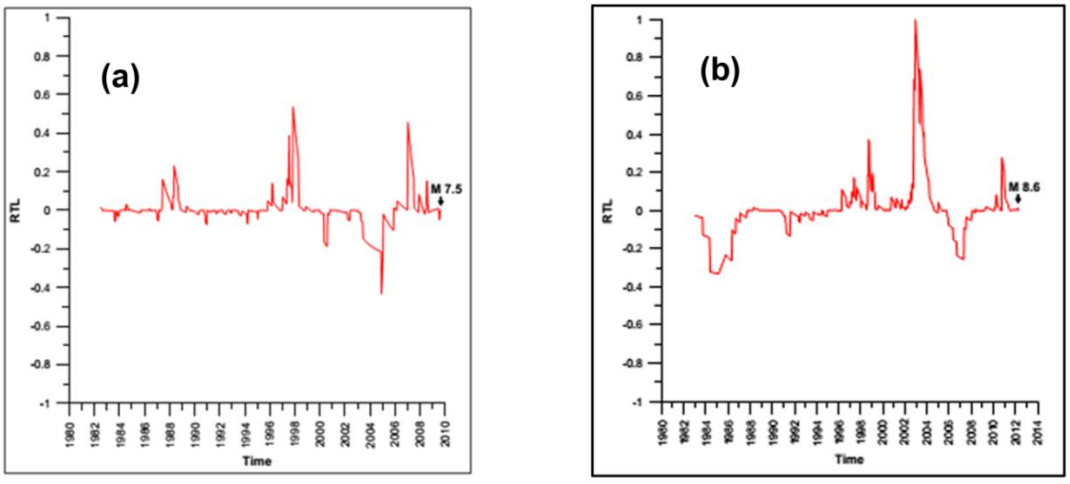

Figure 6.11. The variation pattern of RTL in III-type before (a) M_w-7.5 earthquake on August 10, 2009 and (b) M_w-8.6 earthquake on April 11, 2012.

6.8 Prospective Areas of the Upcoming Earthquake Sources

In this work, the obtain results were compared with b-value of FMD (Pailoplee et al., 2013). Seismotectonically, the lower RTL and higher Z value implied the higher of seismic quiescence. Meanwhile, the lower b-value of FMD relates empirically to higher stress accumulated. After comparing all methods mentioned above, the results revealed that the time span is not same and different of data set with b-value lead to the low of RTL and high Z region (this study) are in the southern part comparing with the area showing low b anomalies which analyzed from the seismicity data recorded during 1984-2010 mentioned by Pailoplee et al. (2013) (Figure 6.12). Furthermore, there is one location, where Z, RTL and b anomalies are very clear which is Andaman and Nicobar Islands which is still quiescence from the major earthquakes. Therefore, the effective mitigation plan should be contributed urgently.

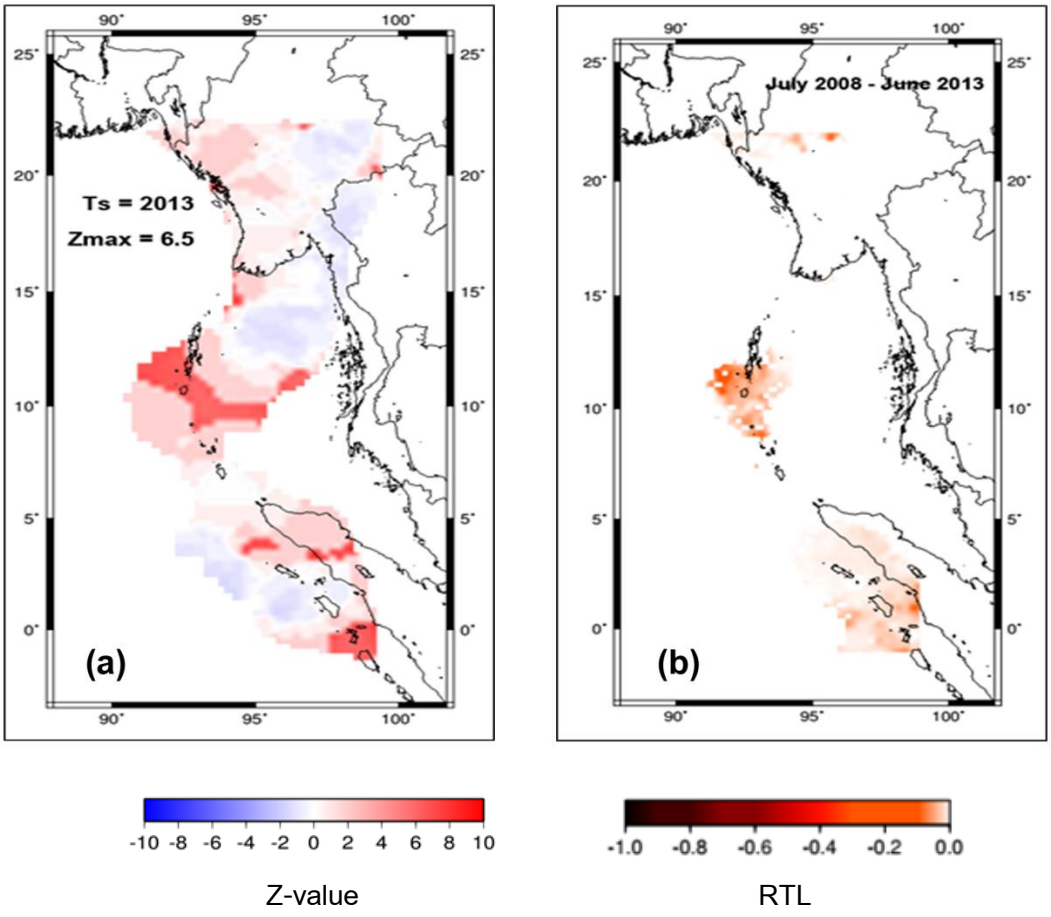

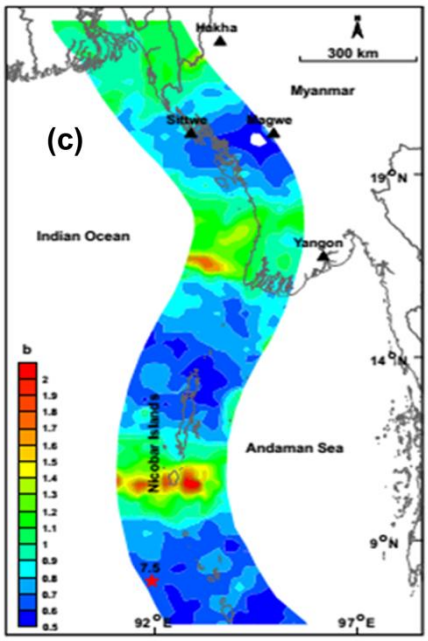

Figure 6.12. Spatial distribution of a) Z values evaluated at the time slice 2013, b) RTL values mapped during July 2008 – June 2013 time span, and c) b values analyze from the seismicity data recorded during 1984 – 2010 (Pailoplee et al., 2013).

6.9 Correlation Coefficient of RTL Algorithm

Regarding to several studies of RTL algorithm mentioned that the characteristic parameters (r_0 and t_0) affect directly to the RTL investigation (Chen and Wu, 2006; Huang, 2004; Huang, 2005). Therefore, in order to observe such changes, this work repeated the RTL calculations by using the different characteristic RTL parameters, subsequently plotted the results of RTL curves at each conditions for considering the suitable characteristic RTL parameters. Furthermore, after varied that conditions, this research also computes the correlation coefficient in each condition of major earthquakes for determining whether the values of two variables are associated. For simplification briefly, the suitable condition r_0= 100 km and t_0= 1.25 years were calculated correlation coefficient by comparison with different RTL conditions which increase/decrease r_0 = 25 km and increase/decrease t_0 = 0.25 years from the suitable characteristic RTL parameter used in this study. Then, the significance in each

correction coefficient was considered by using Pearson correlation coefficient r (P-value). If the probability of P-value is lower than the conventional 5% ($P<0.05$) the correlation coefficient is called statistically significant. Hence, the maximum level of P-value for determining whether the anomalies are random samples or normal distribution was set equal to 0.05 (Bendat and Piersol, 2000) (Table 6.1). In addition, The RTL score at the epicenter of the major earthquake was investigated temporally in Appendix.

After evaluating the correlation coefficient in each major earthquake which found the correlation coefficients indicated that most the varied cases listed in Table 6.1 correlated at a significance of 0.05. As a result, one can conclude that the values of r_0 = 100 km and t_0 = 1.25 year utilized in this study are meaningful for RTL investigation along the SASZ and that the seismic quiescence obtained here is not an artifact due to parameter selections.

Table 6.1. Correlation of RTL values between different characteristic parameters r_0 and t_0 of the (a) M_w-9.0 earthquake on December 26, 2004, (b) M_w-8.6 earthquake on March 28, 2005, (c) M_w-7.2 earthquake on July 24, 2005, (d) M_w-7.3 earthquake on February 20, 2008, (e) M_w-7.5 earthquake on August 10, 2009, (f) M_w-7.8 earthquake on April 6, 2010, (g) M_w-7.5 earthquake on June 12, 2010 and (h) M_w-8.6 earthquake on April 11, 2012. Case A shows the suitable values of independent characteristic parameters, case B the different characteristic RTL parameters that we using for comparison with suitable conditions.

(a) M_w-9.0 earthquake on December 26, 2004

Case	A	(a) r_0 = 100 km, t_0 = 1.25 years			
	B	(b) r_0 = 75 km	(c) r_0 = 125 km	(d) t_0 = 1 year	(e) t_0 = 1.5 years
correlation between A and B		0.817	0.579	0.854	0.816

(b) M_w-8.6 earthquake on March 28, 2005

Case	A	(a) r_0 = 100 km, t_0 = 1.25 years			
	B	(b) r_0 = 75 km	(c) r_0 = 125 km	(d) t_0 = 1 year	(e) t_0 = 1.5 years
correlation between A and B		0.817	0.579	0.854	0.816

(c) M_w-7.2 earthquake on July 24, 2005

Case	A	(a) r_0 = 100 km, t_0 = 1.25 years			
	B	(b) r_0 = 75 km	(c) r_0 = 125 km	(d) t_0 = 1 year	(e) t_0 = 1.5 years
correlation between A and B		0.804	0.847	0.914	0.912

(d) M_w-7.3 earthquake on February 20, 2008

Case	A	(a) r_0 = 100 km, t_0 = 1.25 years			
	B	(b) r_0 = 75 km	(c) r_0 = 125 km	(d) t_0 = 1 year	(e) t_0 = 1.5 years
correlation between A and B		0.337	0.415	0.428	0.460

(e) M_w-7.5 earthquake on August 10, 2009

Case	A	(a) r_0 = 100 km, t_0 = 1.25 years			
	B	(b) r_0 = 75 km	(c) r_0 = 125 km	(d) t_0 = 1 year	(e) t_0 = 1.5 years
correlation between A and B		0.621	0.907	0.765	0.844

(f) M_w-7.8 earthquake on April 6, 2010

Case	A	(a) r_0 = 100 km, t_0 = 1.25 years			
	B	(b) r_0 = 75 km	(c) r_0 = 125 km	(d) t_0 = 1 year	(e) t_0 = 1.5 years
correlation between A and B		0.394	0.417	0.429	0.468

(g) M_w-7.5 earthquake on June 12, 2010

Case	A	(a) r_0 = 100 km, t_0 = 1.25 years			
	B	(b) r_0 = 75 km	(c) r_0 = 125 km	(d) t_0 = 1 year	(e) t_0 = 1.5 years
correlation between A and B		0.886	0.865	0.851	0.904

(h) M_w-8.6 earthquake on April 11, 2012

Case	A	(a) r_0 = 100 km, t_0 = 1.25 years			
	B	(b) r_0 = 75 km	(c) r_0 = 125 km	(d) t_0 = 1 year	(e) t_0 = 1.5 years
correlation between A and B		0.925	0.493	0.744	0.766

จุฬาลงกรณ์มหาวิทยาลัย
Chulalongkorn University

6.10 Stochastic Tests of Z and RTL

According to Huang (2005), in order to constrain that the anomalous areas of Z value and RTL algorithm investigation are not involved the random phenomena of earthquake occurrence, the statistical method called stochastic test is used here. For explaining the details of stochastic test, at first, the random seismicity catalogues (e.g., N = 10,000) were produced by randomizing the space (longitude and latitude) and time of earthquake data. Afterward, for each random catalogue, the Z value and RTL parameter were computed at the location of main shock of the investigated major earthquake. The identical criteria applied in the computations for the real catalogue

were chosen in the investigations. After quantifying the positive anomaly of Z-value and the negative anomaly of the RTL parameter, one can consider whether Z and RTL anomalies appear or not. Eventually, one can analyze the Z-value and RTL parameters at the location of main shock for all random catalogues and estimate the probability of occurrence of Z and RTL anomalies. According to Huang (2005), in order to corroborate that the Z and RTL anomalies are not synthesized, the prospective probability of the observed Z and RTL anomalies before the occurrence of major earthquake should be nearly 0.

After investigating stochastic of the positive Z and the negative RTL anomalies. The results indicated that the probability of Z value higher than that obtained the RTL algorithm. Statistically, it can mention that the anomalies of RTL algorithm are more significant than the anomalies of Z parameter. The detailed study of stochastic of Z value and RTL parameter impending to the occurrence major earthquake along the SASZ showed in Figures 6.13 and 6.14. Therefore, using RTL algorithm analysis of precursory seismicity rate change along the SASZ generate more reliable anomalies than Z.

(a) M_w-9.0 earthquake on December 26, 2004

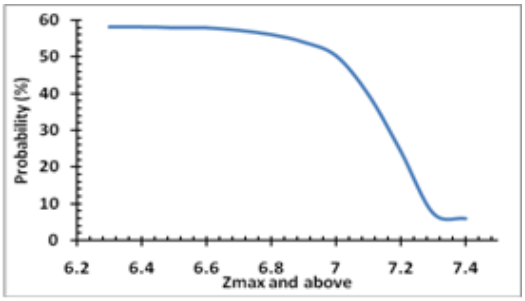

(b) M_w-8.6 earthquake on March 28, 2005

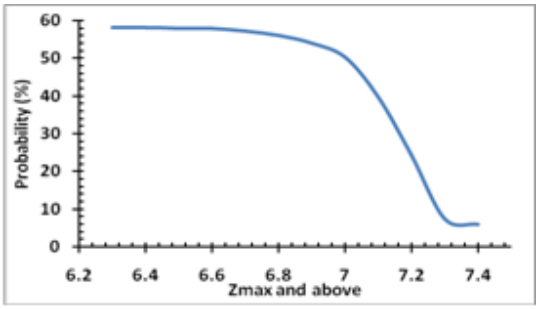

(c) M_w-7.2 earthquake on July 24, 2005

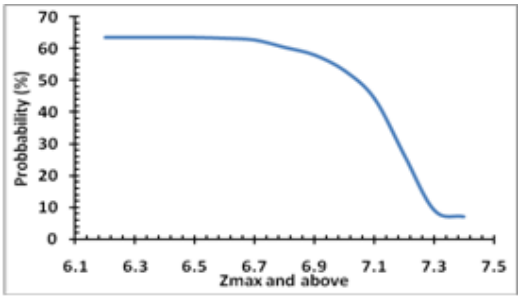

(d) M_w-7.3 earthquake on February 20, 2008

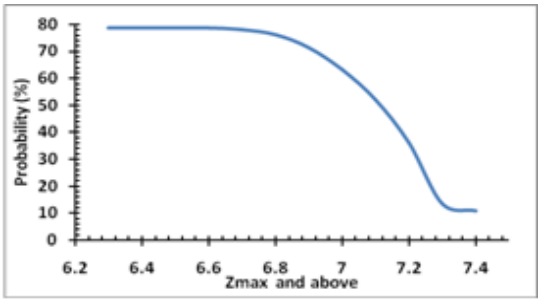

(e) M_w-7.5 earthquake on August 10, 2009

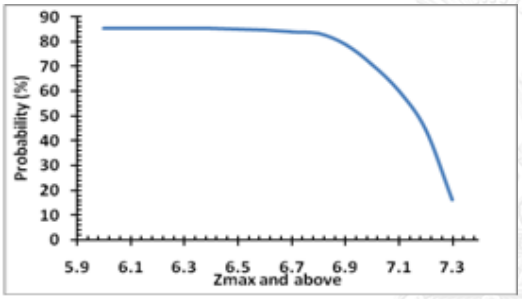

(f) M_w-7.8 earthquake on April 6, 2010

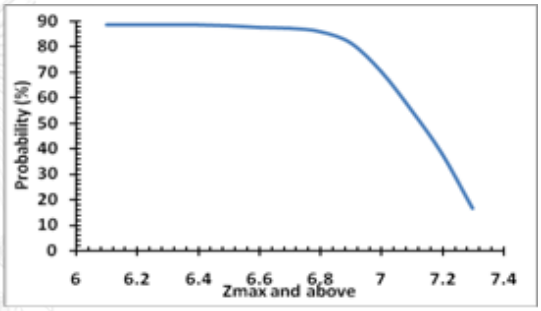

(g) M_w-7.5 earthquake on June 12, 2010

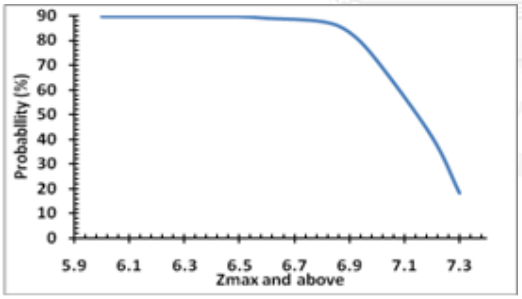

(h) M_w-8.6 earthquake on April 11, 2012

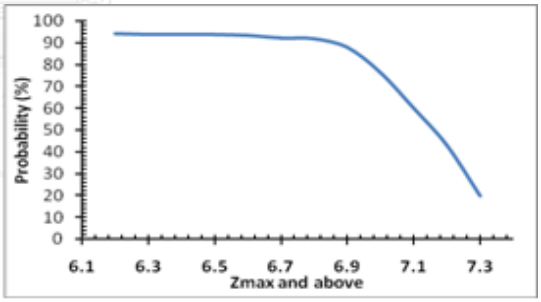

Figure 6.13. Stochastic tests of Z values at the epicenters of (a) M_w 9.0 earthquake on December 26, 2004, (b) M_w-8.6 earthquake on March 28, 2005, (c) M_w-7.2 earthquake on July 24, 2005, (d) M_w-7.3 earthquake on February 20, 2008, (e) M_w-7.5 earthquake on August 10, 2009, (f) M_w-7.8 earthquake on April 6, 2010, (g) M_w-7.5 earthquake on June 12, 2010 and (h) M_w-8.6 earthquake on April 11, 2012.

(a) M_w-9.0 earthquake on December 26, 2004

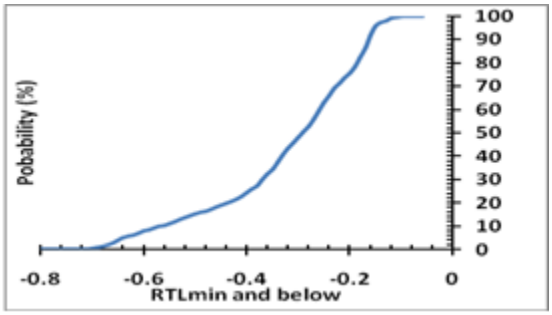

(b) M_w-8.6 earthquake on March 28, 2005

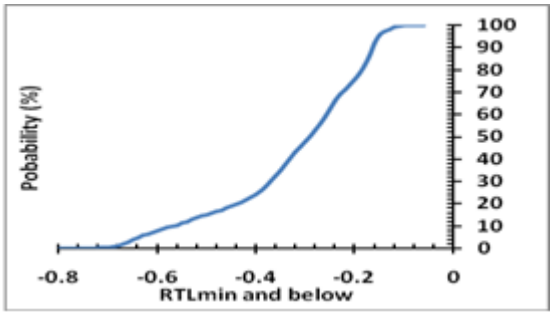

(c) M_w-7.2 earthquake on July 24, 2005

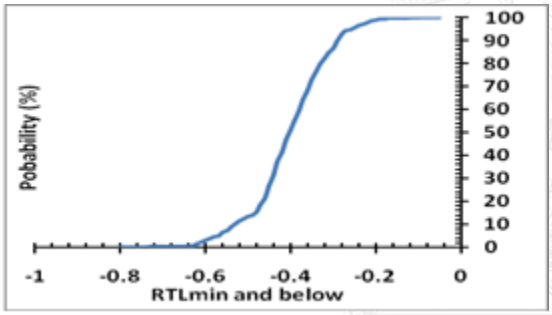

(d) M_w-7.3 earthquake on February 20, 2008

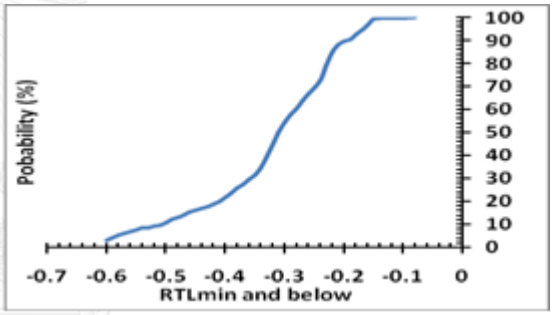

(e) M_w-7.5 earthquake on August 10, 2009

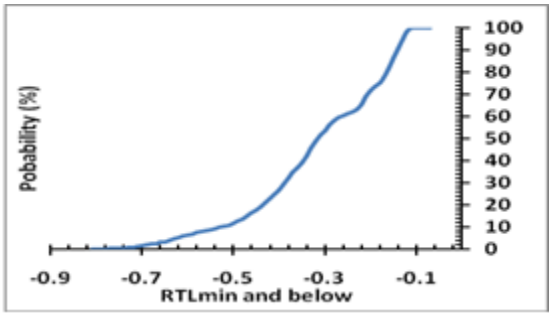

(f) M_w-7.8 earthquake on April 6, 2010

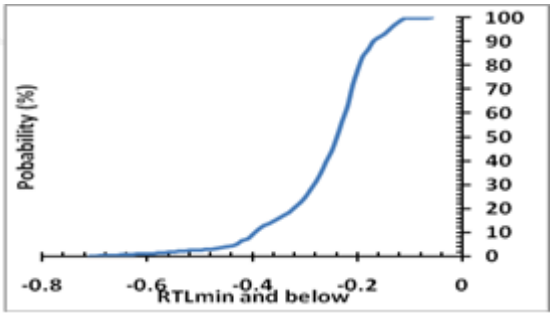

(g) M_w-7.5 earthquake on June 12, 2010 **(h)** M_w-8.6 earthquake on April 11, 2012

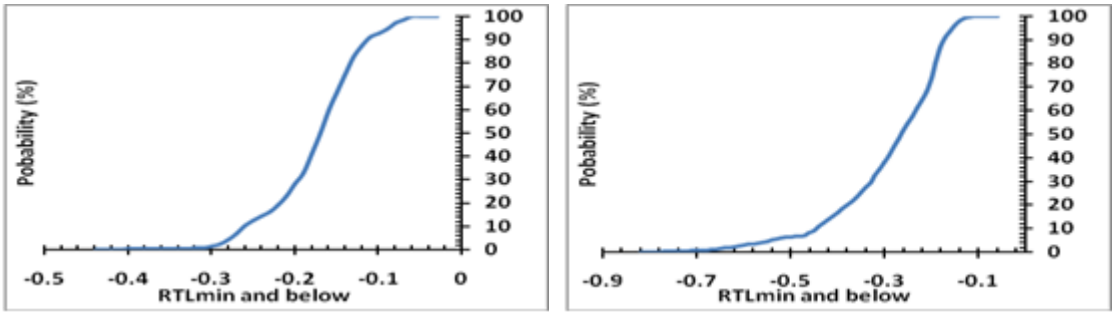

Figure 6.14. Stochastic tests of RTL values at the epicenters of (a) M_w-9.0 earthquake on December 26, 2004, (b) M_w-8.6 earthquake on March 28, 2005, (c) M_w-7.2 earthquake on July 24, 2005, (d) M_w-7.3 earthquake on February 20, 2008, (e) M_w-7.5 earthquake on August 10, 2009, (f) M_w-7.8 earthquake on April 6, 2010, (g) M_w-7.5 earthquake on June 12, 2010 and (h) M_w-8.6 earthquake on April 11, 2012.

จุฬาลงกรณ์มหาวิทยาลัย
Chulalongkorn University

CHAPTER VII
CONCLUSION AND RECOMMENDATION

7.1 Conclusion

This study attempt to investigate the precursory seismic quiescence before the major earthquakes along the SASZ by using simultaneously both Z value and RTL algorithm. The obtained results lead to the conclusion as follows;

i) After complete all recommended improving procedures of the earthquake catalogue, the cumulative number rate trend in straight line indicates the completeness of seismicity data obtained in this study.

ii) The Z value anomalies show clearly decreasing of the seismicity rate at $Z \geq 6.7$. Comparing with Z obtained from the other areas mentioned in the number of previous works, it is concluded that such $Z \geq 6.7$ is significant as the precursory anomalies noticeable before the major earthquake along the SASZ.

iii) In this study, the time span between the seismic quiescence and the following major earthquake are in the range of 2-7 year. Comparing with the previous works, it reveals that both Z and RTL are effective for the intermediate-term earthquake forecasting, i.e., month-10 years, along the SASZ.

iv) Although the higher Z value were found before the larger earthquake, the seismic quiescence are not clear to relate the magnitude of the earthquake. Meanwhile, for the RTL, the lower of RTL score relate significantly to the larger earthquake magnitude.

v) Regarding to temporal investigation, the anomalies of Z are normally found before the anomalous RTL was generated. After that, the following earthquakes were reported.

vi) Regarding to spatial distribution, the distribution of Z and RTL anomalies relate to the epicenters of major earthquake indicate location of an upcoming major earthquake along the SASZ.

vii) In this study, seismicity pattern change can be classified to be 4 types of precursor and the most variation pattern of the RTL are Type I, i.e., the variation pattern of the RTL is complete and dropping from 0 and turning to the background level before main shock.

viii) According to the present-day activities, the Nicobar Islands are covered by Z and RTL anomalies which still quiescence from the major earthquake and represent the risk area.

ix) The correlation coefficient in each major earthquake show that RTL anomalies found before the major earthquakes are not an artifact due to parameter selections indicate significance of precursory seismic quiescence.

x) The stochastic of Z value and RTL parameter indicate the anomalies of RTL algorithm are more significant than the anomalies of Z parameter along the SASZ.

จุฬาลงกรณ์มหาวิทยาลัย
Chulalongkorn University

7.2. Recommendation

According toShearer and Burgmann (2010), it is notable that although both M_w-9.0 and M_w-8.6 earthquake were reported preliminarily the earthquake epicenter at the similar location, the rupture process of these earthquake mentioned above are different. The M_w-9.0 earthquake generate northward to the Nicobar Islands meanwhile the M_w-8.6 generate southward to the Java Island. Therefore although both RTL and Z anomalies can be defined in the same locations in this study, the more details of both tectonic and geological data should be interpreted.

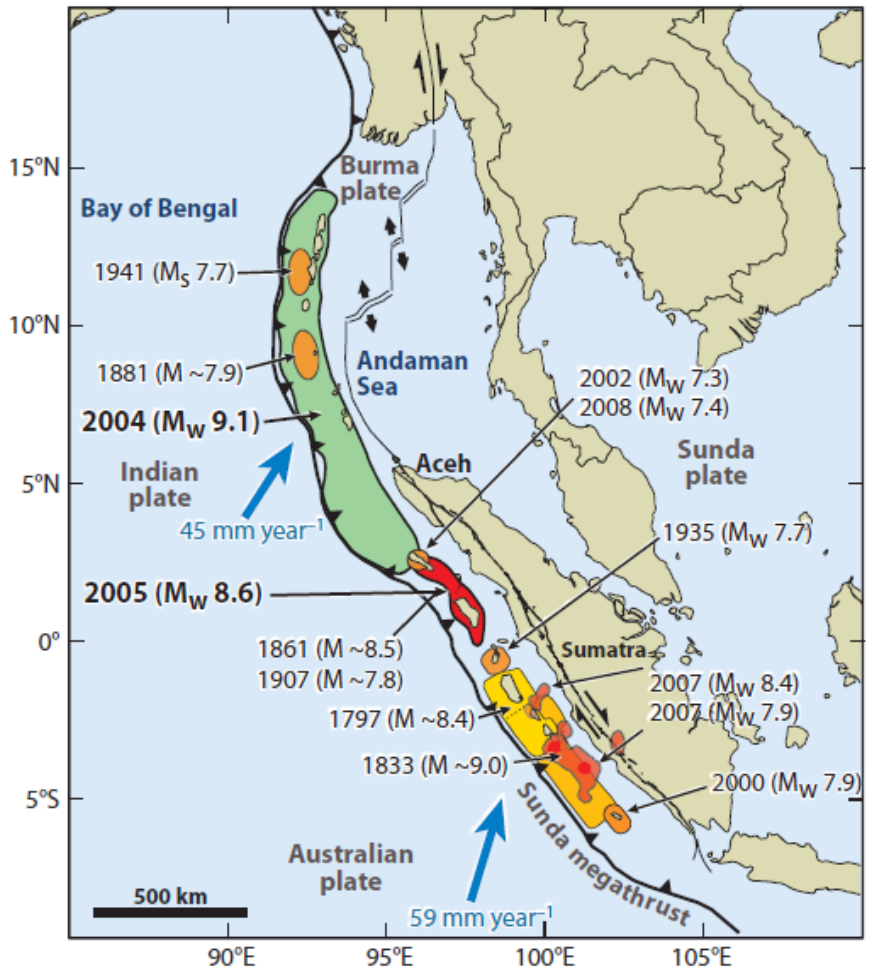

Figure 7.1. Map showing tectonic context and earthquake history along the SASZ (Shearer and Burgmann, 2010).

REFERENCES

Banghar, A.R., 1987. Seismo-tectonics of the Andaman-Nicobar Islands. Tectonophysics 133: 95-104.

Bendat, J.S. and Piersol, A.G., 2000. Random data: analysis and measurement procedures

Bilham, R., Engdahl, E.R., Feldl, N. and Satyabala, P., 2005. Partial and complete rupture of the Indo-Andaman plate boundary 1847–2004. . Seismological Research Letters, 76: 299-311.

Caceres, D. and Kulhanek, O., 2000. Seismic Hazard of Honduras. Natural Hazards 22: 49-69.

Campbell, K.W., 1985. Strong motion attenuation relations: a tenyear perspective. Earthquake Spectra, 1: 759-804.

Chen, C. and Wu, Y., 2006. An improved region-time-length algorithm applied to the 1999 Chi-Chi, Taiwan earthquake. Geophysical Journal International, 166: 1144-1147.

Chouliaras, G., 2009. Seismicity anomalies prior to 8 June 2008, Mw=6.4 earthquake in Western Greece. Natural Hazards and Earth System Sciences, 9: 327-335.

Chouliaras, G. and Stavrakakis, G.N., 2001. Current seismic quiescence in Greece: Implications for seismic hazard. Journal of Seismology, 5: 595-608.

Dasgupta, S. and Mukhopadhyay, M., 1993. Seismicity and plate deformation below the Andaman arc, northeastern Indian Ocean. Tectonophysics, 225: 529-542.

Dasgupta, S., Mukhopadhyay, M., Bhattacharya, A. and Jana, T.K., 2003. The geometry of the Burmese-Andaman subducting lithosphere. Journal of Seismology, 7: 155-174.

Eguchi, T., Ueda, S. and Maki, T., 1979. Seismotectonics and tectonic history of the andaman sea. Tectonophysics, 57: 35-51.

Felzer, K.R., Abercrombie, R.E. and Ekstrom, G., 2004. A common origin for aftershocks, foreshocks, and multiplets. Bulletin of the Seismological Society of America, 94: 88-98.

Gahalaut, V.K., Nagrajan, B., Catherine, J.K. and Kumar, S., 2006. Constraints on 2004 Sumatra-Andaman earthquake rupture from GPS measurements in Andaman-Nicobar Islands Earth and Planetary Science Letters, 242: 365-374.

Gambino, S., Laudani, A. and Mangiagli, S., 2014. Seismicity Pattern Changes before the M=4.8 Aeolian Archipelago (Italy) Earthquake of August 16, 2010. The Scientific World Journal, 2014: 8.

Gardner, J.K. and Knopoff, L., 1974. Is the sequence of earthquakes in Southern California, with aftershocks removed, Poissonian? . Bulletin of the Seismological Society of America, 64(1): 363-367.

Gentili., S., 2010. Distribution of seismicity before the larger earthquakes in Italy in the time interval 1994-2004. Pure and Applied Geophysics, 167: 933-958.

Gutenberg, B. and Richter, C.F., 1944. Frequency of earthquakes in California. Bulletin of Seismological Society of America, 34: 185-188.

Habermann, R.E., 1987. Man-made changes of Seismicity rates. Bulletin of the Seismological Society of America 77: 141-159.

Habermann, R.E., 1991. Seismicity rate variations and systematic changes in magnitudes in teleseismic catalogs. Tectonophysics, 193: 277-289.

Habermann, R.E. and Creamer, F., 1994. Catalog errors and the M8 earthquake prediction algorithm. Bulletin of the Seismological Society of America 84: 1551-1559.

Habermann, R.E. and Wyss, M., 1984. Background seismicity rates and precursory seismic quiescence: Imperial Valley, California. Bulletin of the Seismological Society of America, 74: 1743-1755.

Hanks, T.C. and Kanamori, H., 1979. A moment-magnitude scale. Journal of Geophysical Research 84: 2348-2350.

Huang, Q., 2004. Seismicity pattern changes prior to large earthquakes-An approach of the RTL algorithm. Terrestrial Atmospheric and Oceanic Science 15: 469-491.

Huang, Q., 2005. A method of evaluating reliability of earthquake precursors. Chinese Journal of Geophysics, 48(3): 701-707.

Huang, Q., 2008. Seismicity changes prior to the Ms8.0 Wenchuan earthquake in Sichan, China. Geophysical Research Letters, 35: L23308.

Huang, Q. and Ding, X., 2012. Spatiotemporal variations of seismic quiescence prior to the 2011 M 9.0 Tohoku Earthquake revealed by an improved region–time–length algorithm. Bulletin of the Seismological Society of America 102(4): 1878-1883.

Huang, Q. and Nagao, T., 2002. Seismic quiescence before the 2000 M=7.3 Tottori earthquake. Geophysical Research Letters, 29: 1578.

Huang, Q., Oncel, A.O. and Sobolev, G.A., 2002. Precursory seismicity changes associated with the Mw=7.4, 1999 August 17 Izmit (Turkey) earthquake. Geophysical Journal International, 151: 235-242.

Huang, Q. and Sobolev, G.A., 2002. Precursory seismicity changes associated with the Nemuro Peninsula earthquake, January 28, 2000. Journal of Asian Earth Sciences, 21: 135-146.

Huang, Q., Sobolev, G.A. and Nagao, T., 2001. Characteristics of the seismic quiescence and activation patterns before the M= 7.2 Kobe earthquake, January 17, 1995. Tectonophysics, 337: 99-116.

Ishimoto, M. and K., I., 1939. Observations sur les seismes enregistres par le microsismographe construit dernierement Bulletin of Earthquake Research Institute University of Tokyo 17: 443-478.

Jaffe, B.E., Borrero, J.C., Prasetya, G.S., Peters, R., McAdoo, B., Gel-fenbaum, G., Morton, R., Ruggiero, P., Higman, B., Dengler, L., Hidayat, R., Kingsley, E., Kongko, W., Lukijanto, Moore, A., Titov, V.V. and Yulianto, E., 2006. Northwest Sumatra and Offshore Islands Field Survey after the December 2004 Indian Ocean tsunami. . Earthquake Spectra, 22: S105-S135.

Jankaew, K., Atwater, B.F., Sawai, Y., Choowong, M., Charoentitirat, T., Martin, M.E. and Prendergast, A., 2008. Medieval forewarning of the 2004 Indian Ocean tsunami in Thailand. nature, 455: 1228-1231.

Jiang, H., Hou, H. and Zhou, H., 2004. Region-time-length algorithm and its application to the study of intermediate-short term earthquake precursor in North China. Acta Seismologica Sinica, 17(2): 164-176.

Katsumata, K., 2011a. Precursory seismic quiescence before the Mw=8.3 Tokachi-Oki, Japan, earthquake on 26 September 2003 revealed by a re-examined earthquake catalog. Journal of Geophysical Research, 116: B10307.

Katsumata, K., 2011b. A long-term seismic quiescence started 23 years before the 2011 off the Pacific coast of Tohoku Earthquake (M=9.0). Earth Planets Space, 63: 709-712.

Katsumata, K. and Sakai, S., 2013. Seismic quiescence and activation anomalies from 2005 to 2008 beneath the Kanto district, central Honshu, Japan Earth Planets Space 65(1463-1475).

Kawamura, M., Chen, C. and Wu, Y., 2014. Seismicity change revealed by ETAS, PI, and Z-value methods: A case study of the 2013 Nantou, Taiwan earthquake. Tectonophys.

Kumar Ravi, M., Purnachandra, N. and Chalam, S.V., 1996. A seismotectonic study of the Burmar and Andaman arc regions using centroid moment tensor data. Tectonophysics, 253: 155-165.

Liu, H. and Su, Y.J., 2006. Application of region-time-length algorithm to Yunnan area. Journal of Seismology, 29(1): 25-29.

Martin, S., 2005. Intensity distribution from the 2004 M 9.0 Sumatra-Andaman earthquake. Seismological Research Letters 76: 321-330.

Matthews, M.V. and Reasenberg, P., 1988. Statistical methods for investigating quiescence and other temporal seismicity patterns. Pure and Applied Geophysics, 126: 357-372.

จุฬาลงกรณ์มหาวิทยาลัย
CHULALONGKORN UNIVERSITY

Monecke, K., Finger, W., Klarer, D., Kongko, W., McAdoo, B., Moore, A.L. and Sudrajat, S.U., 2008. A 1000-year sediment record of tsunami recurrence in northern Sumatra. Nature, 455: 1232-1234.

Murru, M., Console, R. and Montuori, C., 1999. Seismic quiescence precursor to the 1983 Nihonkai-Chubu (M7.7) earthquake, Japan. Annals of Geophysics, 42: 871-882.

Nuannin, P., Kulhánek, O. and Persson, L., 2005. Spatial and temporal b-value anomalies preceding the devastating off coast of NW Sumatra earthquake of December 26, 2004. Geophysical Research Letters 32: L11307.

Oishi, M. and Sato, T., 2007. Moment release budget at oblique convergence margin as revealed by the 2004 Sumatra-Andaman earthquake. Earth Planets and Space, 59: 913-921.

Ortiz, M. and Bilham, R., 2003. Source area and rupture parameters of the 31 December 1881 MW=7.9 Car Nicobar earthquake estimated from tsunamis recorded in the Bay of Bengal. Journal of Geophysical Research, 108(22): 15-31.

Ozturk, S. and Bayrak, Y., 2009. Precursory seismic quiescence before 1 May 2003 Bingol (Turkey) earthquake: A statistical evaluation. Journal of Functional Analysis, 4(4): 600-610.

Pailoplee, S. and Choowong, M., 2014. Earthquake frequency-magnitude distribution and fractal dimension in mainland Southeast Asia. Earth Planets and Space, 66: 1-8.

Pailoplee, S., Surakiatchai, P. and Charusiri, P., 2013. b-value anomalies along the northern segment of the Sumatra-Andaman subduction zone: Implications for upcoming earthquake. Journal of Earthquake and Tsunami 7(3): 1350030.

Paris, R., Lavigne, F., Wassimer, P. and Sartohadi, J., 2007. Coastal sedimentation associated with the December 26, 2004 tsunami in Lhok Nga, west Banda Aceh (Sumatra, Indonesia). Marine Geology, 238(1-4): 93-106.

Park, J., Butler, R., Anderson, K., Berger, J., Benz, H., Davis, P., Hutt, C., McCreery, C., Ahern, T., Ekstrom, G. and Aster, R., 2005. Performance Review of the Global

Seismographic Network for the Sumatra-Andaman Megathrust Earthquake. Seismological Research Letters 76: 331-343.

Petersen, M., Dewey, J., Hartzell, S., Mueller, C., Harmsen, S., Frankel, A.D. and Rukstales, K., 2004. Probabilistic seismic hazard analysis for Sumatra, Indonesia and across the Southern Malaysian Peninsula Tectonophysics, 390: 141-158.

Rudolf-Navarro, A.H., Munoz-Diosdado, A. and Angulo-Brown, F., 2010. Seismic quiescence patterns as possible precursors of great earthquakes in Mexico. International Journal of Physical Sciences, 5(6): 651-670.

Rydelek, P.A. and Sacks, I.S., 1989. Testing the completeness of earthquake catalogues and the hypothesis of self-similarity. Nature, 337: 251-243.

Shashidhar, D., Kumar, N., Mallika, K. and Gupta, H., 2010. Characteristics of seismicity patterns prior to the M ~ 5 earthquakes in the Koyna Region, Western India – application of the RTL algorithm. International Union of Geological Sciences, 33: 83-90.

Shearer, P. and Burgmann, R., 2010. Lessons Learned from the 2004 Sumatra-Andaman Megathrust Rupture. Annual Review of Earth and Planetary Science, 38: 103-131.

Sobolev, G.A., 1995. Fundamental of Earthquake Prediction. Electromagnetic Research Centre, Moscow: 162.

Sobolev, G.A. and Tyupkin, Y.S., 1997. Low-seismicity precursors of large earthquakes in Kamchatka. Volcano Seismology, 18: 433-446.

Sorbi, M.R., Nilfouroushan, F. and Zamani, A., 2012. Seismicity patterns associated with the September 10th, 2008 Qeshm earthquake, South Iran. International Journal of Earth Science, 101: 2215-2223.

Sun, J. and Pan, T., 1995. Seismic characteristics of Sumatra and its relevance to Peninsular Malaysia and Singapore. Journal of Southeast Asian Earth Sciences, 12: 105-111.

จุฬาลงกรณ์มหาวิทยาลัย
Chulalongkorn University

Taylor, D.A., Snoke, J.A., Sacks, I.S. and Takanami, T., 1990. Nonlinear frequency magnitude relationship for the Hokkaido corner, Japan. Bulletin of the Seismological Society of America, 80: 340-353.

Wiemer, S., 2001. A software package to analyze seismicity: ZMAP. Seismological Research Letters, 72: 373-382.

Wiemer, S. and Wyss, M., 1994. Seismic quiescence before the Landers (M = 7.5) and Big Bear (M= 6.5) 1992 earthquakes. Bulletin of the Seismological Society of America, 84: 900-916.

Wiemer, S. and Wyss, M., 2000. Minimum Magnitude of Completeness in Earthquake Catalogs: Examples from Alaska, the Western United States, and Japan. Bulletin of the Seismological Society of America, 90: 859-969.

Woessner, J. and Wiemer, S., 2005. Assessing the Quality of Earthquake Catalogues: Estimating the Magnitude of Completeness and Its Uncertainty. Bulletin of the Seismological Society of America, 95(2): 684-698.

Wyss, M., 1991. Reporting history of the central Aleutians seismograph network and the quiescence preceding the 1986 Andreanof Island earthquake. Bulletin of the Seismological Society of America, 81: 1231-1254.

Zuniga, F.R., Reyners, M. and Villamor, P., 2005. Temporal variations of the earthquake data in the catalogue of seismicity of New Zealand. Bulletin of the New Zealand Society for Earthquake Engineering, 38: 87-107.

Zuniga, F.R. and Wiemer, S., 1999. Seismicity patterns: are they always related to natural causes? Pure and Applied Geophysics, 155: 713-726.

APPENDIX

จุฬาลงกรณ์มหาวิทยาลัย
Chulalongkorn University

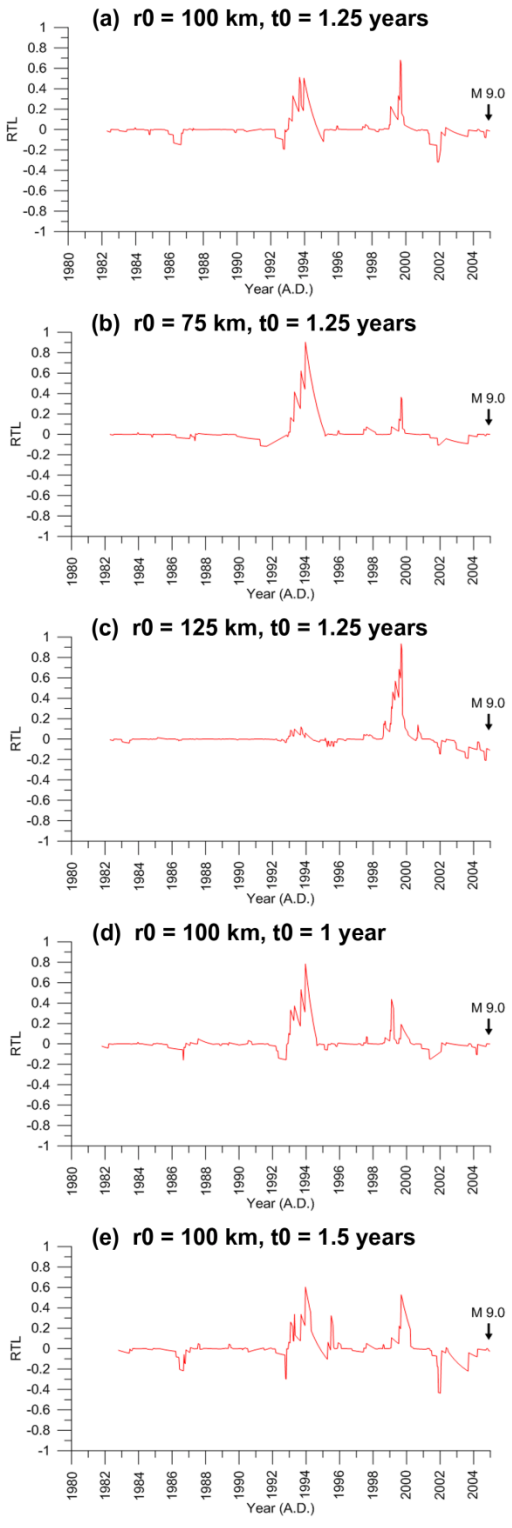

M_w-9.0 earthquake on December 26, 2004

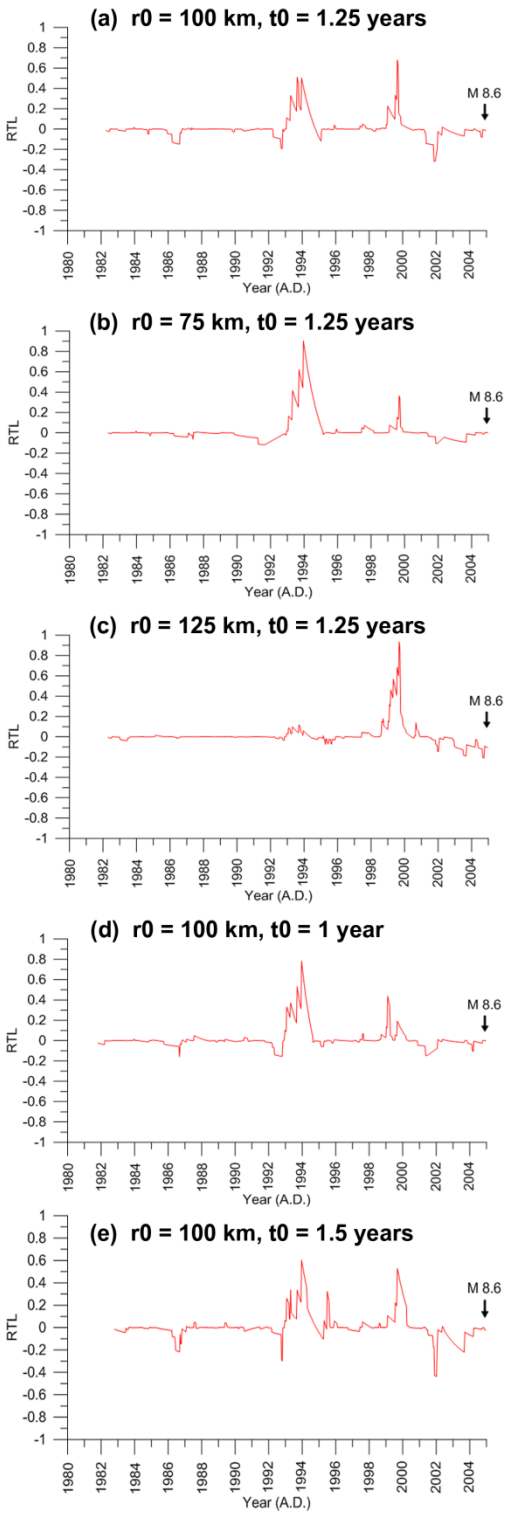

M_w-8.6 earthquake on March 28, 2005

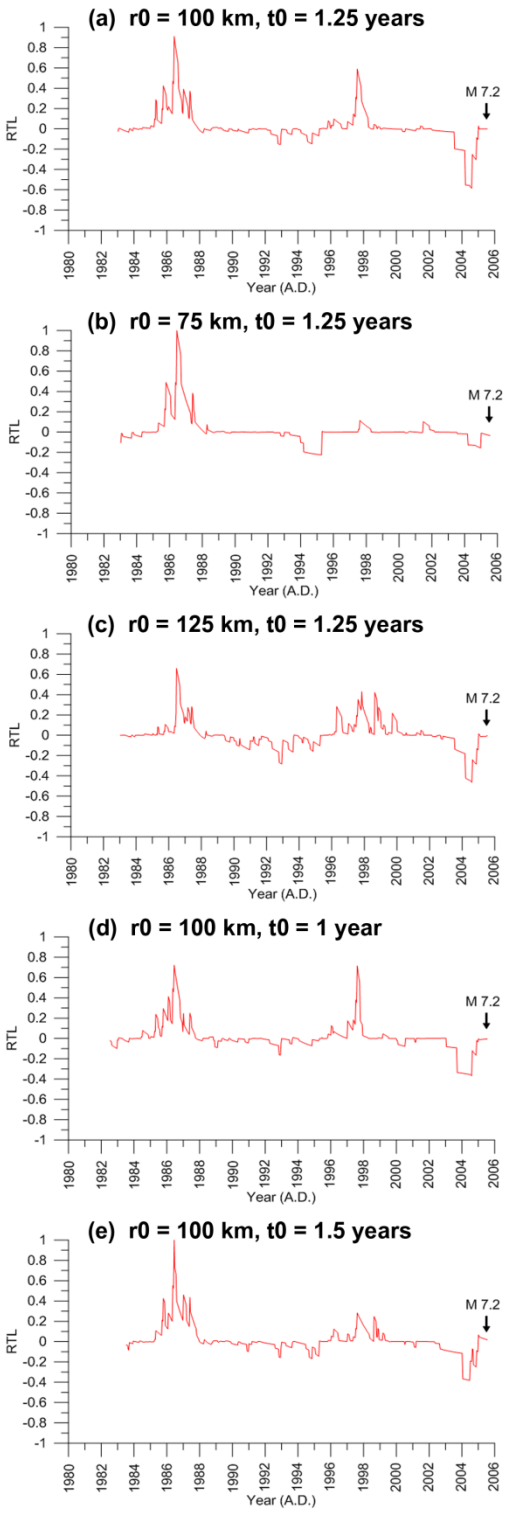

M_w-7.2 earthquake on July 24, 2005

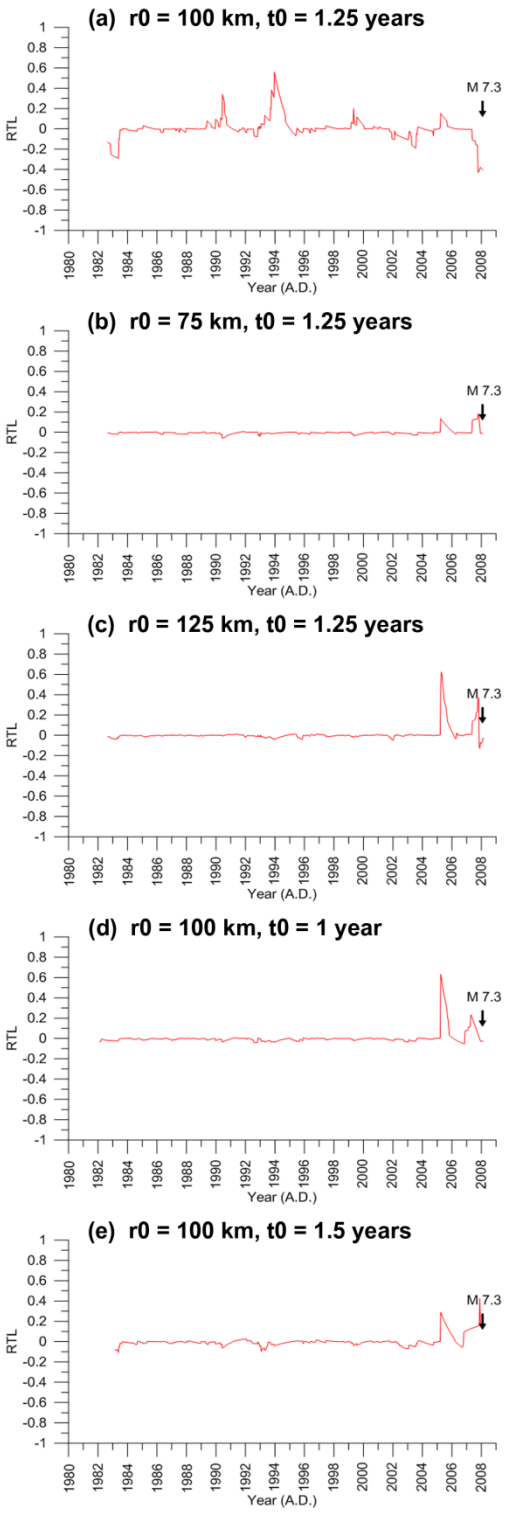

M_w-7.3 earthquake on February 20, 2008

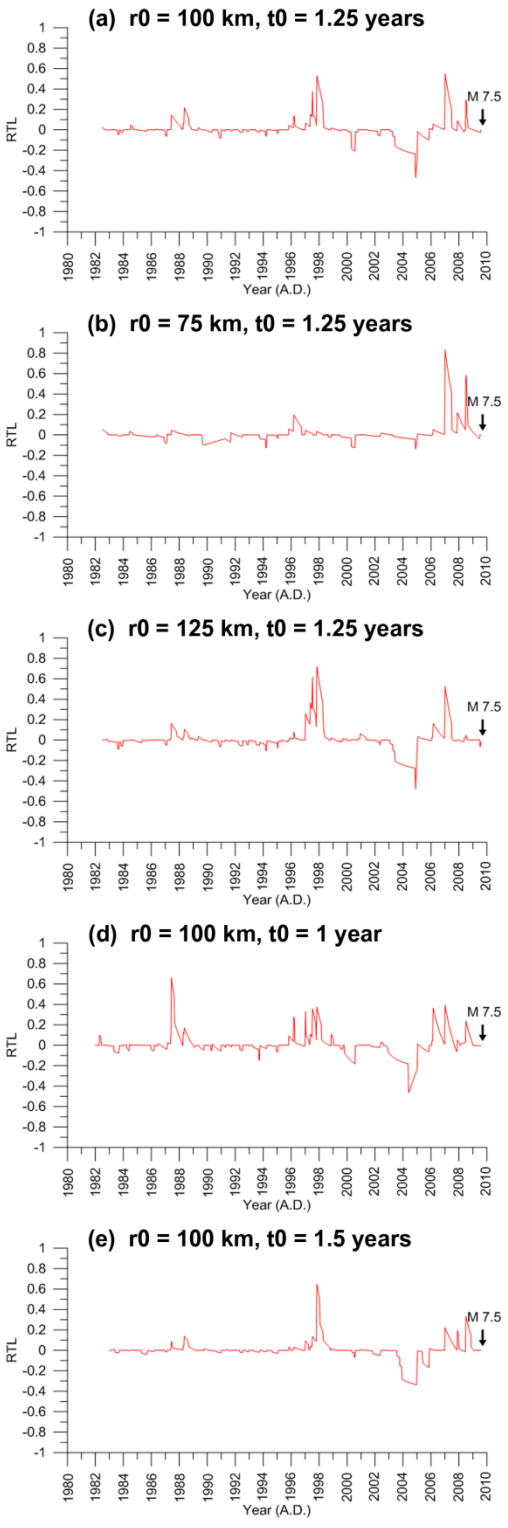

M_w-7.5 earthquake on August 10, 2009

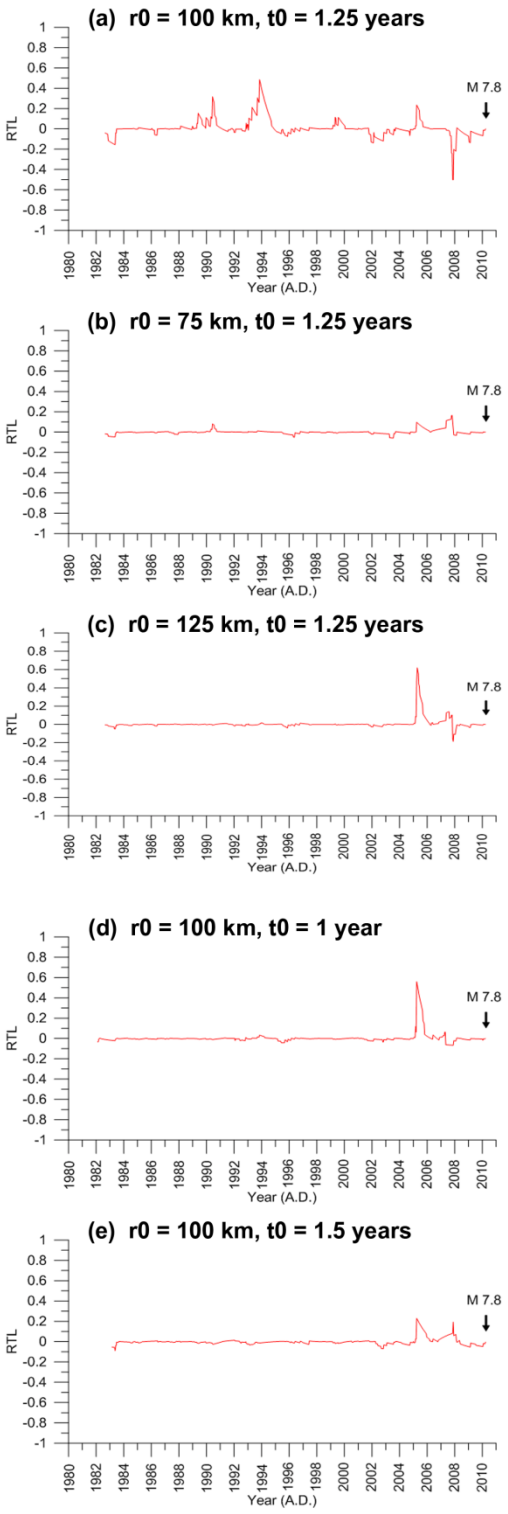

M_w-7.8 earthquake on April 6, 2010

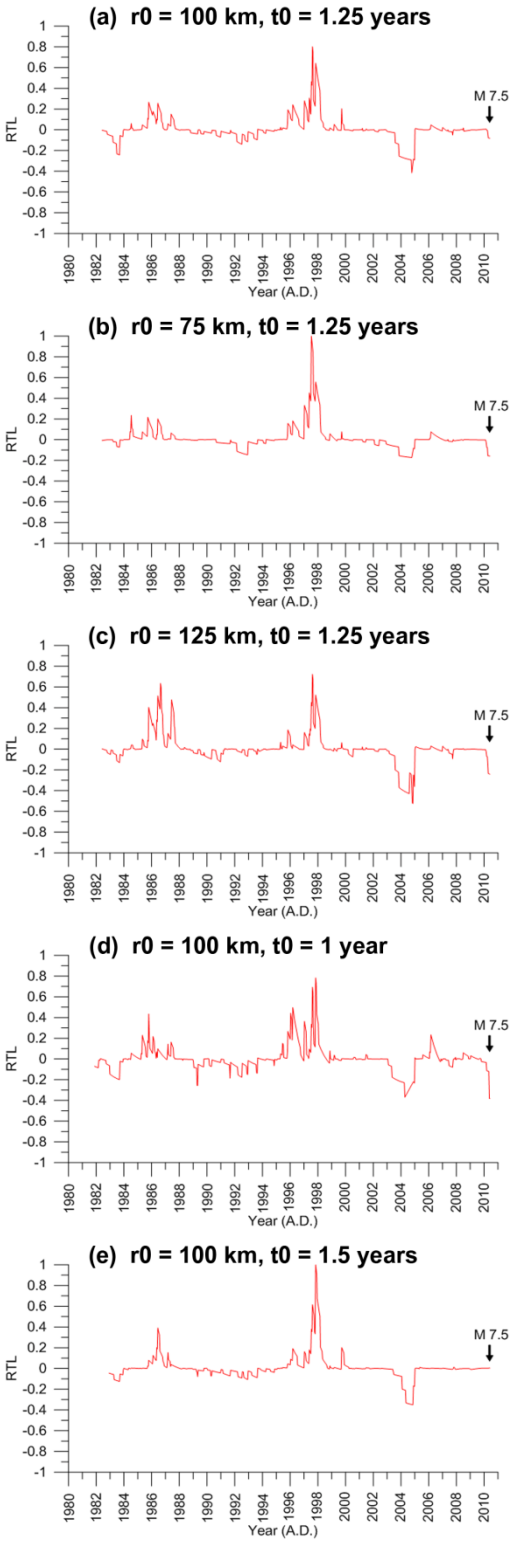

M_w-7.5 earthquake on June 12, 2010

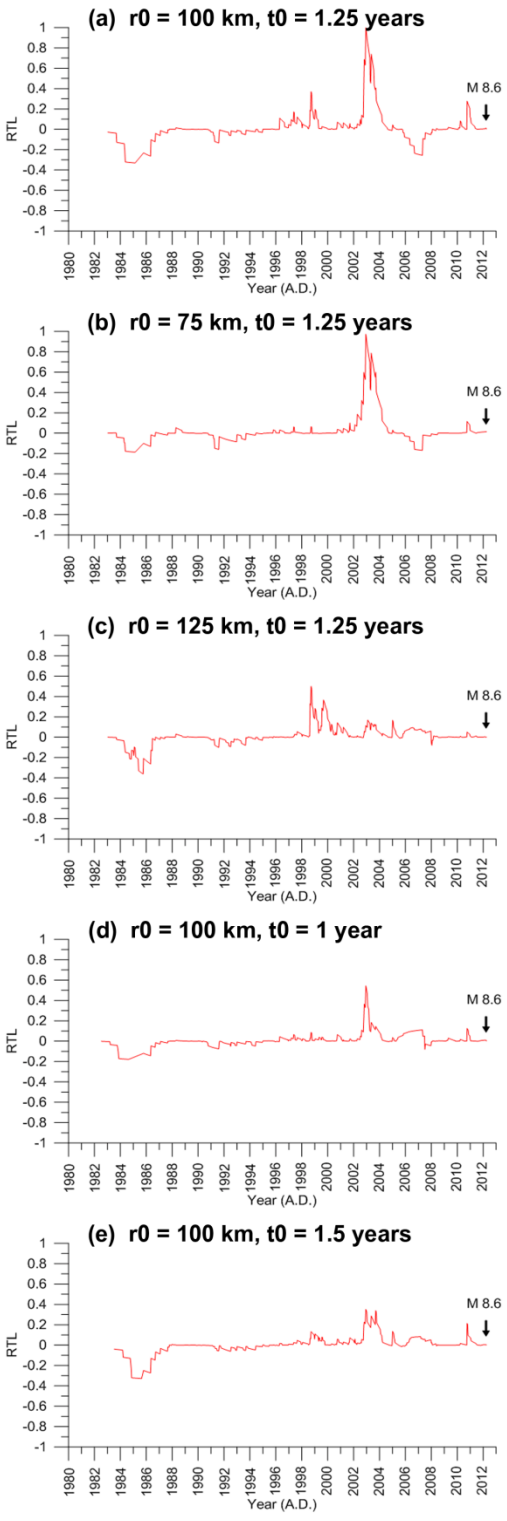

M_w-8.6 earthquake on April 11, 2012

VITA

Mr. Santawat Sukrungsri was born in Bangkok, Thailand on June 7, 1982. In 2004 he received a Bachelor of Science degree in Physics with the computer simulation and acoustic wave experience from Department of Physics, Faculty of Science, Chulalongkorn University. After graduation, he has been employed under the position of Geologist with experience in geophysical survey and seismic wave by the Department of Mineral Resources then he joined the Seismological Bureau, Thai Meteorological Department, as a Meteorologist with skill in analyses earthquakes within Thailand and internationally. Since 2012, he has entered the Earth Sciences program, Department of Geology, Faculty of Science, Chulalongkorn University with a focus on the earthquake forecasting for a Master of Science degree study.

จุฬาลงกรณ์มหาวิทยาลัย
Chulalongkorn University